Geoff Smith
Leicester School of Pharmacy

A focus on PAT in freeze-drying

APS Parenteral Focus Group meeting on Freeze Drying and Alternative Drying Technologies for Parenterals, Burleigh Court, Loughborough University.28 January 2015

BIOPHARMACEUTICAL QUALITY BY DESIGN

Overview

- Freeze-drying – Process steps and questions?
- QbD in Freeze-Drying
- Freezing Stage
  - Critical process parameters : solidification end point, eutectic formation, glass formation
  - PAT in the freezing Stage (development & production)
- Primary Drying Stage
  - Critical process parameters : collapse temperature, drying rate, drying end point
  - PAT in the 1ry drying Stage (development & production)
- LyoDEA – A new PAT

Problems with lyophilizing biologicals

Biologicals are labile, complex, often multi-domain macromolecules

- Freeze drying can strip stabilising water from proteins
  - requiring careful excipient choice to maintain activity
- Freeze-concentration may induce unfolding and aggregation
  - Specific electrolyte balance required to control the weak forces
- Final product storage stability may be problematic (cold chain)
- Instability on reconstitution
  - May require chilling during dispensing to minimise degradation
  - May suffer from aggregation and denaturation
- May lose active material by non specific adsorption to glass/metal/plastics

So process optimisation is a key issue for manufacturers whose processes include freeze drying.

QbD in Freeze Drying

- Identify Critical Quality Attributes for the freeze dried product
  - Stability, Reconstitution time, cake structure, mechanical strength
- Determine critical thermal properties of the product
  - Eutectic temperatures, glass transition (Tg) and collapse temperature (Tc)
- Develop & implement in-line PAT tools to monitor the process
  - Freezing onset, freezing rate, amount of ice formation, solidification end point
  - Primary drying rate and end point
- Use DoE the to establish the Design Space for safe operation
  - Assess the impact of product, formulation, container and dryer
  - Develop models for each stage of the process to assess the impact of changes
  - Risk assess the impact of excursion outside of this space (product & Equipment failure)

Process Analytical Technologies

- A system for designing, analyzing, and controlling manufacturing through timely measurements (i.e. during processing) of critical quality and performance attributes of raw and in-process materials and processes with the goal of ensuring final product quality

- In the PAT framework (FDA September 2004) these tools can be categorized according to the following:
  - Multivariate tools for design, data acquisition and analysis
  - Process analyzers
  - Process control tools
  - Continuous improvement and knowledge management tools

- http://www.fda.gov/downloads/Drugs/Guidances/ucm070305.pdf

PAT in production : The expectations are high

Global load monitoring	As freeze-drying is dependent upon heat and mass thermal transfer, some heterogeneities may limit control. It may be erroneous to rely on individual vial measurement to control the whole load.
loading/unloading	Compatibility with automatic loading/unloading devices. The placement and removal of vials must not be impaired.
CIP & stoppering	Compatibility with cleaning in place(CIP)/stoppering devices. No leads should compromise the movement of shelves, CIP ramps, or nozzles
Aseptic handling compliance	Compliance with aseptic handling. There should be no source of contamination within the materials or during positioning
Steam sterilization	Steam sterilization. The device must sustain repeated steam sterilization at a minimum of 123 ° C and 2 bars for a duration of 3 h.
Leakage control	Placement of the device should not induce freeze-dryer leakage. It should also support at least a 5 microbar vacuum, and measurement should be independent of equipment leak rate.
Integration	Simple integration into an industrial freeze-dryer. The device should be installed to current existing ports using tri-clamp flanges, and the data acquisition signal should be compatible with 21CFR Scada / recorders

Comparison of PATs for Production

Drying rate & End Point

End point

Success Factor	Monitor Global Load	Automatic Loading	CIP + Stoppering Device	Aseptic Handling	Steam Sterilizable	Leak Rate Control	Simple Integration	Calibration
Temperature probe	NO	NO	NO	+/−	YES	YES	+/−	YES
Wireless product temperature probe	NO	NO	NO	+/−	YES	YES	+/−	YES
Conductivity probe	NO	NO	NO	NO	YES	YES	YES	YES
Microbalance	NO	NO	NO	NO	NO	+/−	NO	YES
FTNIR product probes	NO	NO	NO	NO	YES	YES	NO	YES
Pirani/capacitive differential pressure control	YES	YES	YES	YES	+/−	YES	YES	YES
Moisture probe	YES	YES	YES	YES	NO	YES	YES	YES
Pressure rise measurement	YES	YES	YES	YES	YES	NO	YES	NO
Mass spectrometry	YES	YES	YES	YES	NO	NO	NO	
TDLAS	YES	YES	YES	YES	YES	YES	NO	
Cold plasma	YES	YES	YES	YES	YES	YES	YES	

Modified from Mayeresse et al. PDA J Pharm Sci Technol. 2007 May-Jun;61(3):160-74

Freeze drying cycle design

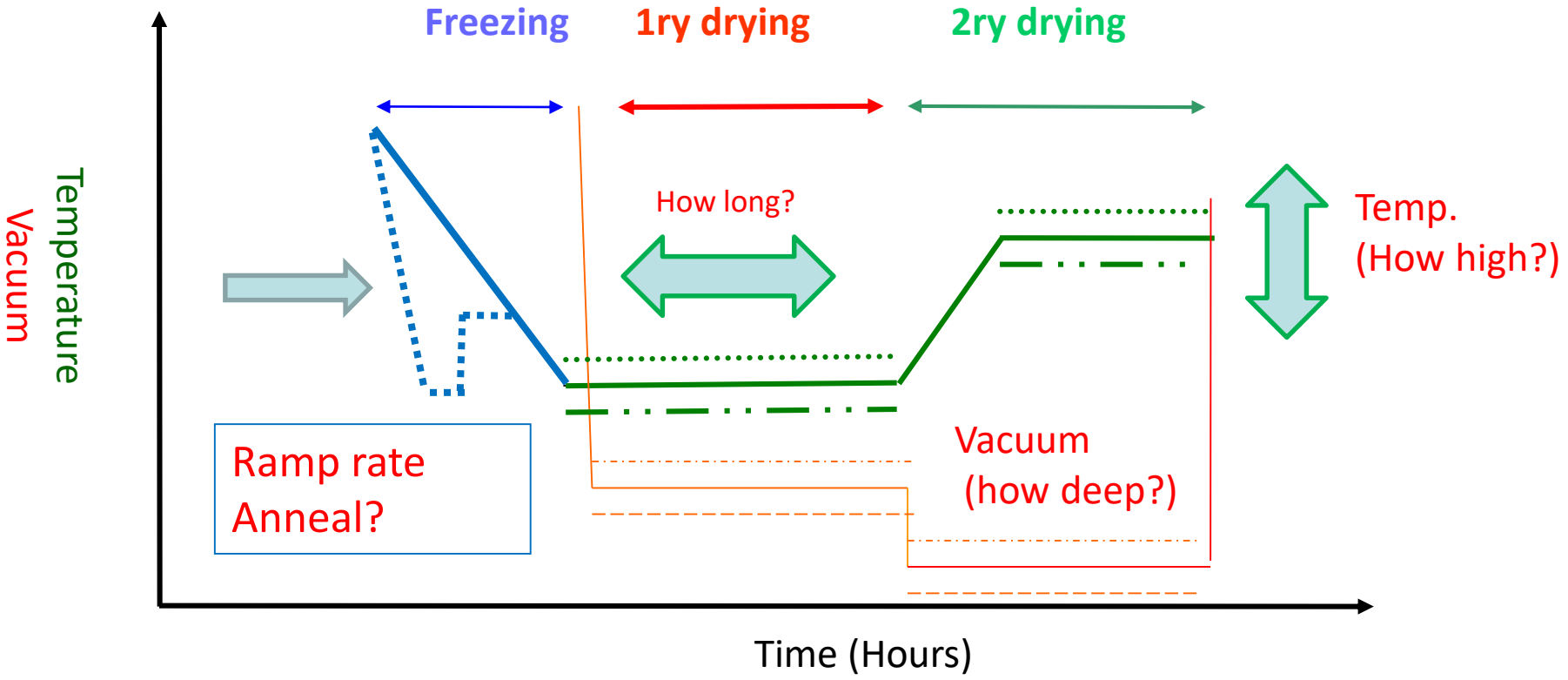

- Process design achieved by multiple cycles to establish high&low operational limits
- Repeatability established by consistency of batches and process trend monitoring

PAT : What do you need to measure and at what scale

Product scales

1: Microscopic : Molecular dynamics in the unfrozen phase (relevance to collapse temperature)

2: Mesoscopic: Ice crystals and connectivity (relevance to drying rates)

3: Macroscopic I : Ice formation from the base (impact on scale 2). Temperature differences across the ice layer, changing ratio of ice layer and dry layer during drying,

4: Macroscopic II : design of vial (size, wall thickness, base characteristics), Impact of vial dimensions in relation to fill height, clustering of vials

Engineering scale

1: size of shelf, separation of shelves, edge effects

2: loading of drier, condenser capacity, coolant capacity, dimensions of ducting between the chamber and condenser (choke flow) etc..

FREEZING STAGE

The Desired state?

(Freezing onset, freezing rate, amount of ice formation, solidification end point)

End of freezing stage : Product temperature stabilises

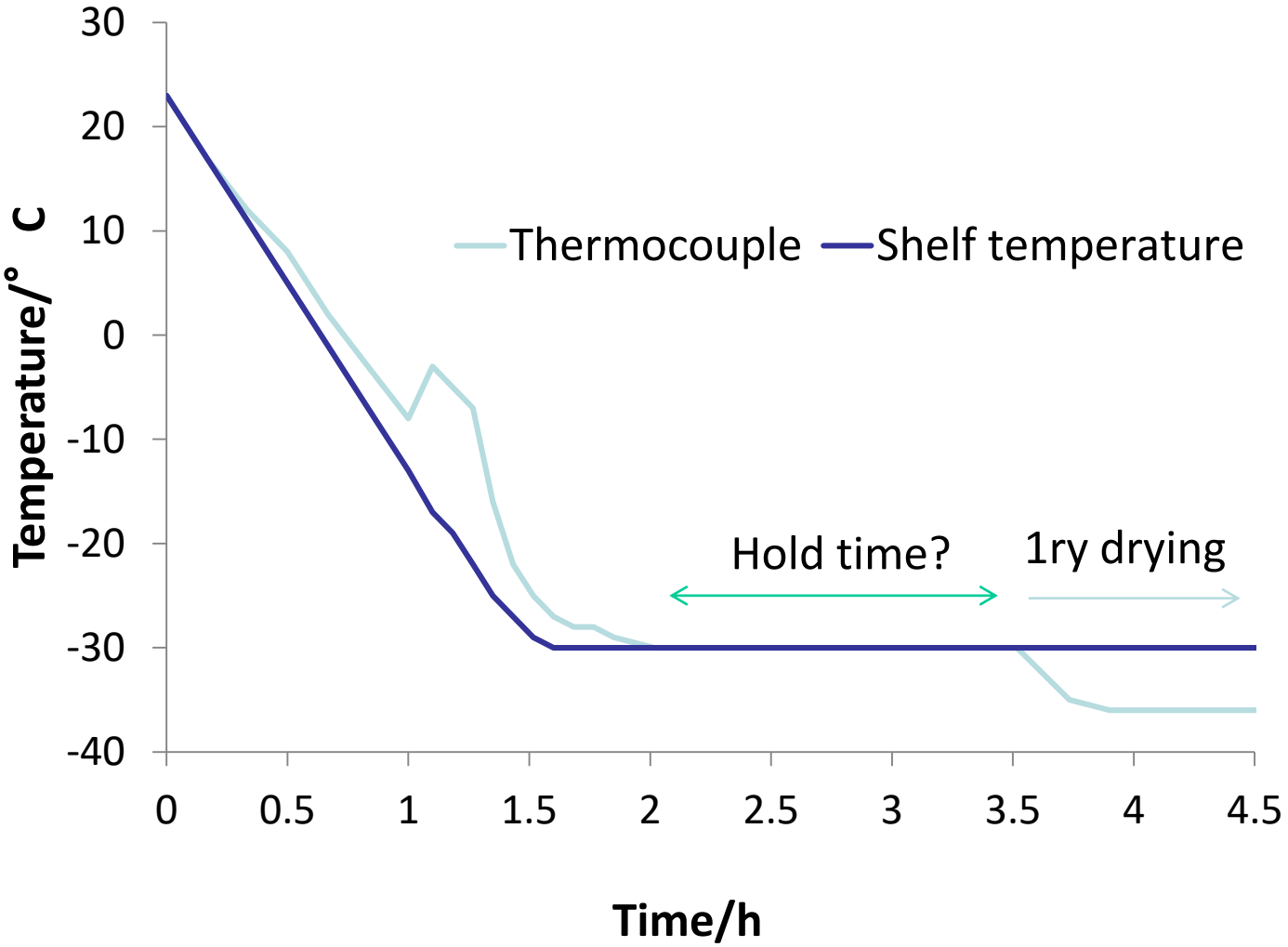

Freezing is a critical step

Super-cooling & nucleation, induction

- Ice nucleation is a random process- can impact homogeneity of product
- **Slower freezing** gives rise to bigger ice crystals and permits faster sublimation JA Searles et al *J Pharm Sci* 90; 860-71 (2001)
- **Rapid freezing** may be needed for labile products (Åkerblom et al Infusions Therapie 1992; 19:283-287)
- **Annealing** (raising the temperature during freezing stage) may improve ice crystal growth JA Searles et al *J Pharm Sci* 90;872-87 (2001)

Impact of formulation on critical temperatures

When freezing : Ice formation followed by **crystallization of excipients** & **drug** and/or **formation of the amorphous state**

- Characteristics of excipient may define whether it is a crystallising excipient (mannitol) or a glass forming excipient (sucrose)
- Freeze to well below the critical temperatures (eutectic) and hold to ensure complete solidification (But for how long?)
- Formulation changes (e.g. mixtures) may result in marked changes in critical temperature (But are off-line measurements representative?)
- Crystallisable excipients may require annealing (But at what temperature and for how long?)

PAT for laboratory studies : Critical temperatures Tm, Te, Tg

Lyotherm2 – integrated electrical Impedance (Zsinϕ) and DTA

designed to measure glass transition (Tg'), eutectic (Teu) and melting (Tm) temperatures relevant to freeze-drying formulations

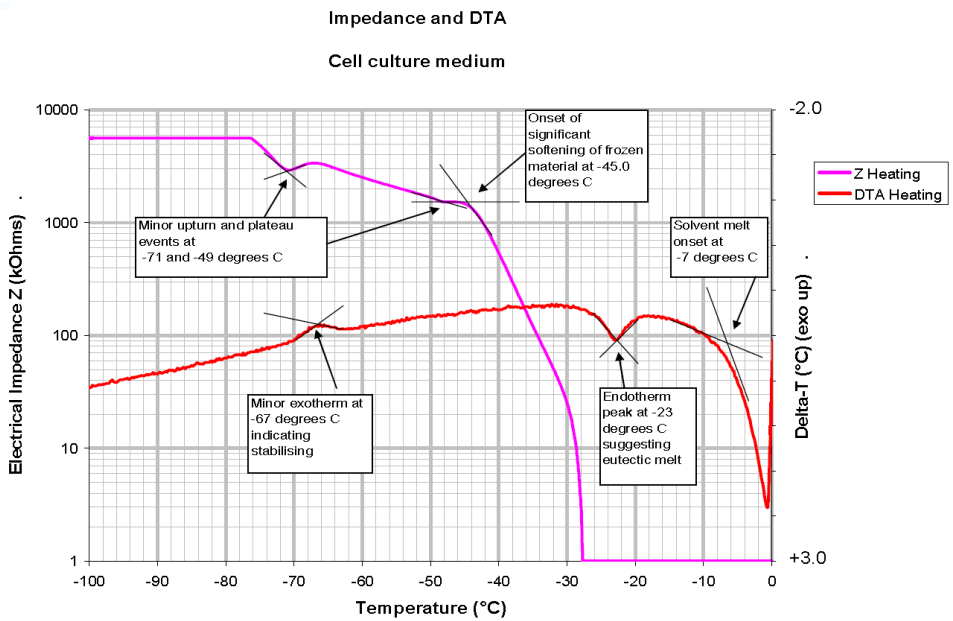

Ward & Matejtschuk , 2010 *in Freeze Drying/ Lyophilization of Pharmaceutical & Biological Products* 3rd ed. Rey,L & May JC eds, Informa Press, New York

PAT in freezing stage limited to Temperature Measurement

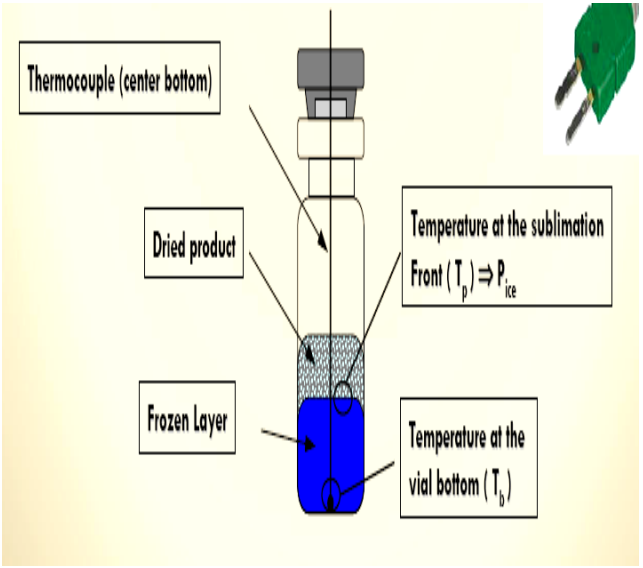

Thermocouple

- positioned *bottom-centre in the vial-*
- less robust (*difficult to handle*, *sterility problems)*
- Used mainly in *laboratory scale*

Resistance thermal detectors

- Reliable, easy to sterilize
- accurate positioning is difficult, limited validity due to measurement of temperature average
- Used primarily in manufacturing

LyoDEA Brief Description

- The system connects via a junction box to 5 individual **LyoDEA™** test vials positioned around the freeze-drier shelf.
- Frequency scans (10 Hz – 1 MHz) of the LyoDEA™ test vial impedance were recorded every 1-5 minutes throughout a freeze-drying cycle (20 s for each spectrum)
- The **LyoDEA™** measurement and control software saves the spectra from each time point

LyoDEA Measurement Vial

Applications

Formulation variables

- Freezing rates/end points
- Eutectic crystallization
- Glass transition
- Structural relaxation

Process variables

- Temperature
- Annealing – ice growth rates
- Drying rates
- Primary drying end points

LyoDEA response surface

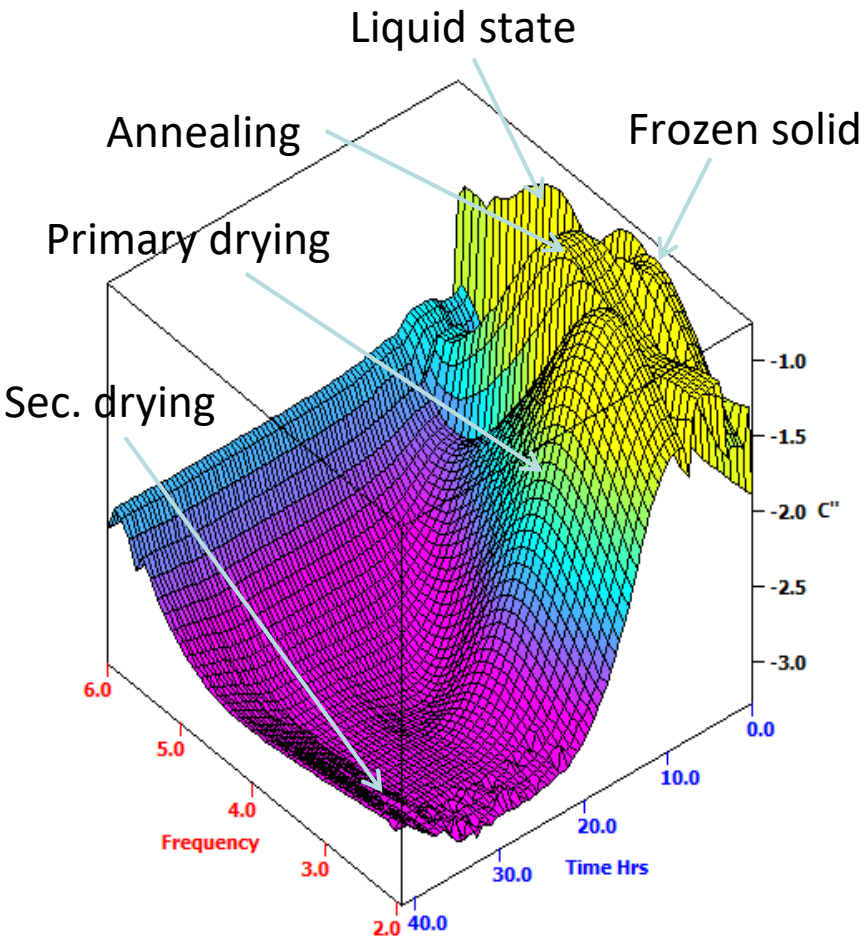

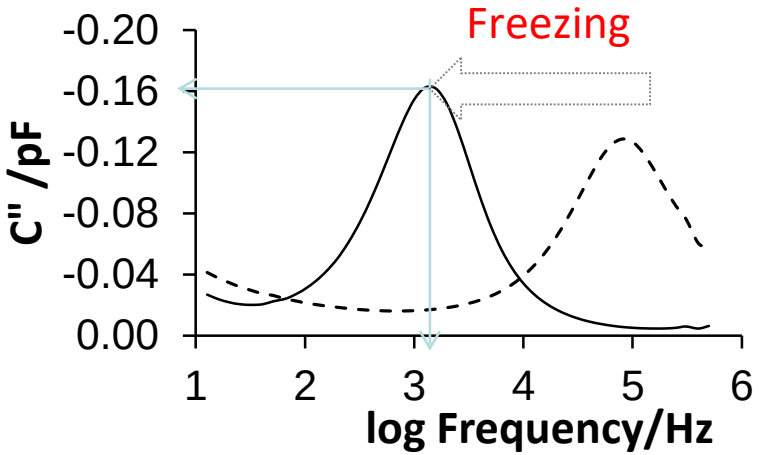

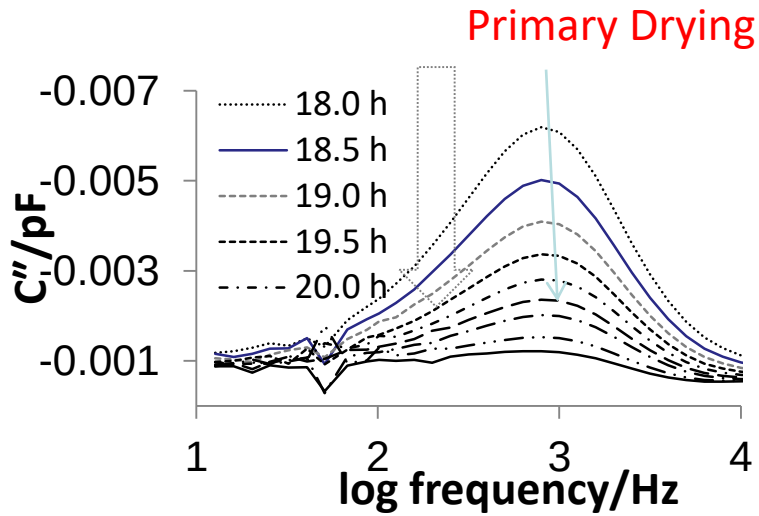

Impedance Modelling

- CPE explains the interfacial impedance of the glass wall of the vial.
- Resistance element records conductivity of ions
- Capacitor element defines dielectric properties of the product.
- The circuit element R was shown to be a sensitive indicator of the phase behavior of the solution, i.e. ice formation and solute crystallization during the freezing cycle

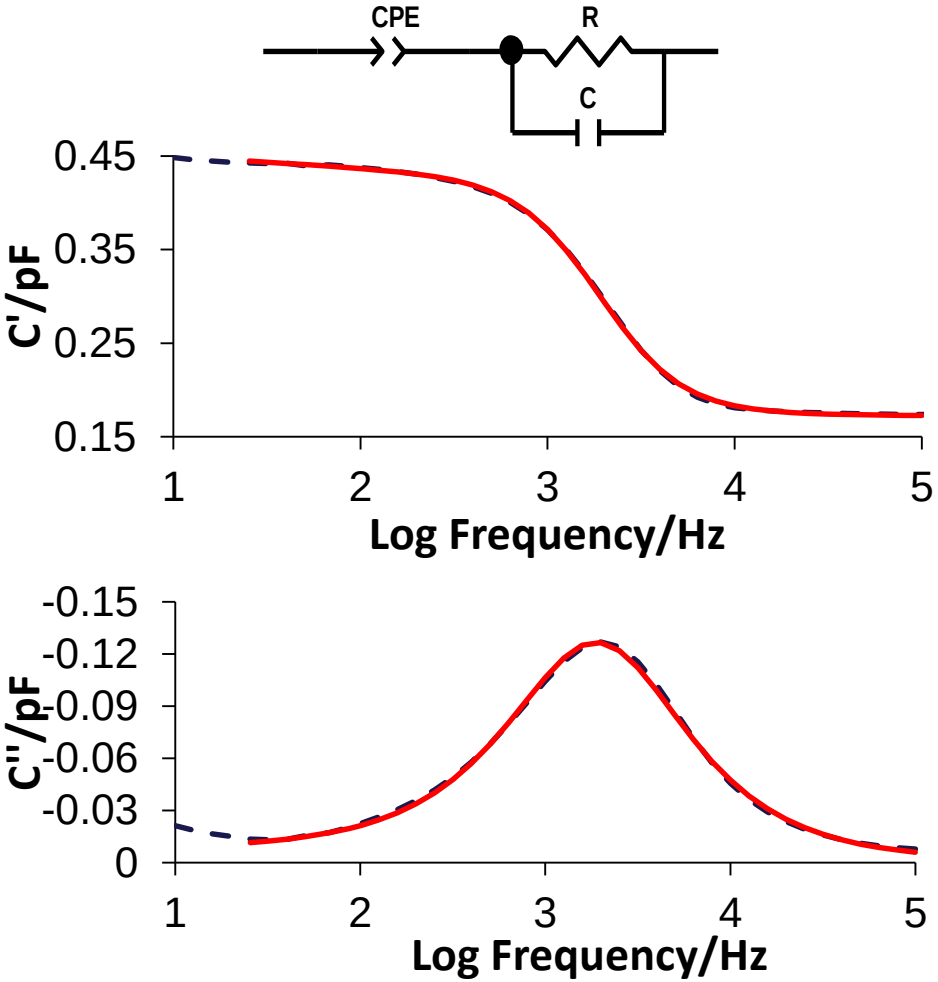

Product Characterization – Ice formation

Fpeak profile records freezing step (B-E) which progress through 2 discrete stages; solidification(B-D) and equilibration(D-E). Time duration for the former increase with the fill height while the latter remain broadly unchanged as it is related to thermal coefficient of the vial base.

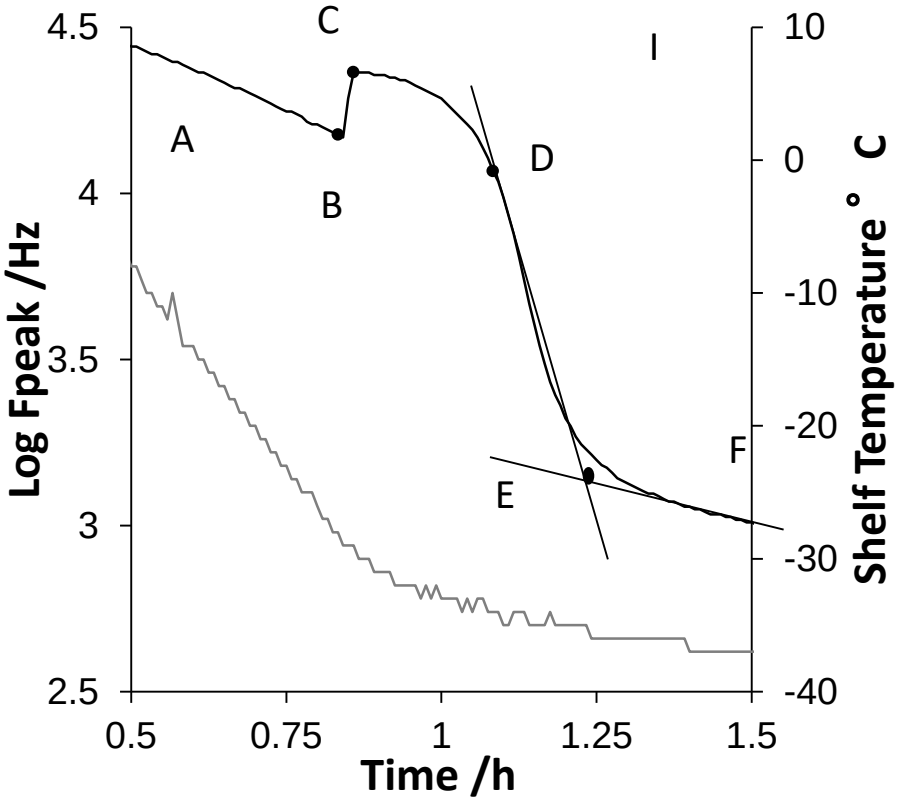

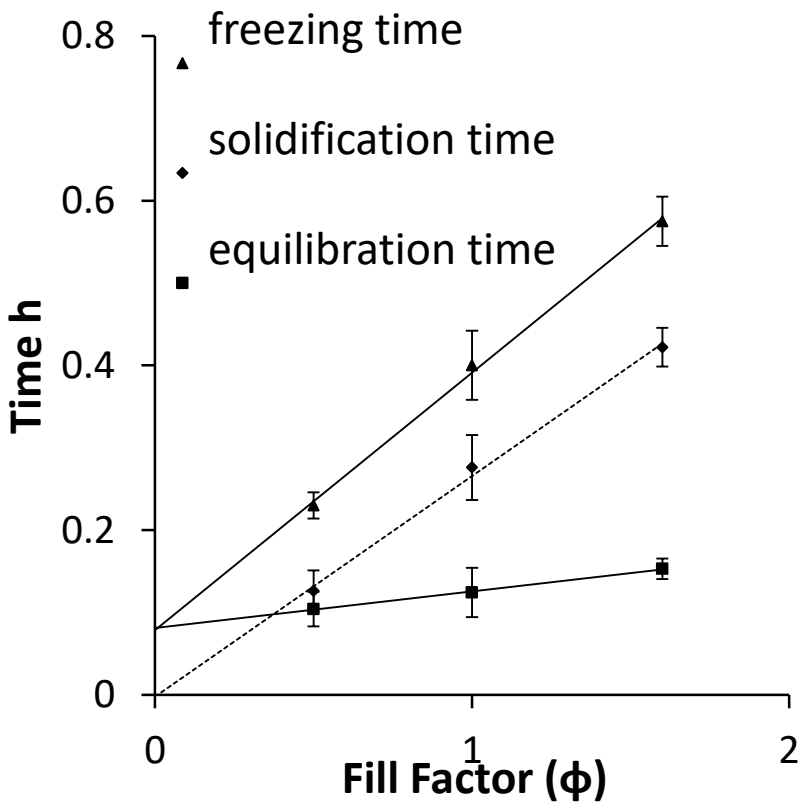

Effect of Sucrose on mannitol crystallization

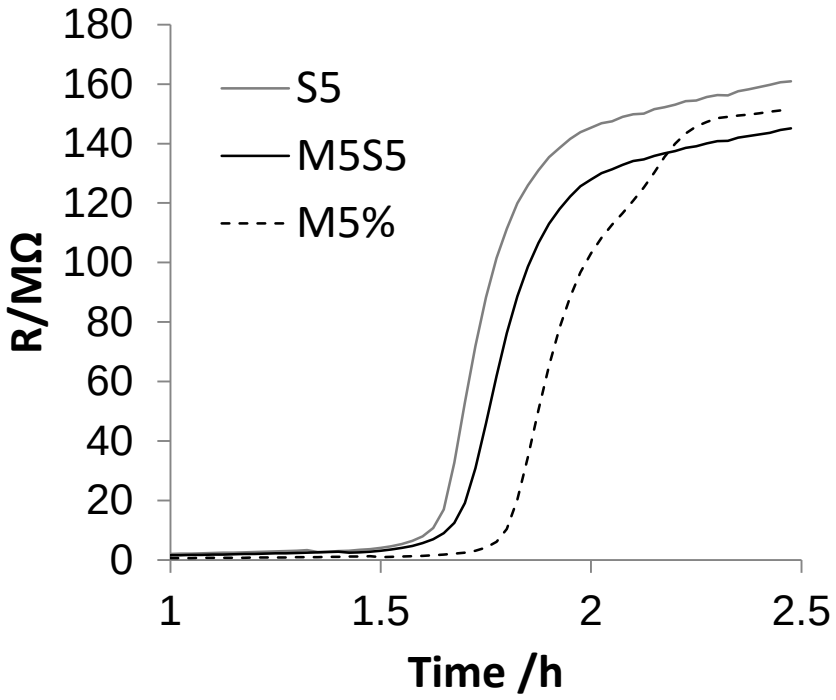

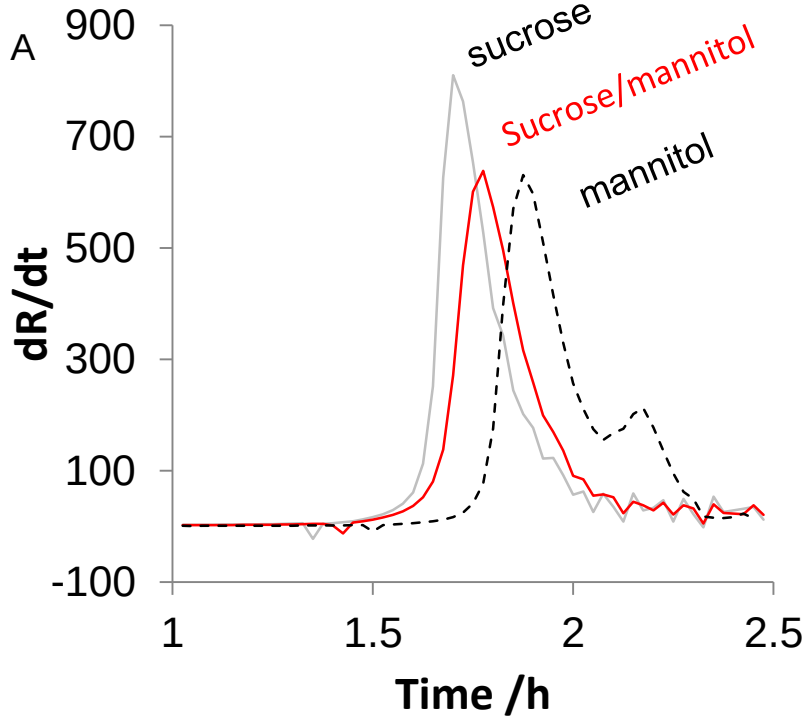

Mannitol crystallization supressed with the inclusion of sucrose in the solution.

Completion of Annealing (Maltodextrin 10% w/v)

- The capacitance of the formulation changes minimally while the resistance changes significantly and plateaus at 3-4 h
- After 3h annealing hold time, both the capacitance and drying time changes insignificantly.

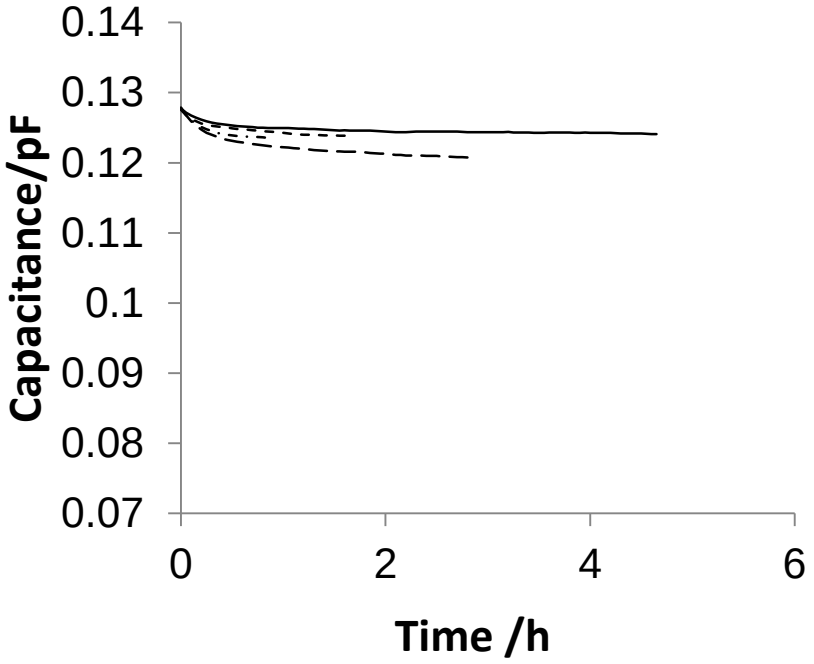

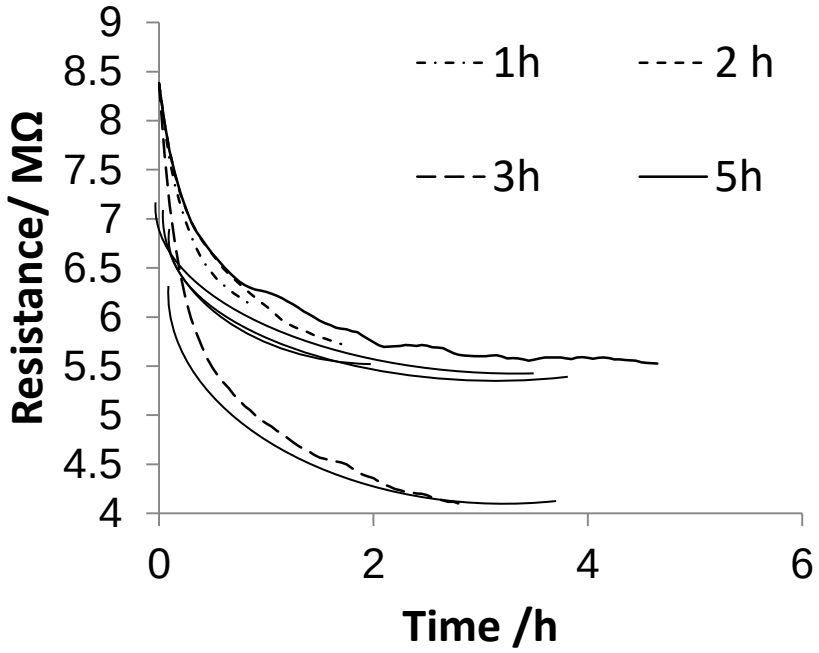

Predictive control of the primary drying time

- Increase in the capacitance correlates well with the decrease in the primary drying time.
- Changes in the Product capacitance during annealing may be predictive of the reduction in primary drying time.

For every ~2% increase in capacitance the primary drying decreases by ~8%

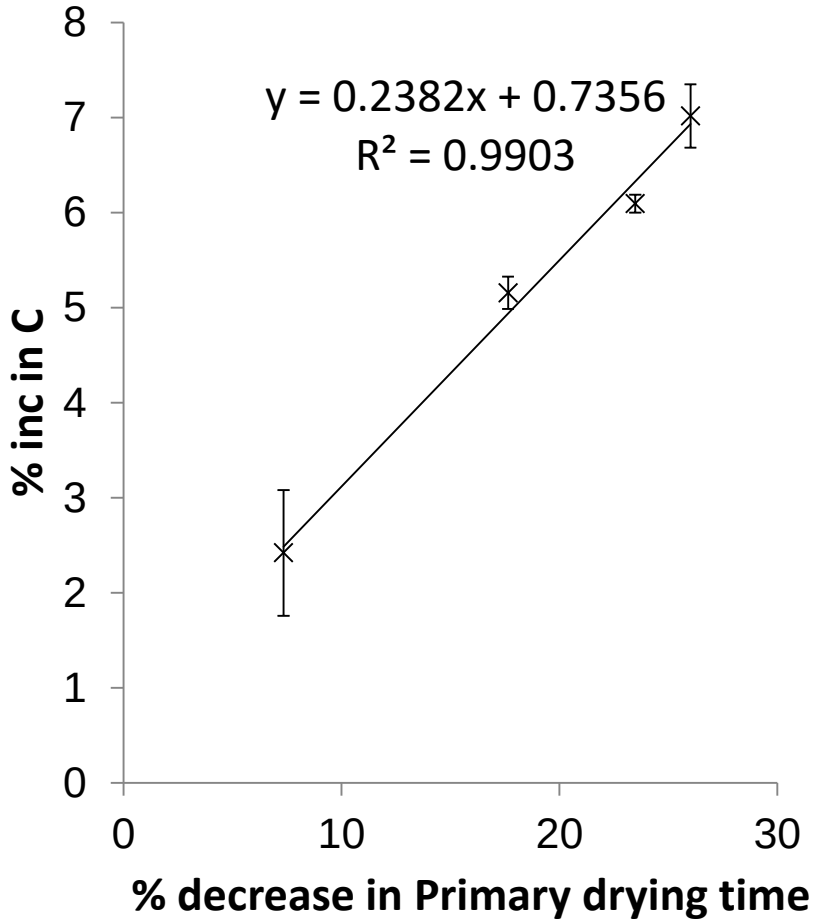

Product Characterization: T_g determination by LyoDEA

Aqueous solution of Maltodextrin 10% w/v by LyoDEA on heating at 1 C min^{-1}

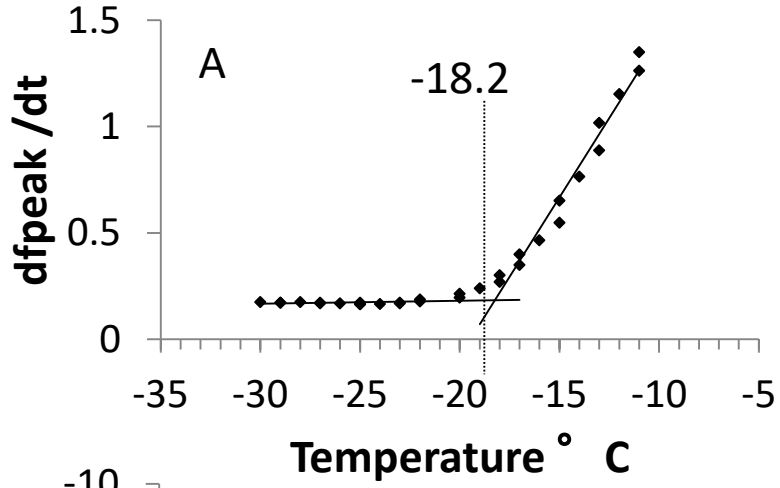

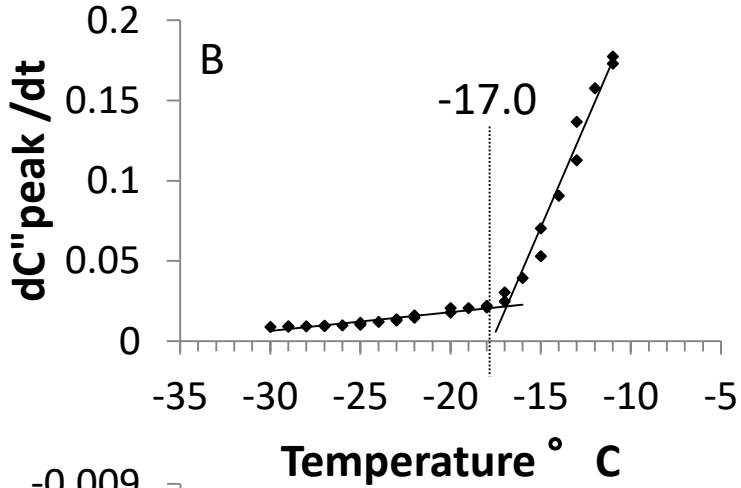

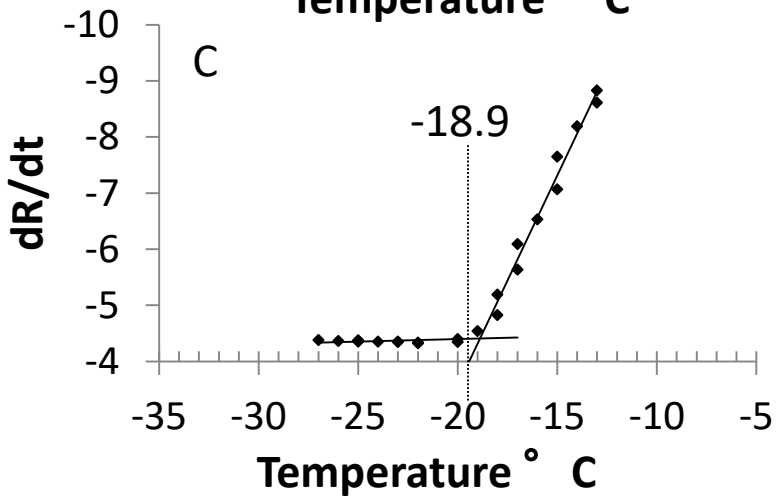

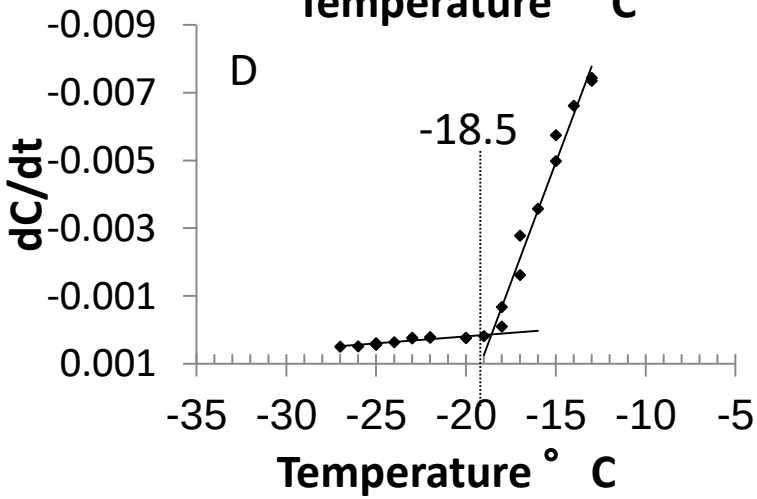

Measurement of Fragility of frozen solution (Maltodextrin 10% w/v)

- Below Tg the changes in product resistance follows Arrhenius trend with Ea ~ 20 KJ.Mol^{-1}.
- Above Tg VTF function models the resistance profile.
- The fragility of the glassy matrix calculated from VTF results and slope of resistance was recorded to be ~0.7; suggesting a fragile glass.

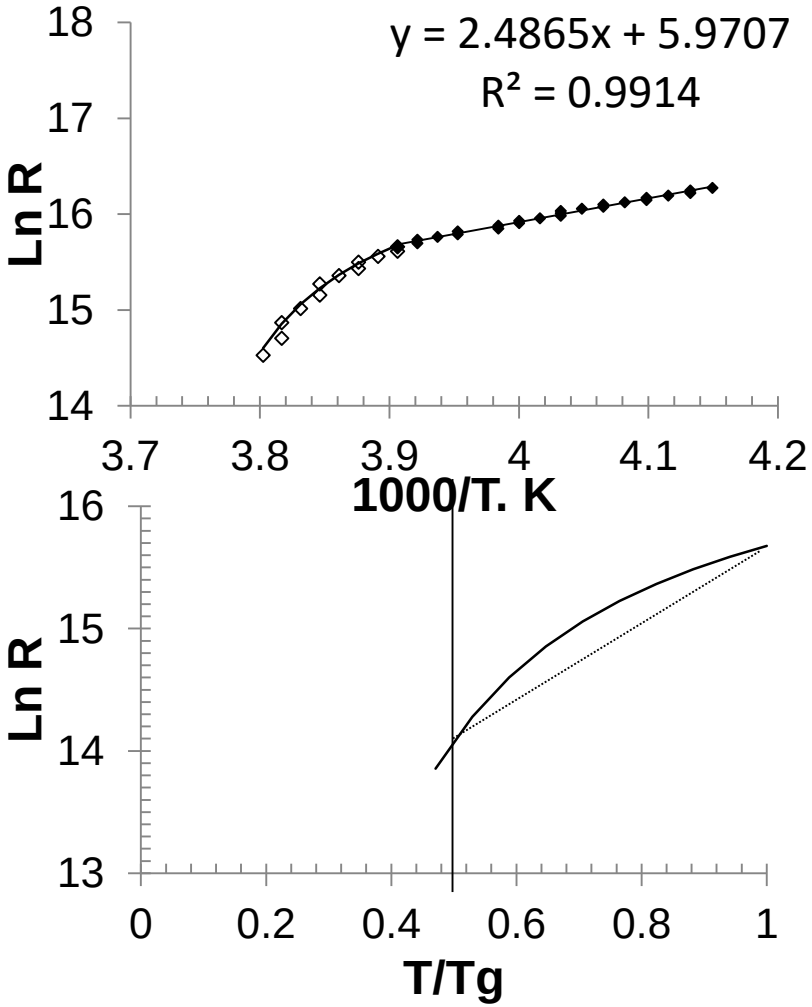

VTF Fit to describe the above Tg' resistance

- Above T_g the temperature dependence of the product resistance follows the Vogel-Tammann-Fulcher function.
- The curvature of the resistance plot decreases following annealing
- which relates to the increased strength of the glassy material.

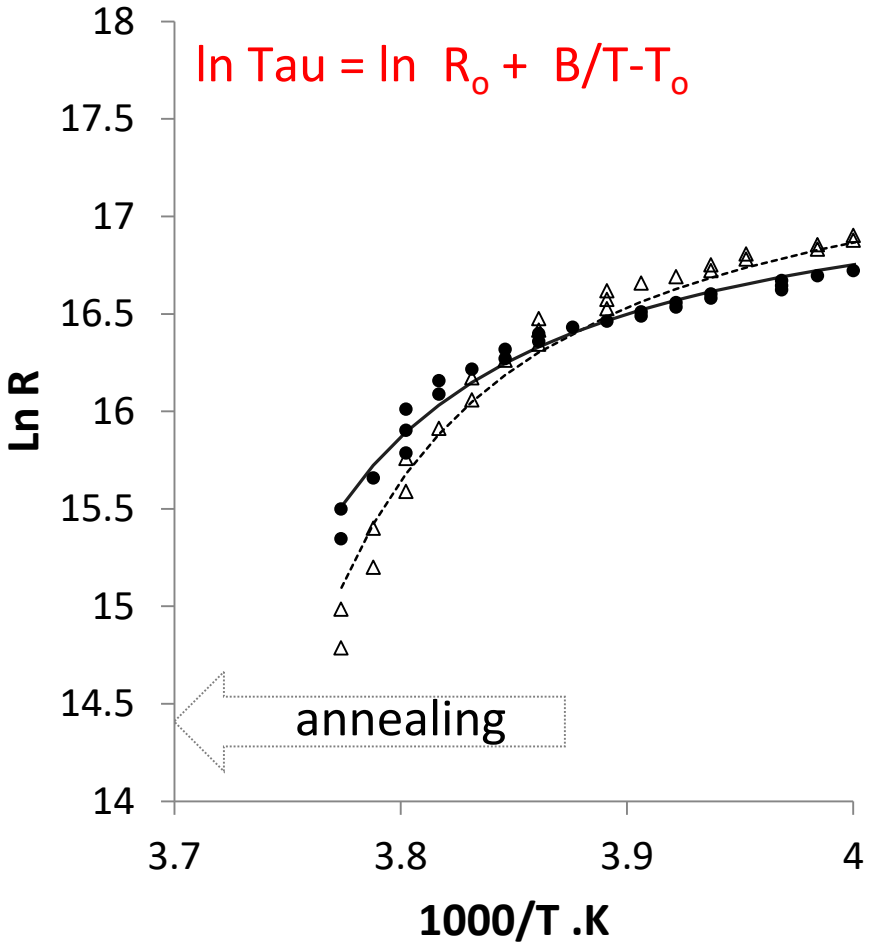

Fragility of different solutions

Solution details	Fragility*
Maltodextrin 10% w/v	0.7
Lysozyme 4.5% w/v	0.8
Lysozyme 4.5 % + trehalose 1.5% w/v	0.6

- The higher the fragility number the more fragile the glass
- A finger print for stability – reproducibility?

Precision of these numbers in relation to relevance requires validation

Pre-heated Lysozyme 4.5% w/v (pre-aggregated)

- Lysozyme solution

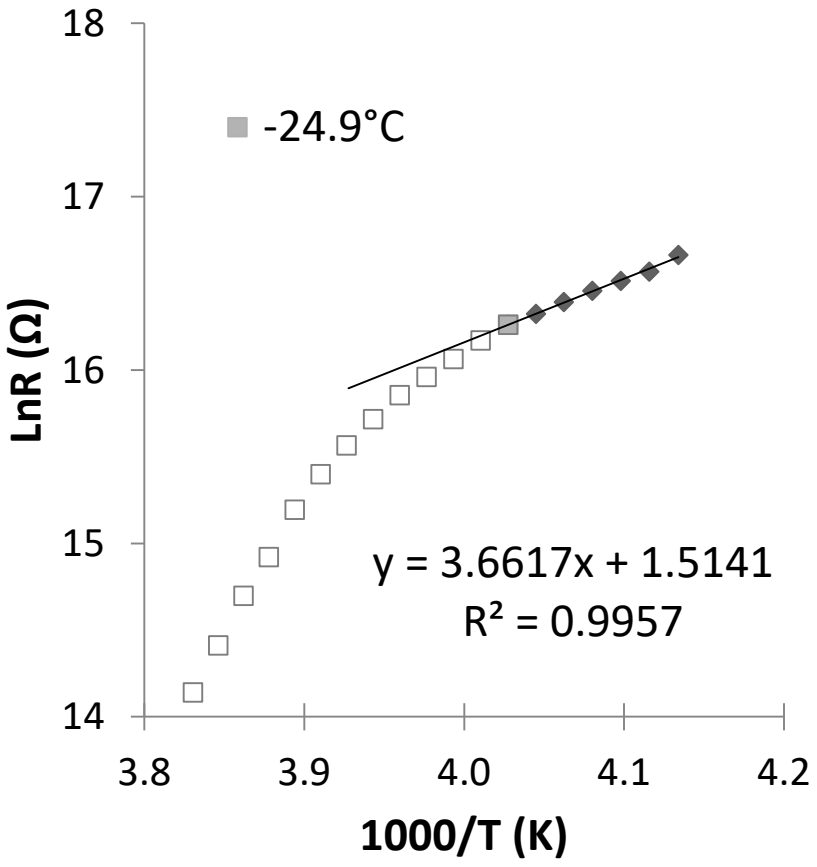

- Pre-heated Lysozyme solution

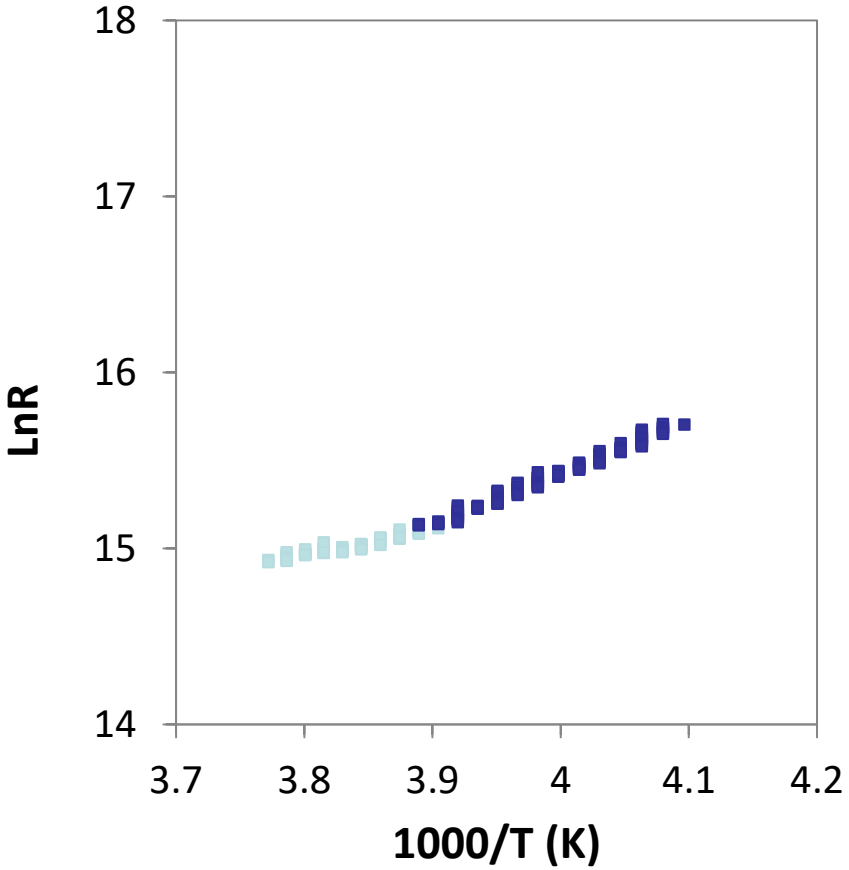

Effect of Sucrose on mannitol crystallization

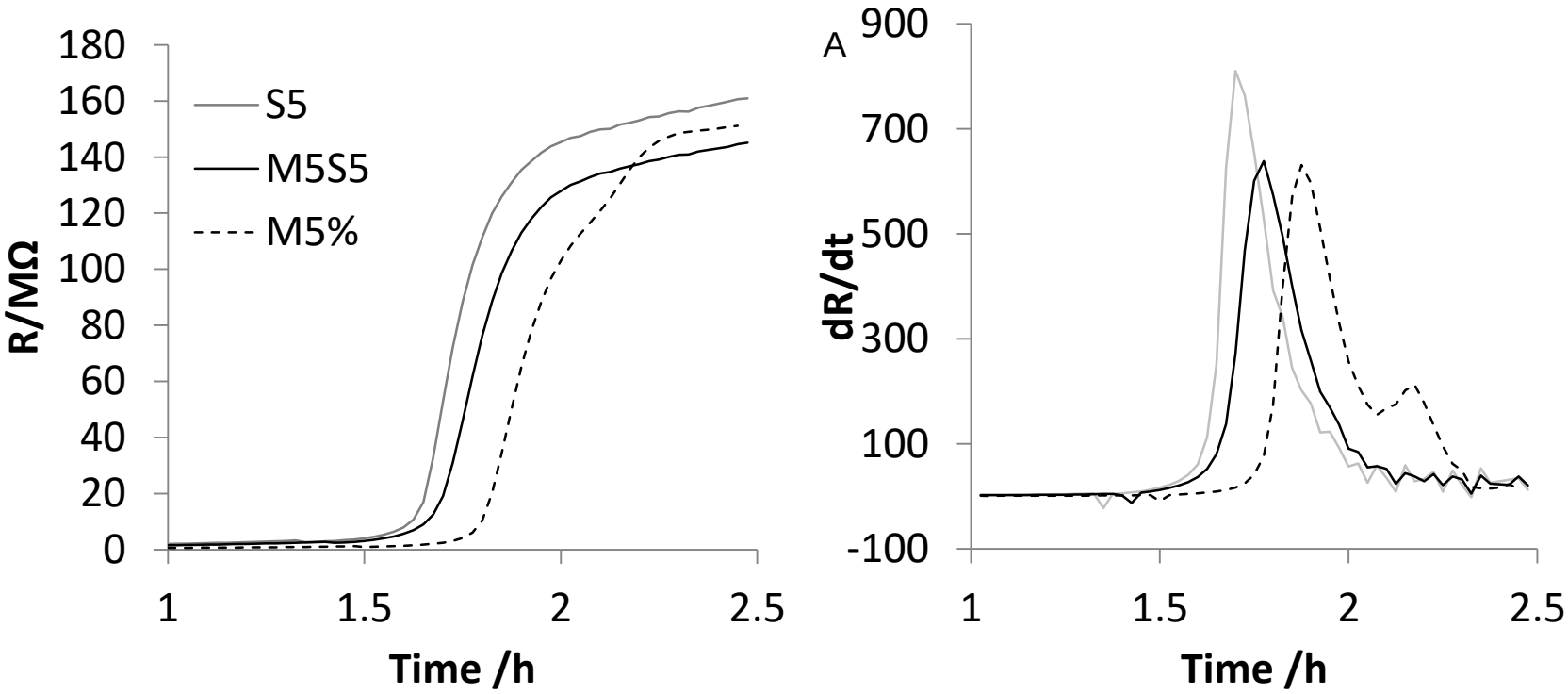

Mannitol crystallization supressed with the inclusion of sucrose in the solution.

PRIMARY DRYING STAGE

The Desired state?

Fast drying rate, without compromising product quality, or operating at limits of equipment

Design Space for Primary Drying

- The aim is to achieve an acceptable drying rate, without
  - compromising product quality
  - operating the equipment at (or beyond) the limits of its capability

- Lab scale instruments for screening formulations and process conditions to optimise drying profiles Microbalance

- PAT and “intelligent” freeze drying software has allowed
  - in process monitoring
  - interactive control of the cycle

PAT in Primary Drying

Methodologies for Production Scale

- pressure rise and MTM (Tang et al *Pharm Res* 2005,22;685-700),
- tunable diode laser absorption spectroscopy (Gieseler et al *J Pharm Sci* 2007,96;1776-93)
- soft sensor probes (Barresi et al *Int J Refrigeration* 2009,32;1003-14)

have enabled critical process parameters (drying rate) to be monitored and used to drive cycle progression and method optimisation.

- Methodologies for Development/lab Scale

  near infra-red & Raman spectroscopy (De Beer et al *J Pharm Sci* 2009,98;3430) to model drying within analytical equipment and to assess stabilization (Hedoux et al *J Pharm Sci* 2013,102;2484-94)

Design Space

- A target sublimation rate can be achieved by two independently controlled variables:

(i) Chamber pressure (shown on the x axis)

(ii) Shelf temperature (shown as a floating variable)

Chang & Fisher 1995

The dotted line is the minimum acceptable drying rate

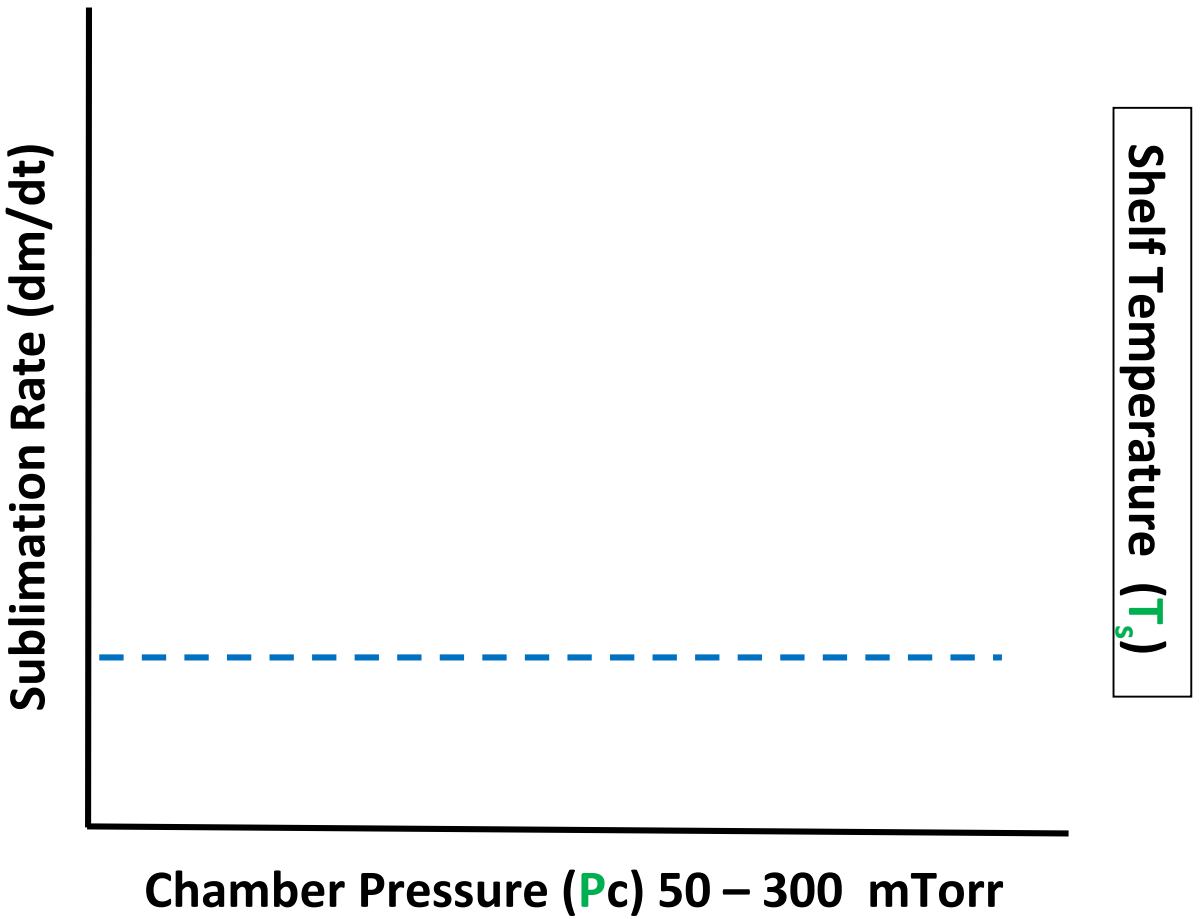

Primary Drying Modelling : Heat and Mass Transfer

$$dm/dt = \frac{A_v(P_i - P_c)}{R_{ps}}$$

$$dq/dt = A_v K_v (T_s - T_p)$$

$$dq/dt = \Delta H_s \, dm/dt$$

$$\ln P_i = -145/T_p + 24.02$$

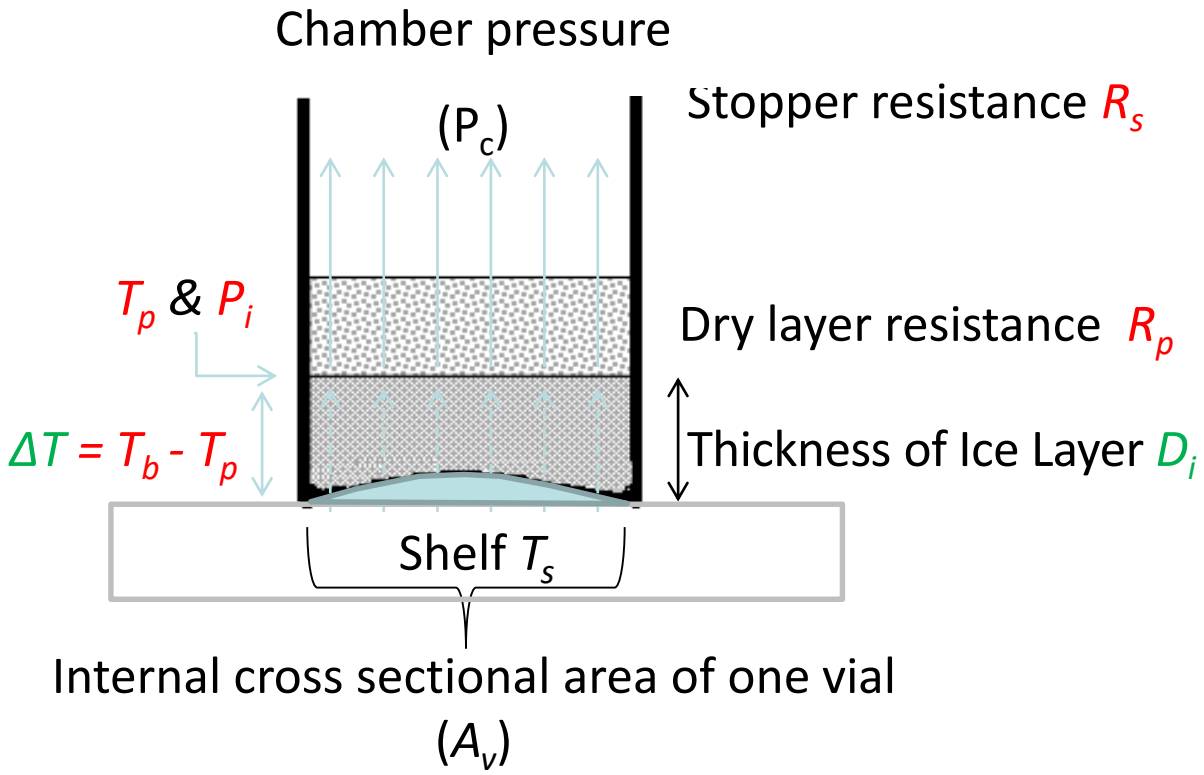

Design Space

$dm/dt \propto (P_i - P_c)$

- **Lower chamber pressures** (P_c) increases the driving force for sublimation

$$dm/dt \propto (P_i - P_c)$$

- Effect seen for a constant ice vapour pressure, P_i
- i.e. A constant product temperature (T_p)
- Linear increase in rate with decreasing chamber pressure

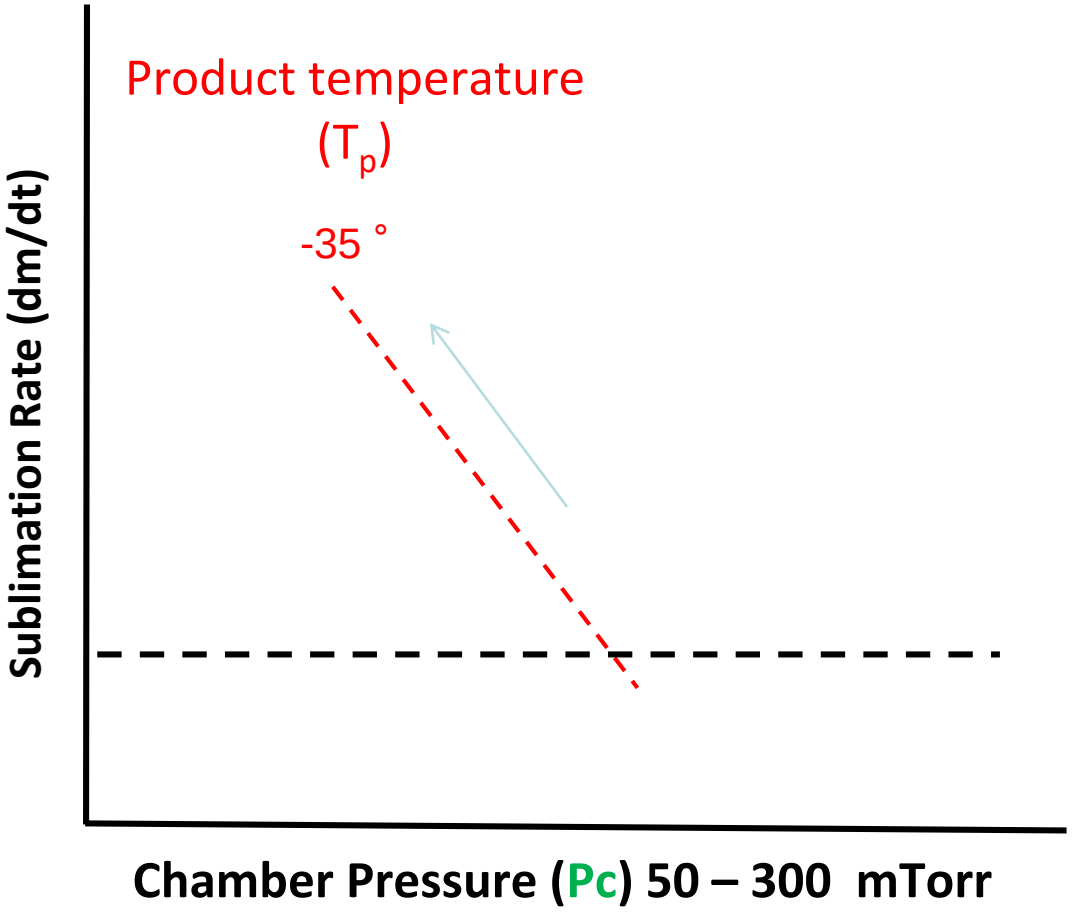

Design Space

$dq/dt = A_v K_A (T_s - T_p)$

$dm/dt = -DH_i \, dq/dt$

- Increases sublimation rates requires greater rate of heating (dq/dt),

$$dm/dt = -DH_i \, dq/dt$$

- which, for a constant product temperature, can only come from increasing the shelf temperature (T_s)

$$dq/dt = A_v K_v (T_s - T_p)$$

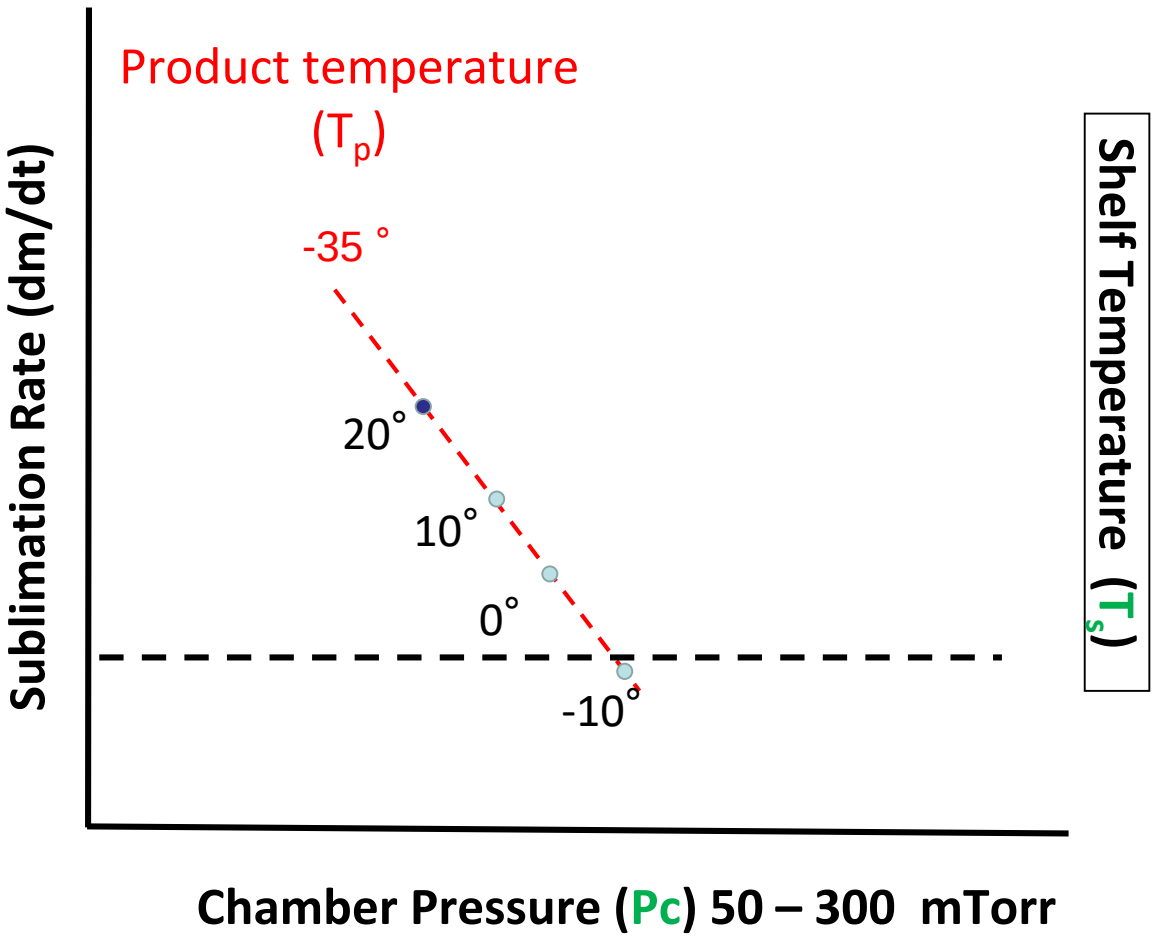

Design Space

$dq/dt \propto K_v K_G$ | $T_p \propto dq/dt$ | $P_i \propto T_p$ | $dm/dt \propto (P_i - P_c)$

- **Higher chamber pressures** also increases rate of heat transfer by increasing the thermal conductance of the gas in the gap between the shelf and the bottom of the vial (K_G)
- This in effect increases the product temperature (T_p) which increases the ice vapor pressure, increasing driving force for flow of vapour in the chamber

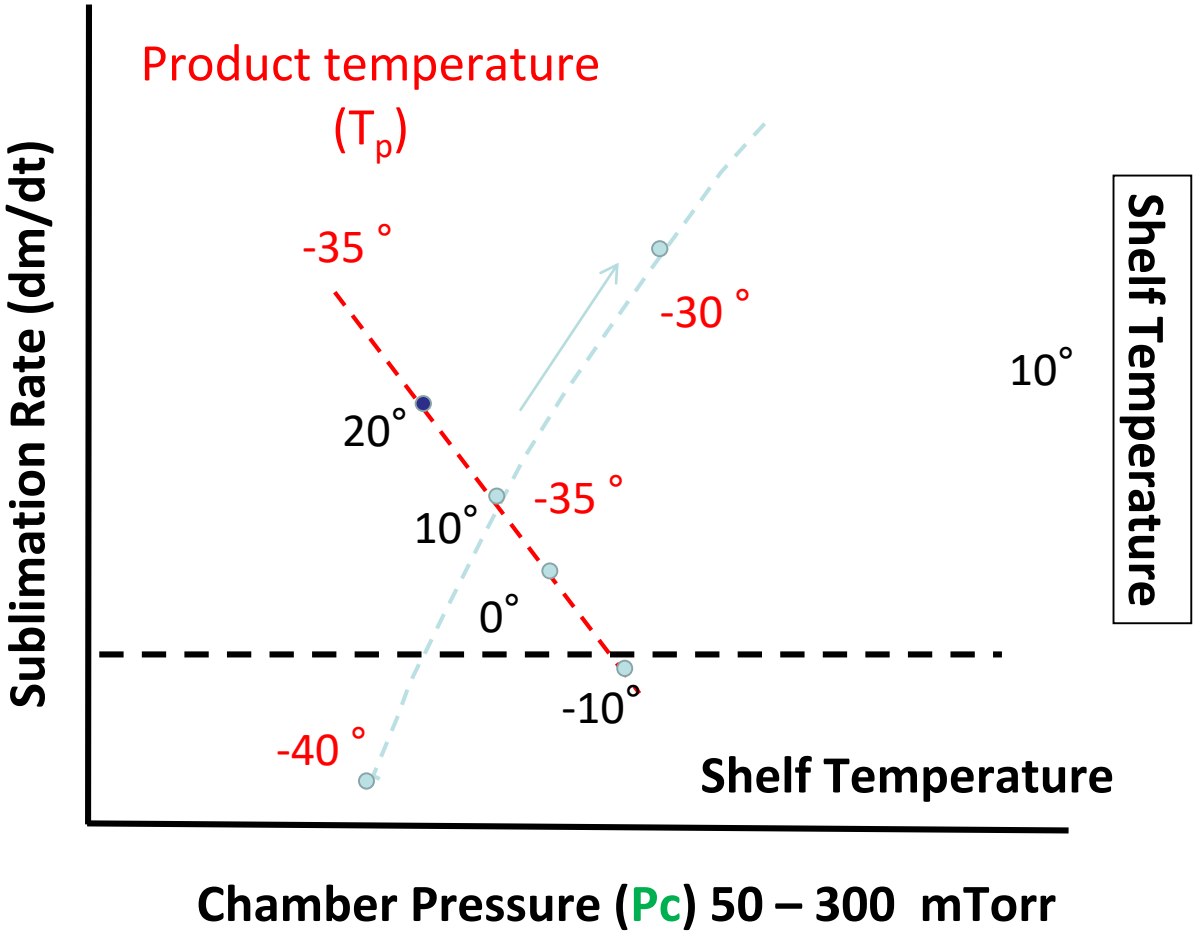

Design Space

$dq/dt \propto K_v K_A$ | $T_p \propto dq/dt$ | $P_i \propto T_p$ | $dm/dt \propto (P_i - P_c)$

Two conflicting driving forces associated with increased chamber pressure

$dm/dt \propto (P_i - P_c)$

AND

$dm/dt \propto (P_i - P_c)$

THE RESULT

$dm/dt \propto P_i$

THE LESSON

Drive process via T_p

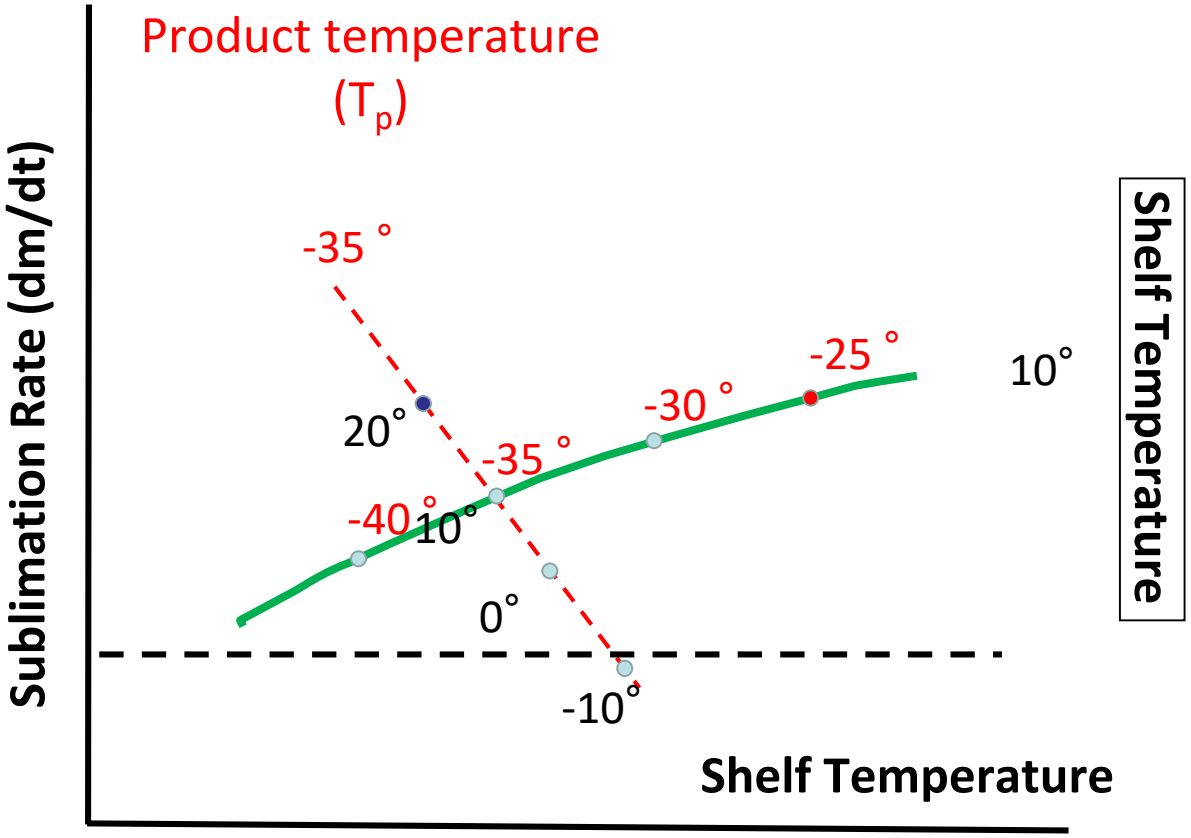

Design Space – Failure Modes

There are two failure points resulting from

(i) Formulation

(ii) Equipment

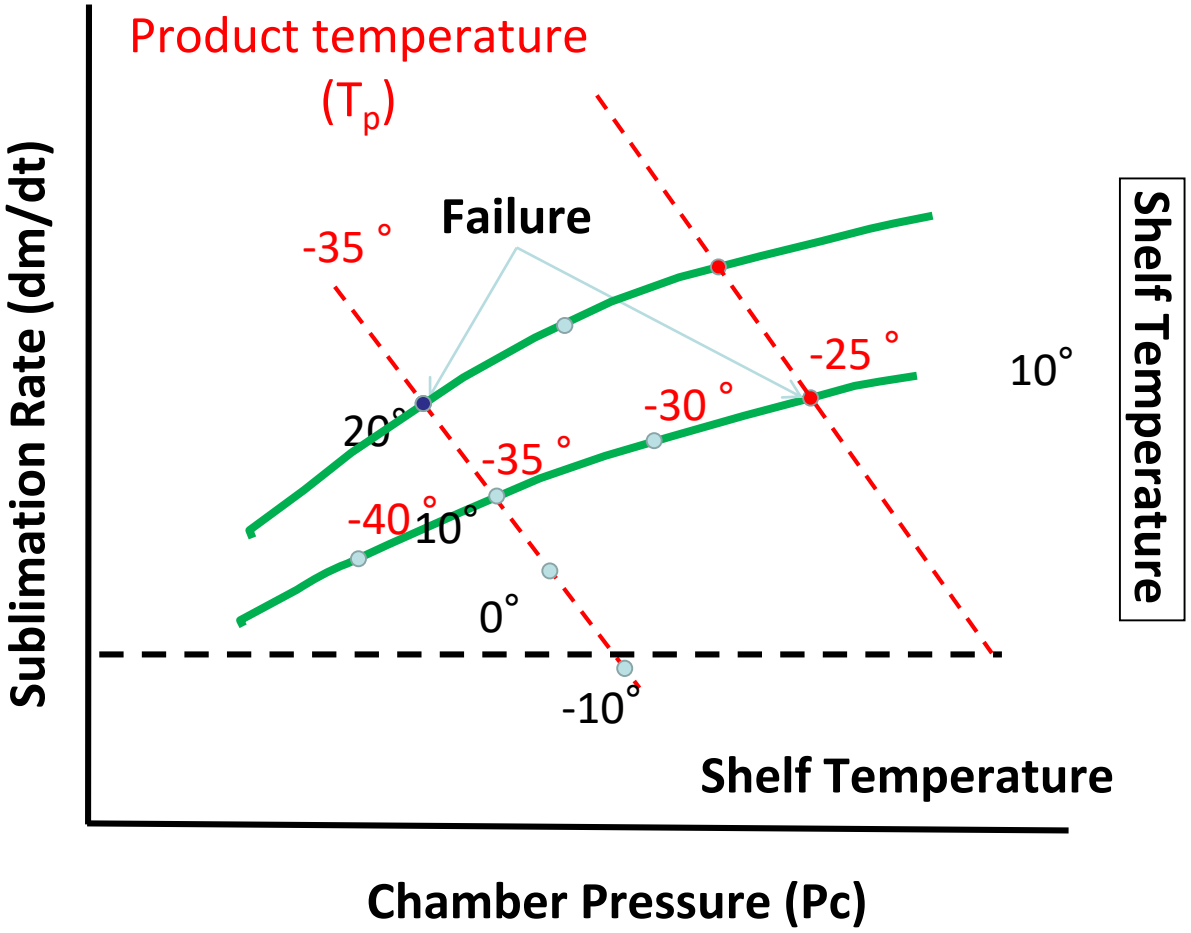

Design Space

There are two failure points resulting from

(i) Formulation

(ii) Equipment

Formulation Limits

If the product exceeds its a critical temperature at which the viscosity of the unfrozen matrix is too low to support its weight then it collapses (e.g. -25 C)

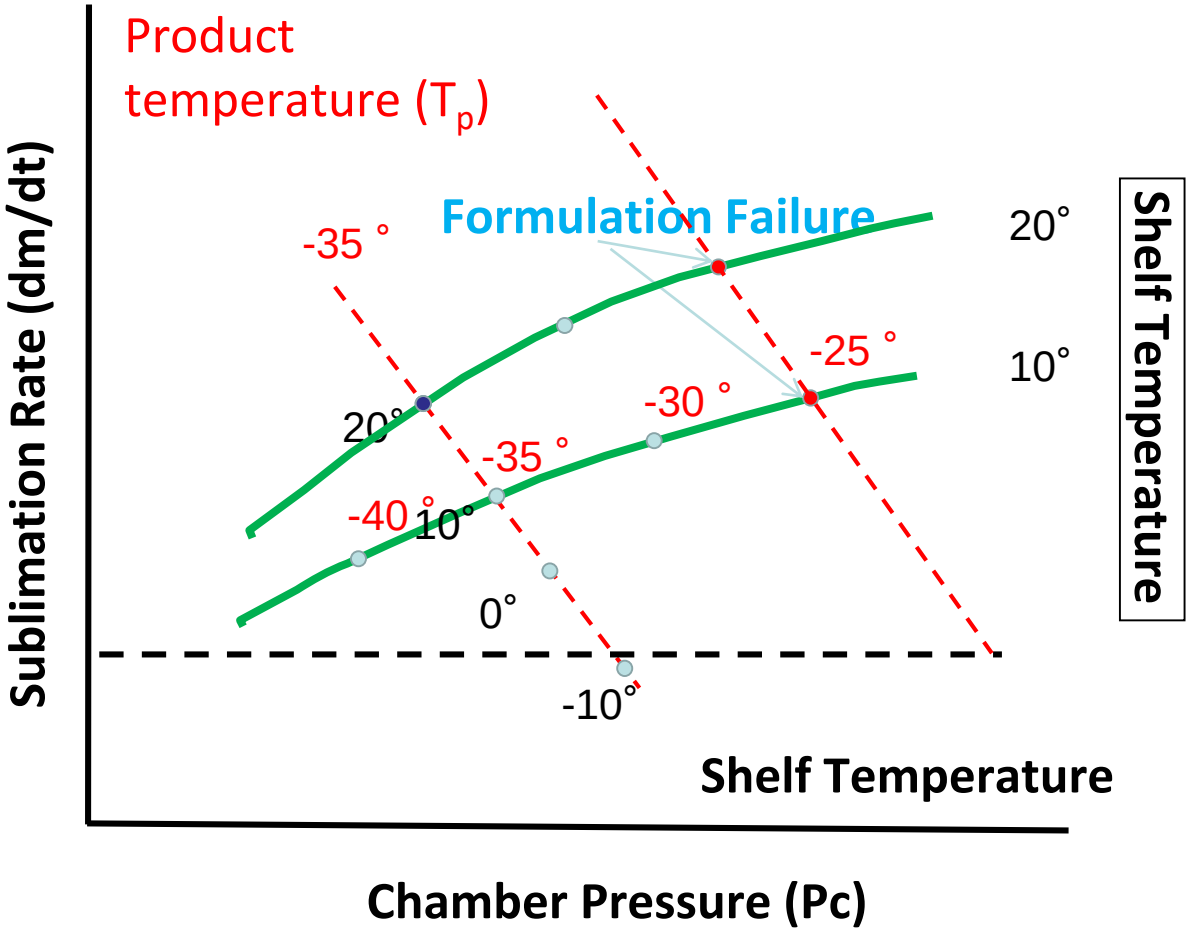

Design Space

There are two failure points resulting from

(i) Formulation

(ii) Equipment

Equipment Limits

Condenser capacity to trap ice and maintain its temperature

Shelf coolant capacity to maintain its temperature

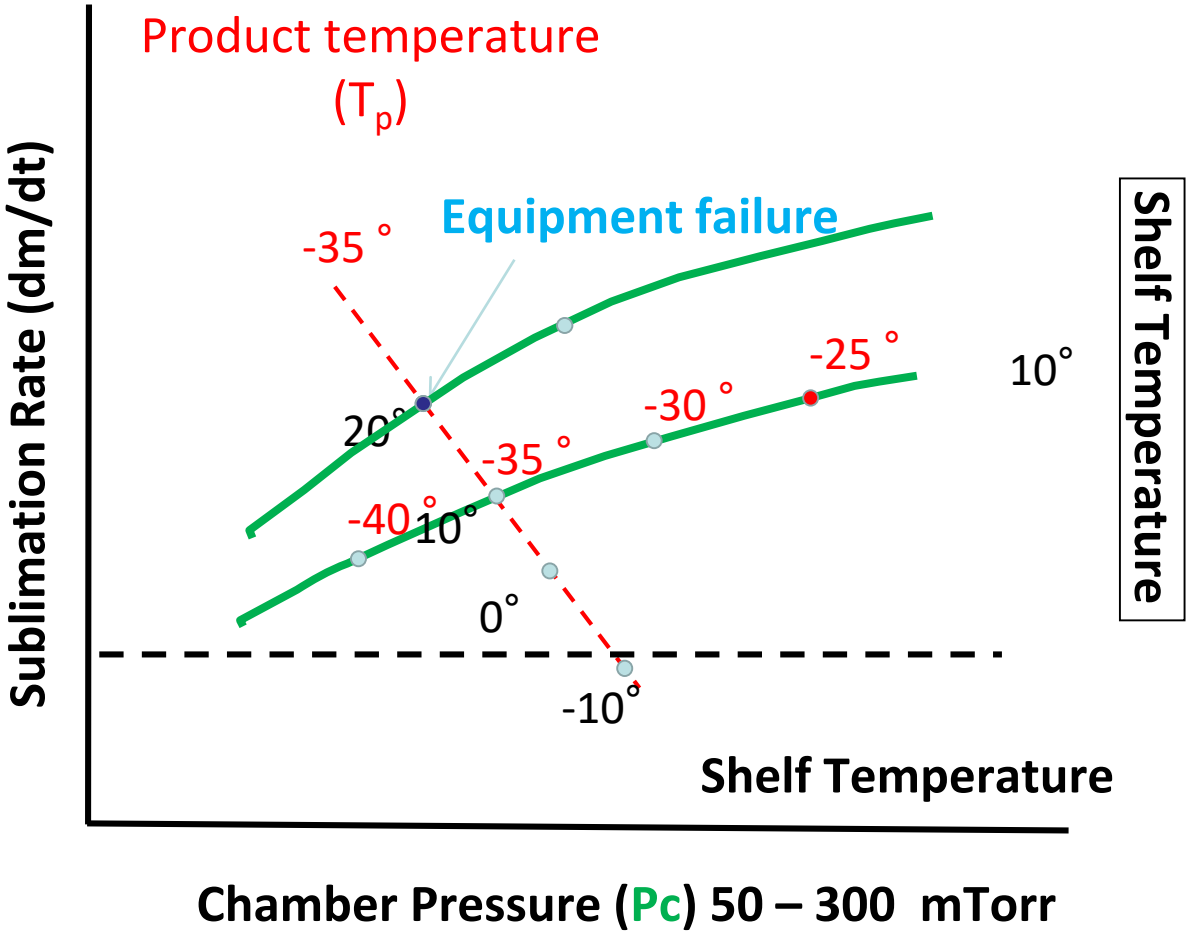

Design Space-Choked flow

$$dm/dt \propto (P_i - P_c) = 0$$

With aggressive drying the sublimation rate is eventually suppressed by the maximum volume of water vapour which could traverse from chamber to condenser in unit time

$$P_i \approx P_c$$

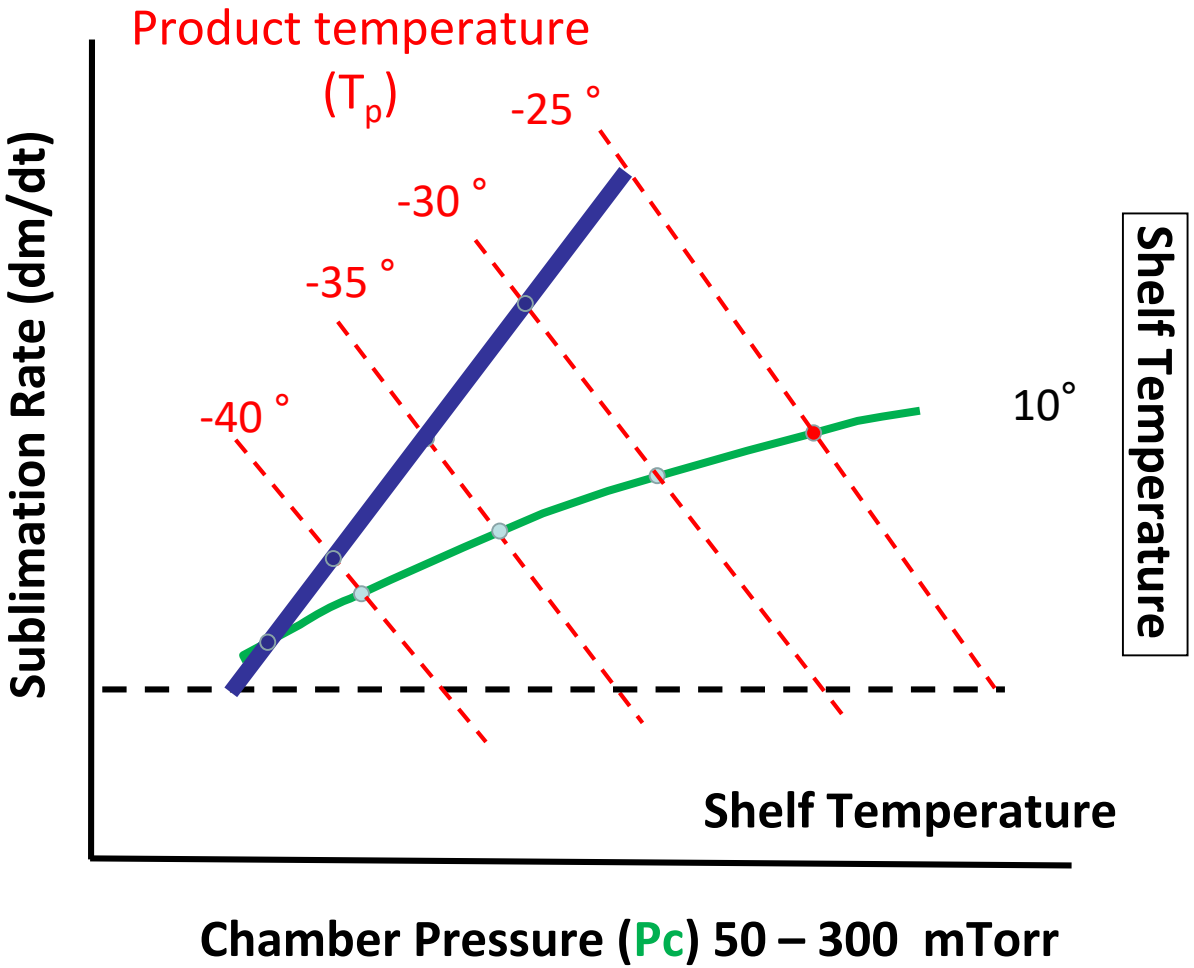

Design Space-Choked flow

$$dm/dt \propto (P_i - P_c) = 0$$

Similar effects have been observed with the physical spacing of the shelves in a stack can also pose a resistance to the increasing sublimative flow,

with pockets of greater chamber pressure building up between narrowly separated shelves and limiting the effective drying rate.

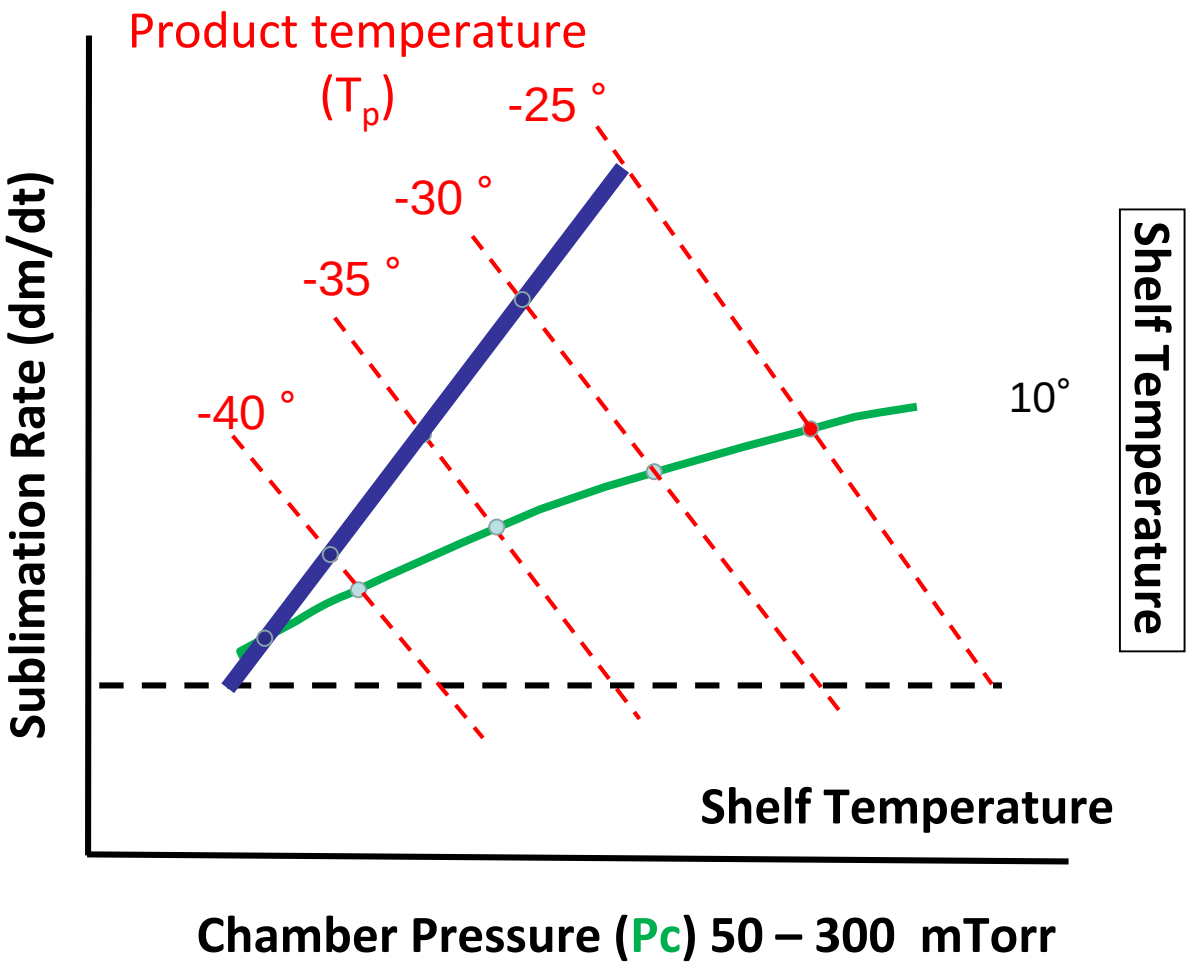

Design Space

Complete the DoE!!

Using a range of chamber pressures and shelf temperatures to establish the limits of the equipment

The design space is shown by the yellow triangle

Operate at the apex of the triangle to drive process efficiencies

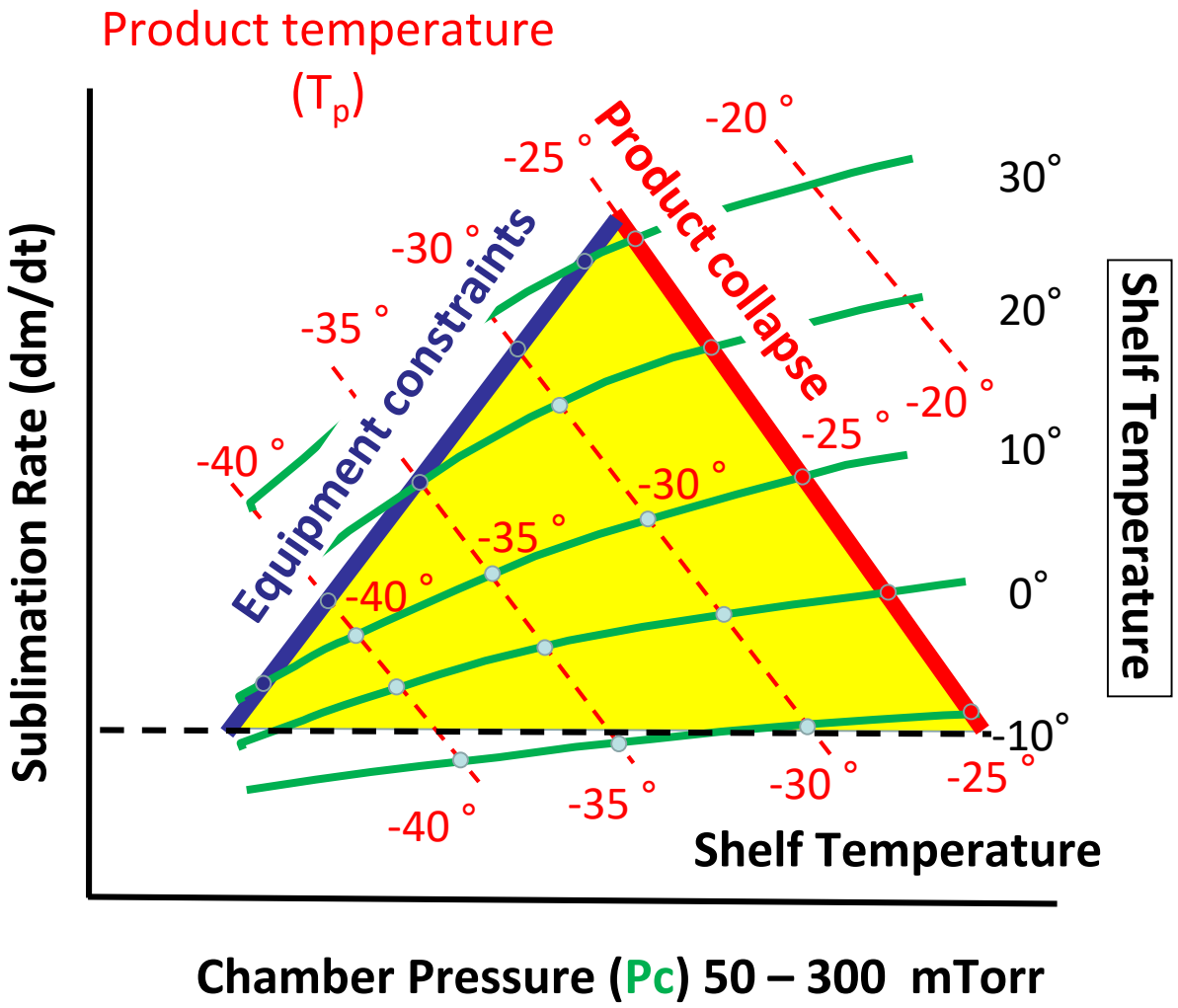

$$P(t) = P_i - (P_i - P_c)\exp\left(-\frac{3.461NvA_vT_s}{V_c(R_p + R_s)}t\right) + 0.0465P_i\Delta T\left[1 - 0.811\exp\left(-\frac{0.114}{D_i}t\right)\right] + Xt$$

$$D_i(t) = \frac{m(0) - m(t)}{\varrho_i A_p \varepsilon}$$

$$\Delta T = T_b - T_p = [24.7\, L_{ice}(P_0 - P_c)/(R_p + R_s) - 0.0102 L_{ice}(T_s - T_p)]/1 - 0.0102 D_{ice}$$

Measure pressure rise $P(t)$

Calculate Ice vapour pressure at sublimation front P_i And resistance to vapour flow $R_{ps} = R_p + R_s$

Calculate Product temperature at sublimation front T_p

$$\ln P_i = (-144.96/T_p) + 24.0189$$

Calculate Product temperature at base of line T_b

$$T_b = \frac{dq/dt}{A_v K_I} D_i + T_p$$

Set Shelf Temperature Ts

$$T_s = T_p + \frac{1}{A_v}\frac{dQ}{dt}\left(\frac{1}{K_v} + \frac{D_i}{K_I}\right)$$

Calculate Mass transport dm/dt

$$dm/dt = A_v(P_i - P_c)/R_{ps}$$

Calculate Thermal coefficient of vial k_v

$$dq/dt = A_v K_v (T_s - T_b)$$

Calculate Mass transport dq/dt

$$dq/dt = (dm/dt)H_s$$

Limitations Smart freeze drying

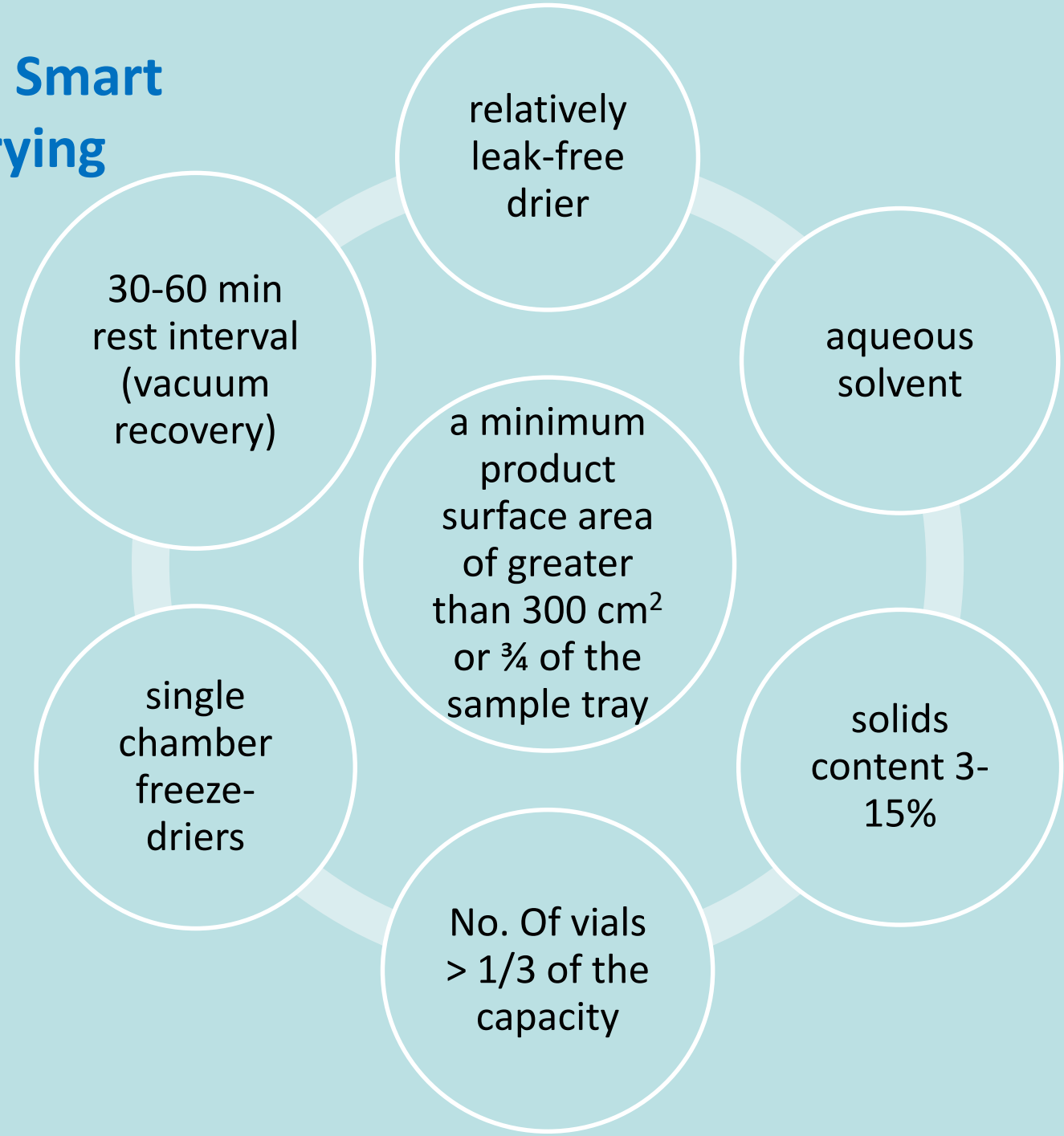

Product Characterization : phase behaviour, temperature

- The f_{peak} showed a good correlation with the product temperature during product cooling (A), freezing (B) and thawing (C)
- Provided there is no change in phase, then a linear correlation exists between Log F and temperature (A, C-D)
- Use LyoDEA response to drive the process

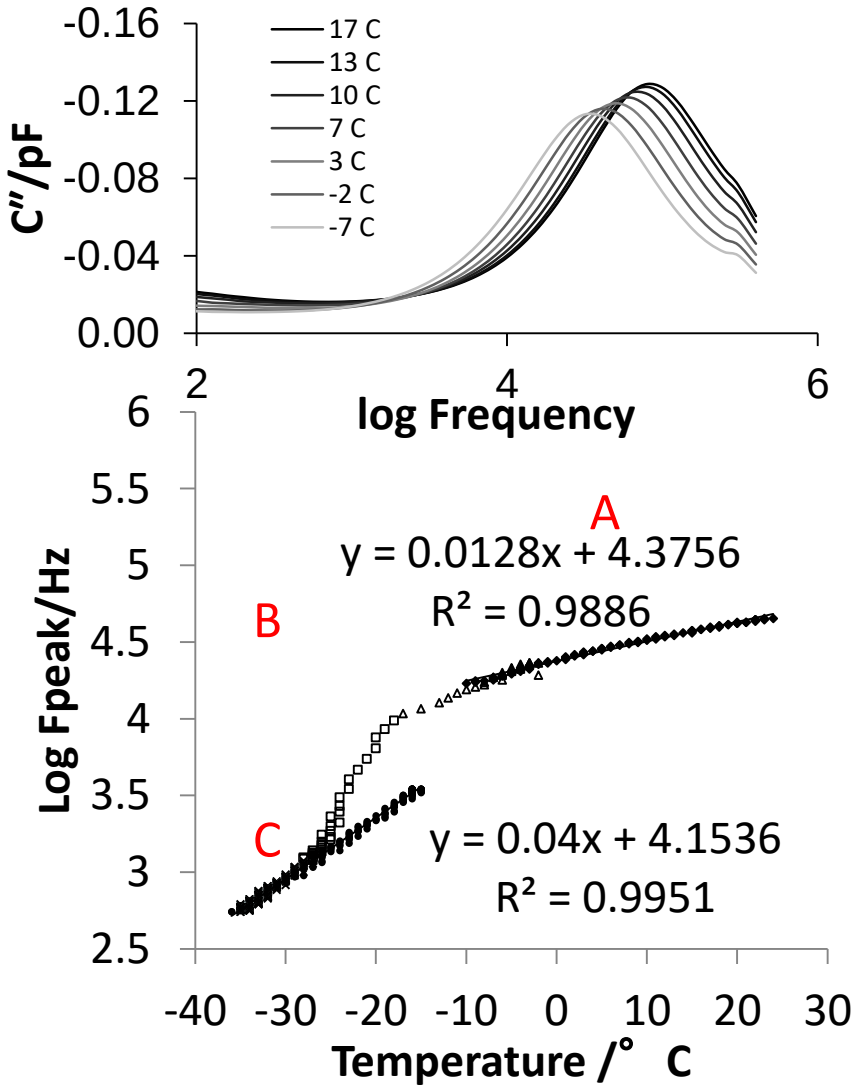

Lactose 3%

- In some cases the maximum in the derivative corresponds to the point at which the ice front has receded to 50% of the height of the product (in the case of lactose)

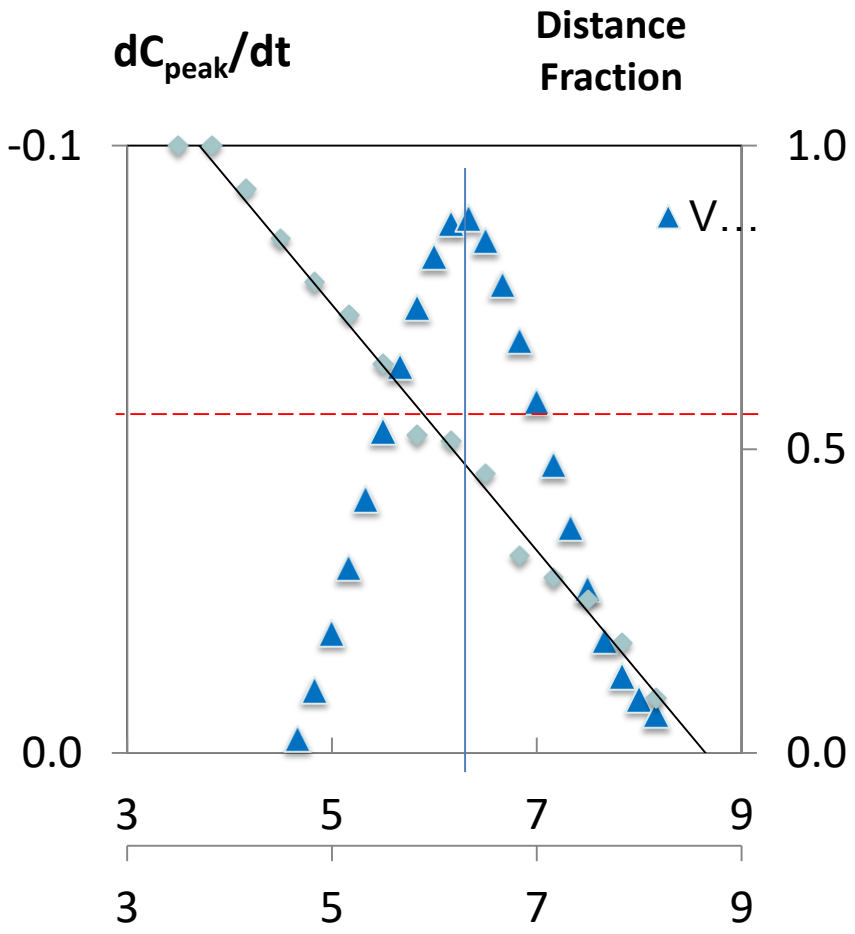

Sucrose 3%

- In other case the maximum in the derivative corresponds to the point at which the external ice front has receded to 100% of the height of the product (in the case of sucrose
- Can these observation be used to indicate/inform the user about the flatness of the drying front?
- In all case the approach of the derivative to a value of zero indicates the end of the primary drying process.

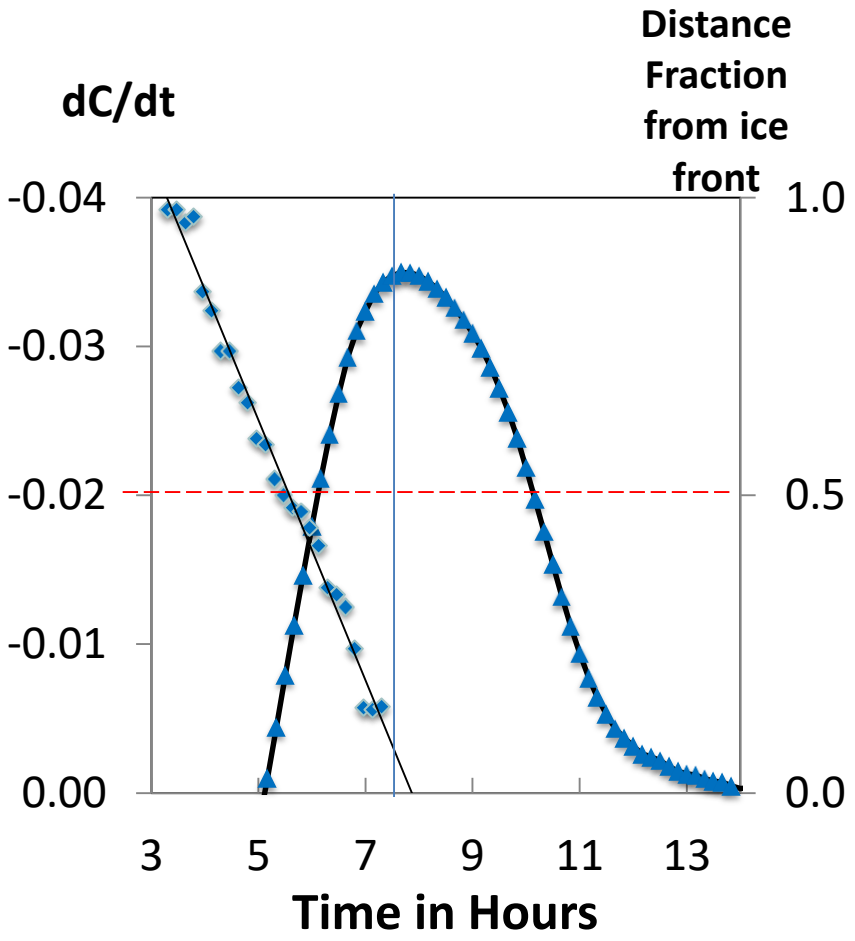

End Point Determination

- Impedance measurement data from sucrose 2.5% w/v were analysed for the determination of primary drying end point.
- Time slice of the imaginary capacitance at 1kHz showed a sharp decline as the ice sublimation was complete.

Results: Defining the End of Primary Drying

LyoDEA offers a non invasive measurement of primary drying time which is in good agreement with the thermocouple.

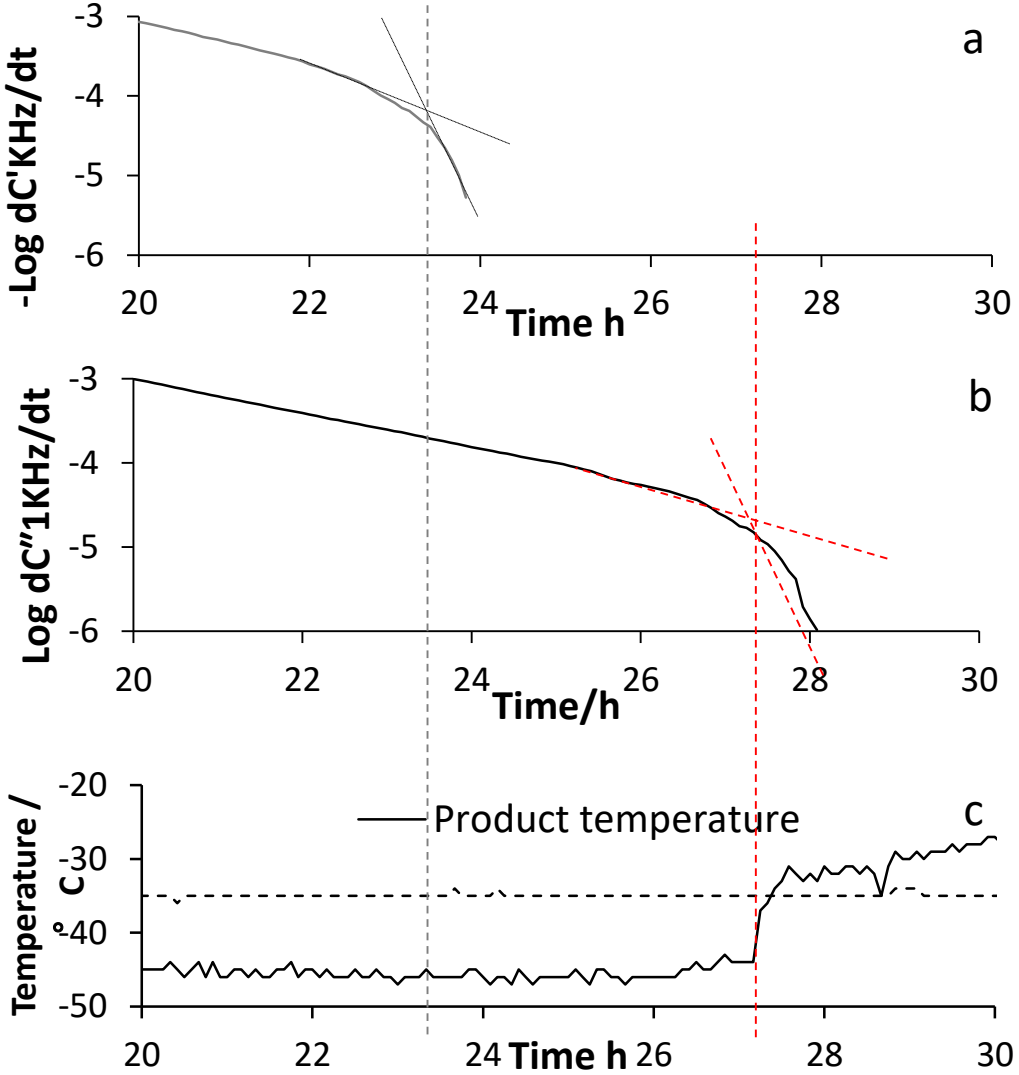

Shelf temperature distribution: Spatial mapping

- The temperature variation measurement during freezing stage.
- Thermocouple measurements of vials filled with oil.
- Gray scale shows minimum-maximum during freezing.
- ΔT ~ 1-2 ° C across shelf can affect ice formation (already stochastic) and impact drying time
- 1 ° C increase in 1° drying T can shorten drying time by ~13%

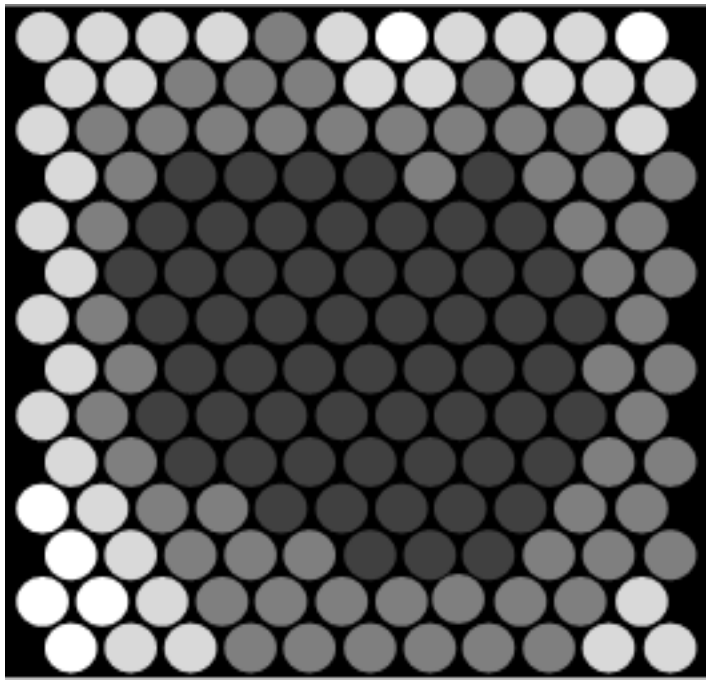

Impact of Spatial Temperature Map on Ice Formation

- Ice crystallization rates can impact the amount of ice and the particle size

Leading to variations in:

1. drying rates (because of the impact on the resistance to vapour flow, R_p)
2. concentration on solutes in the unfrozen fraction, which impacts T_g which impacts the primary drying temperature.

F Rate	Ice Crystal Size	R_p	Unfrozen fraction
Fast	Small	High	High
Slow	Large	Low	Low

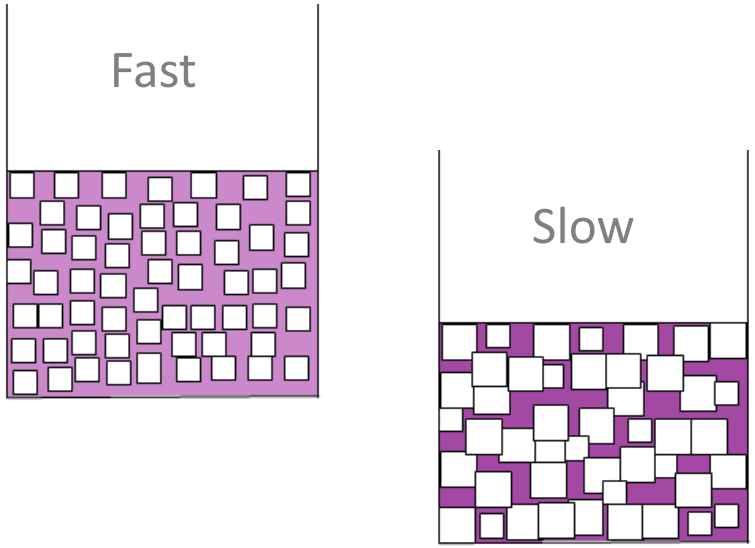

LyoDEA Spatial mapping: Primary drying times

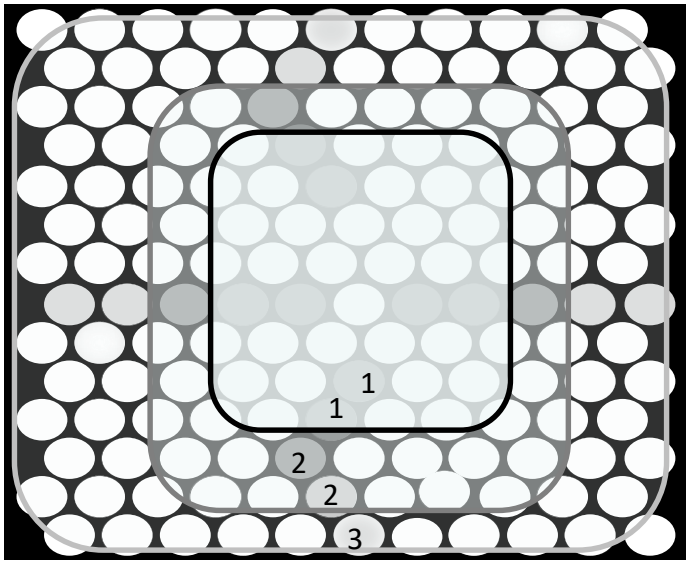

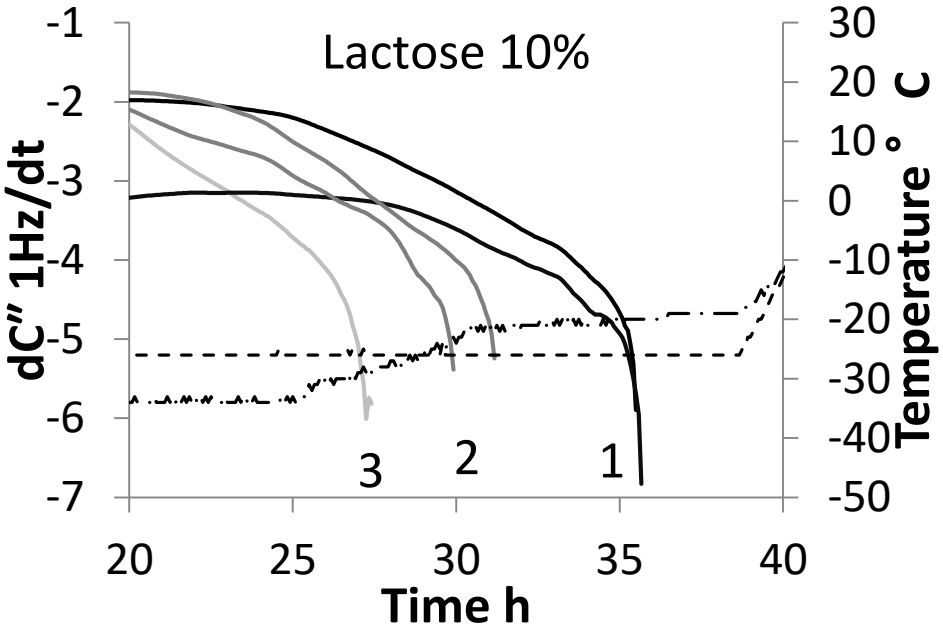

1. Primary drying time distribution across the shelf identifies three distinct spatial regions characteristic of thermal variations in the shelf.
2. Edge effects – may extend across three vials around the periphery of the shelf

Product Collapse

- Conventionally measured by cryo-microscopic images

Sublimation front

Collapsed product

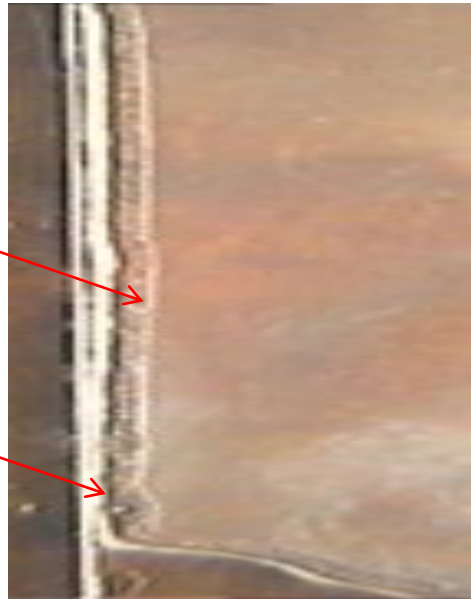

Microscopic images may not account for increase in the vapor pressure at sublimation front ,following increased resistance to vapor flow during the later stage of primary drying; potentially vulnerable to collapse

Collapse measurement within the real conditions may provide such information

Sample lactose 10% w/v

LyoDEA: Product collapse

A sharp spike in the capacitance profile at 1 kHz characterizes the product collapse

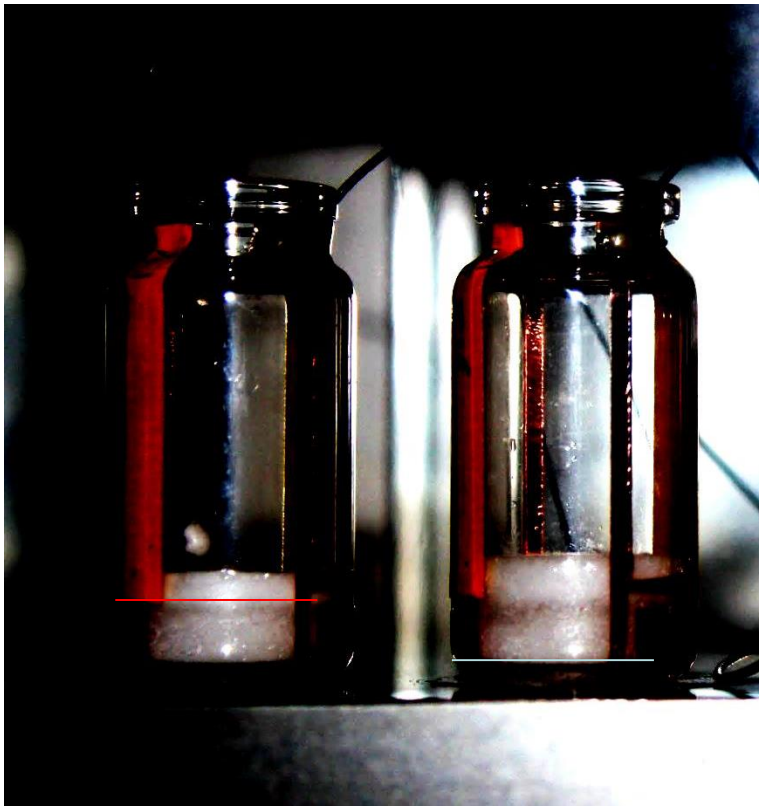

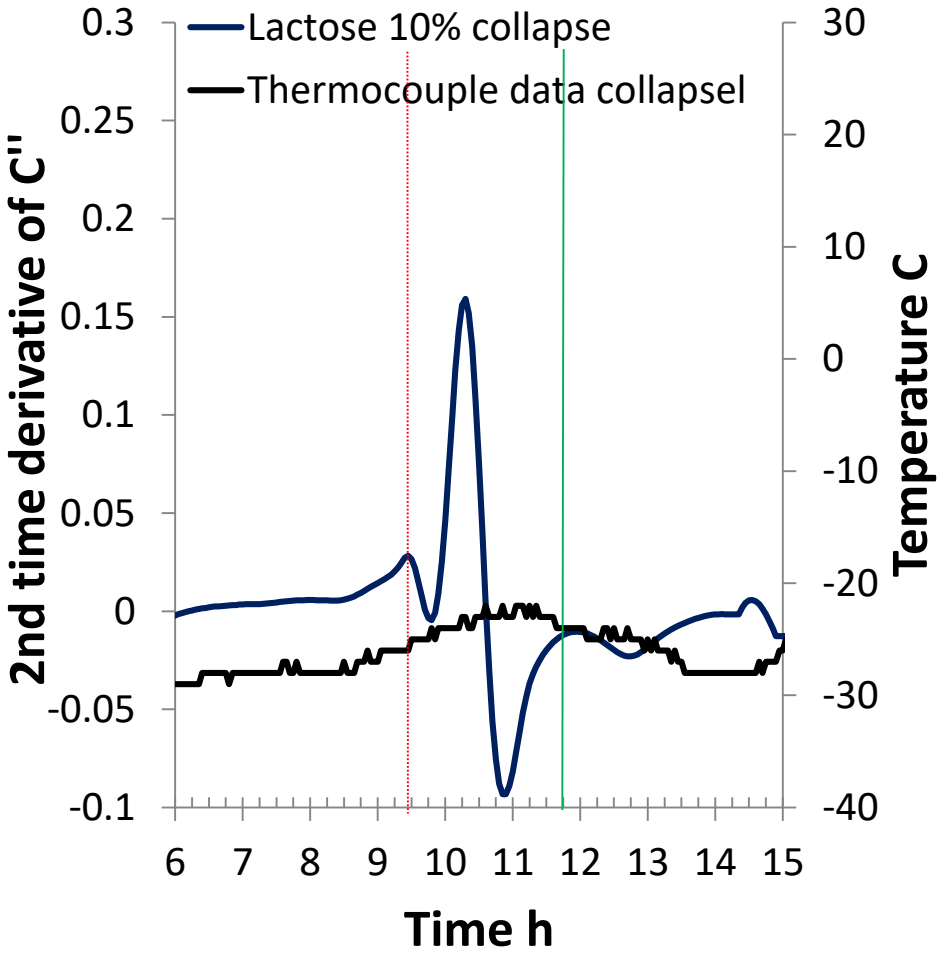

Lactose 10% Collapse : 2nd derivative

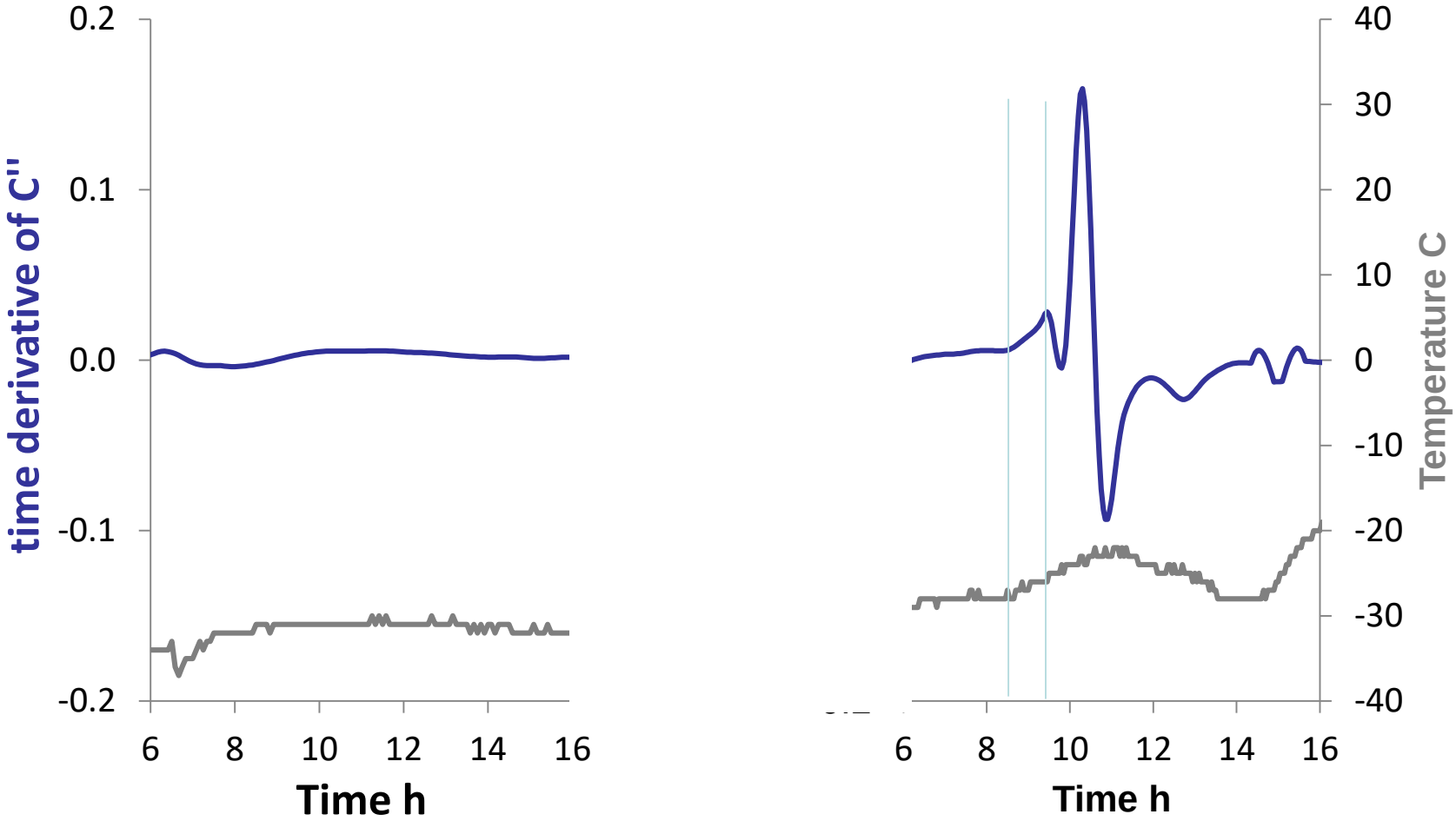

the capacitance profile of collapse free product (LEFT) was seen to be fairly uniform, un-like the collapsed product (RIGHT)

Acknowledgements

- **Paul Matejtschuk** (NIBSC)
- **Tim McCoy** (Genzyme)
- **Sohail Arshad** (Bahauddin Zakariya University, Multan, Pakistan)
- **Evgeny Polgalov** (DMU)
- **Irina Ermolina** (DMU)

LyoDEA References

- Arshad, M.S. Smith, G., Polygalov, E., Ermolina, I. (2014). Through-vial impedance spectroscopy of critical events during the freezing stage of the lyophilization cycle: The example of the impact of sucrose on the crystallization of mannitol. Eur J Pharm Biopharm., 87 (3), pp. 598-605
- Smith, G., Arshad, M.S., Polygalov, E., Ermolina, I. (2014). Through-Vial Impedance Spectroscopy of the Mechanisms of Annealing in the Freeze-Drying of Maltodextrin: The Impact of Annealing Hold Time and Temperature on the Primary Drying Rate. J Pharm. Sci., 103 (6), 1799-1810
- Smith, G., Polygalov, E., Arshad, M.S., Page, T., Taylor, J., Ermolina, I. (2013) An impedance-based process analytical technology for monitoring the lyophilisation process. International Journal of Pharmaceutics, 449 (1-2), pp. 72-83
- Smith, G., Arshad, M.A., Polygalov, E., Irina Ermolina, I. (2013) Factors Affecting the Use of Impedance Spectroscopy in the Characterisation of the Freezing Stage of the Lyophilisation Process: the Impact of Liquid Fill Height in Relation to Electrode Geometry. AAPS PharmSciTech, online first
- Smith, G., Arshad, M.S., Polygalov, E. and Ermolina, I. (2013) An application for impedance spectroscopy in the characterisation of the glass transition during the lyophilization cycle: The example of a 10% w/v maltodextrin solution. European Journal of Pharmaceutics and Biopharmaceutics, 86 (3 Part B), pp. 1130-1140

BIOSTART

An Innovate UK Collaborative R&D Programme

GEA Pharma Systems

DE MONTFORT UNIVERSITY LEICESTER

genzyme
A SANOFI COMPANY

bluefrog
design

NIBSC
Confidence in Biological Medicines

Medicines and Healthcare Products Regulatory Agency

Overview

- Highlight from the CDER PAT guidance document (2004)
- Brief overview of scale lengths
- Features and limitations of existing PAT
- Through Vial Impedance Spectroscopy (TVIS): Overview
- TVIS Applications & Challenges
  - Ice formation
  - Phase behaviour (T_{EU} and T_G)
  - Annealing & structural relaxation
  - Various scales (freeze-drier heterogeneity, ice front shape)
- TVIS Future developments

Process Analytical Technology

The desired state of pharmaceutical manufacturing and regulation may be characterized as follows:

- Product quality and performance are ensured through the design of effective and efficient manufacturing processes
- Product and process specifications are based on a mechanistic understanding of how formulation and process factors affect product performance
- …….. Etc

This defines the role for PAT in the concurrent development of the product and process (and not just for manufacturing controls)

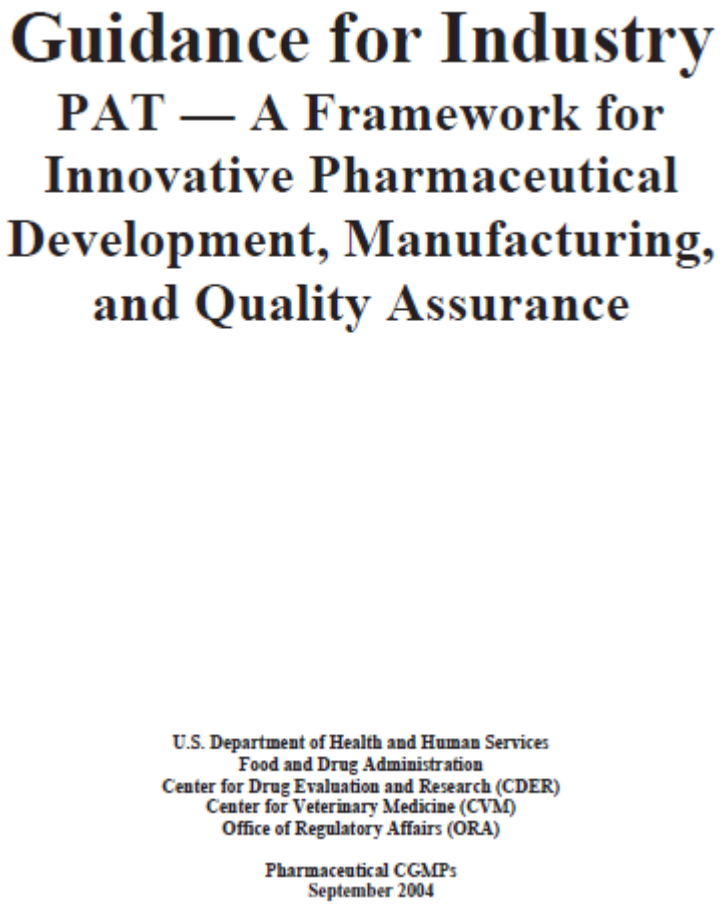
Guidance for Industry

PAT — A Framework for Innovative Pharmaceutical Development, Manufacturing, and Quality Assurance

U.S. Department of Health and Human Services
Food and Drug Administration
Center for Drug Evaluation and Research (CDER)
Center for Veterinary Medicine (CVM)
Office of Regulatory Affairs (ORA)

Pharmaceutical CGMPs
September 2004

Scale of Scrutiny

Nano
(0.1 – 100 nm)
Molecules, macromolecules, nano-particles
CQA : drug stability

Macro-bulk
(cm to m)
Vials (individual & clusters)
engineering scales
CPP:
Temperature & drying rate distributions

Meso 1
(1 nm – 1 µm)
short range order/fractality
co-operativity (CRR) & dynamics,
microviscosity, phase separation
CPP : T_G, T_C

"Meso 2"
(100 µm to cm?)
Pore connectivity
CPP:
dry layer resistance

Micro-bulk
(1 – 50 µm)
- crystal size/shape distributions
- crystal habit
-enthalpy of fusion

CPP : T_{EU}

Mesoscale in amorphous systems

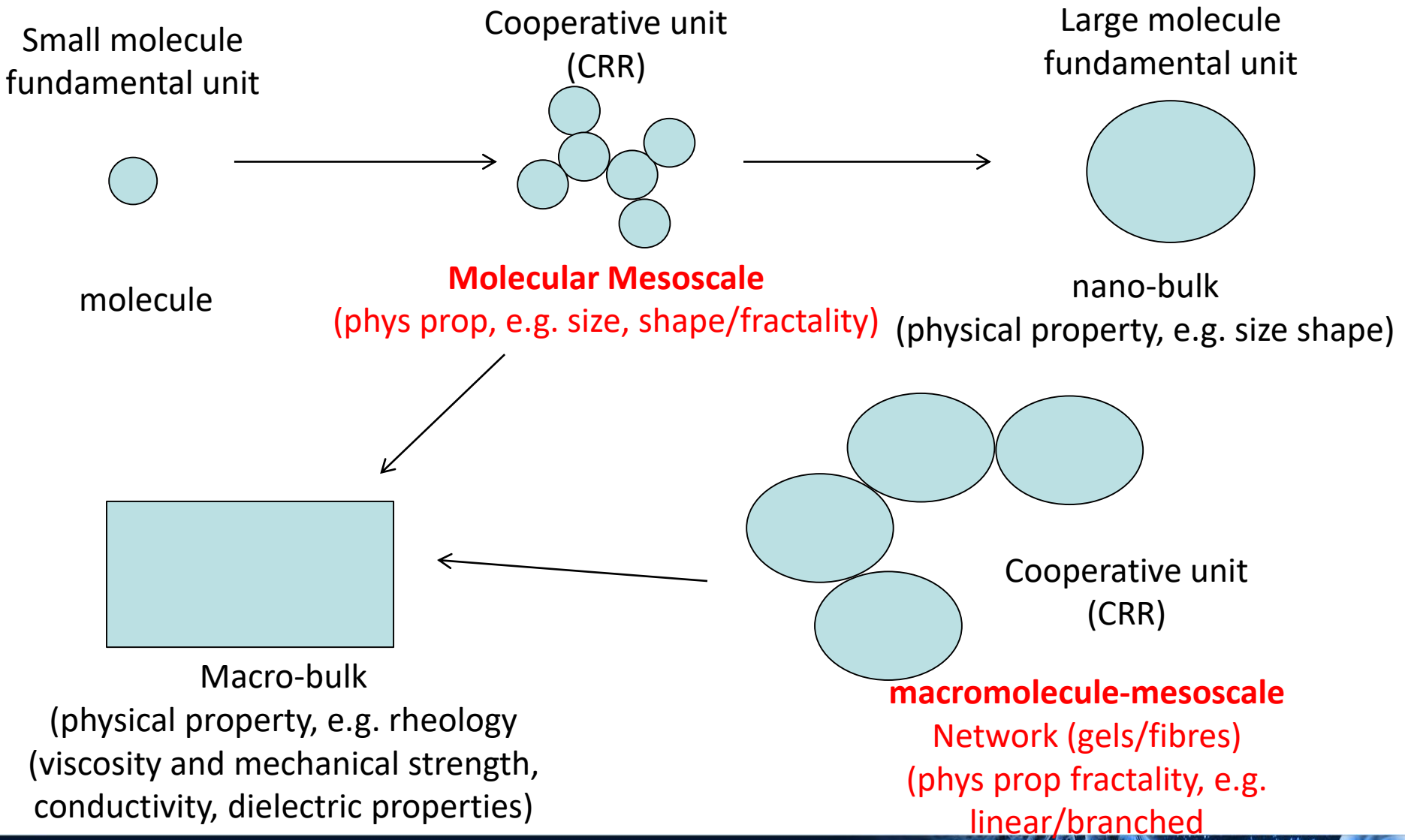

Mesoscales in crystalline materials

fundamental unit

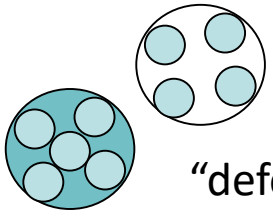

"defect" cell

Unit cell

Defect pathway

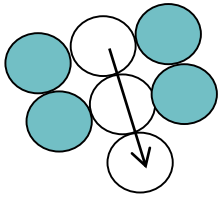

MS 1 : Molecular mesoscale

fundamental unit "crystal"

Nano-micro-bulk
(e.g. ice conductivity, Shape/size)

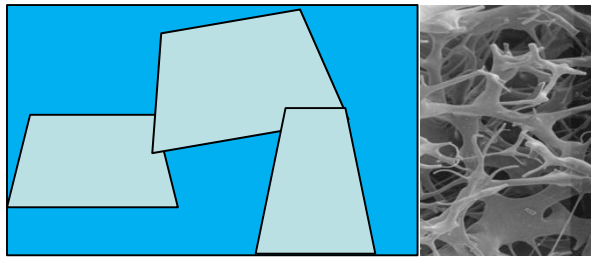

MS 2 "particle-mesoscale"
Percolation pathways, fractality (networks)

sublimation

Macro-bulk
(e.g. porosity, dry layer resistance, shape of drying front, temperature profiles)

PAT and scale length

- PAT can be in-line or off-line (e.g. of the later : DSC and FDM)
- The classic distinction is to divide in-line PAT methods into those applicable to single vials and those that measure the batch

Single vial techniques are for localised measurements

- **Thermal Information** TC & RTD provide pin point measurements of temperature (more suited to small scale R&D if wired sensors, wireless can be used at larger scale)
  - multiple sensors are required to monitor distributions of temperature within an individual vial or across populations of vials
- **Molecular Information** Spectroscopic techniques measure through the glass and may not access the core of a vial (penetration depth depends on absorption coefficient of the contents)
  - Many are difficult to locate within a batch process and are best used for novel continuous processes, whereby the vials can be transported through a sensing region and the ice layer is reduced to 1-2 mm

PAT and scale length

- The classic distinction is to divide PAT methods into those applicable to single vials and those that measure the batch

Batch techniques provide an average measurement

- Good for end point determination in primary drying
- Some cant be used at small scale (TDLAS) so not useful in mini-pilot studies
- In order to ensure that they are representative – need to address the heterogeneity in the thermal behaviour of the system (e.g. through pressure drop, ice fog nucleation and controlled crystal growth)

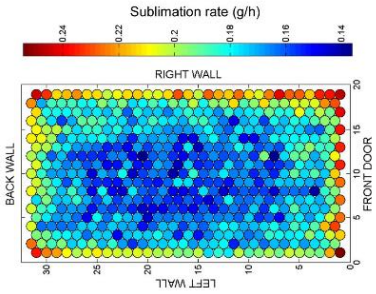

- Given the essential nature of the batch process it is difficult to imagine a single PAT method that can translate across all scales.

"L-histidine-zwitterion-from-xtal-1993-3D-balls-B" by Ben Mills

Nano (1 – 1000 nm)

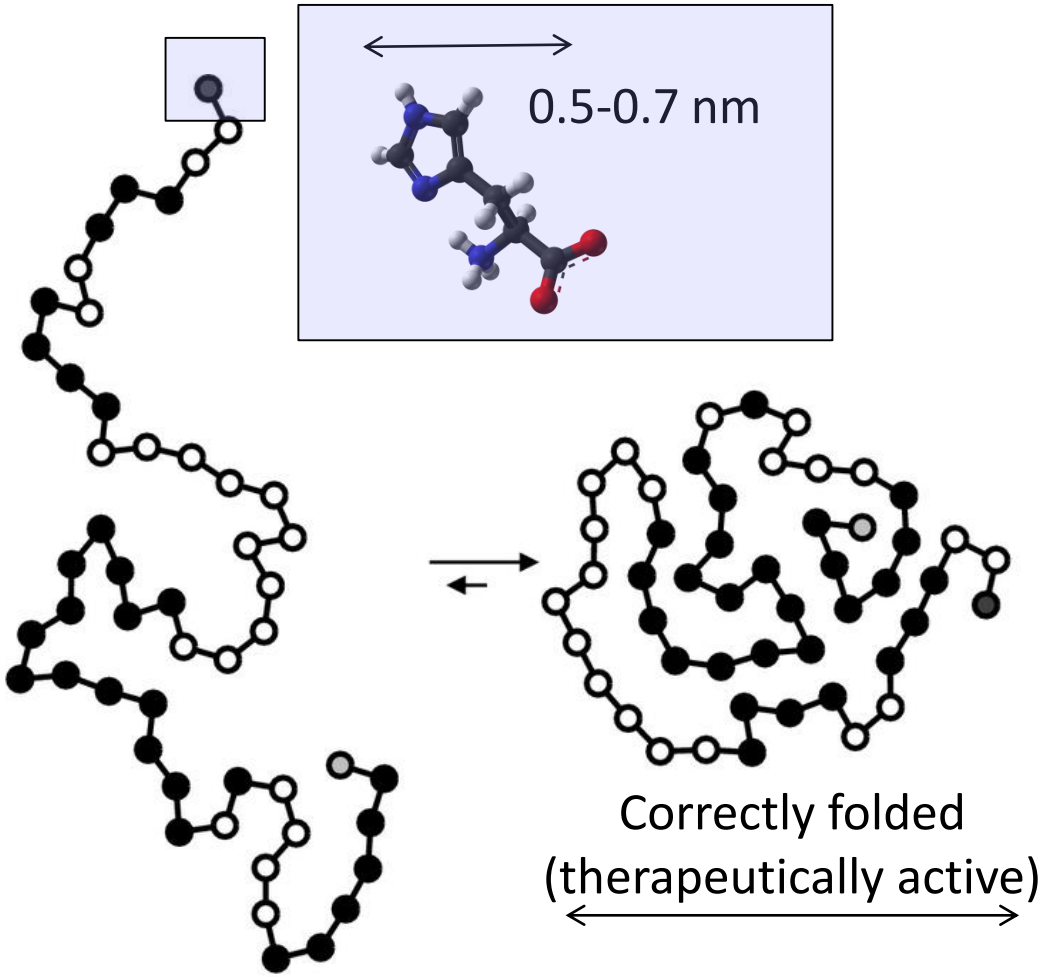

Molecular scale inc size/shape

CQA : Product stability

unfolding and/or Incorrect protein folding can inactivate a therapeutic protein and may lead to irreversible aggregation (& possible immunogenicity)

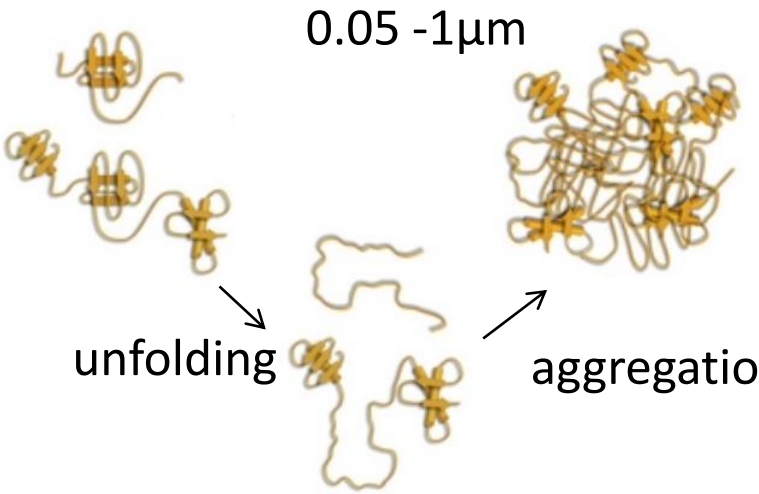

Meso scale (<1 nm – 100 µm?)

- An intermediate scale (between scales) often associated with clusters of fundamental units

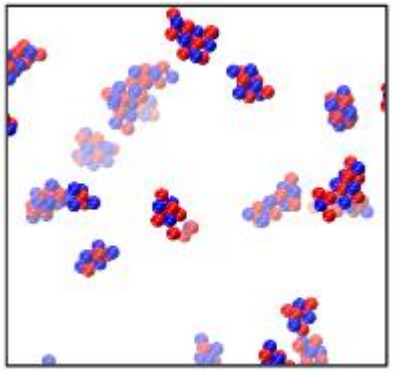

Disordered cluster/CRR

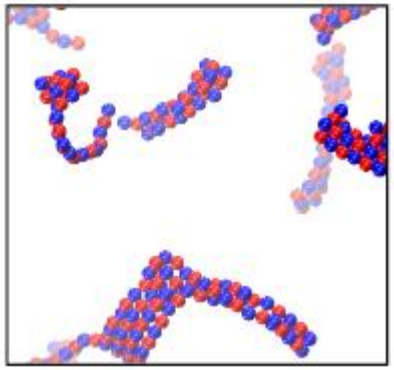

fibrils

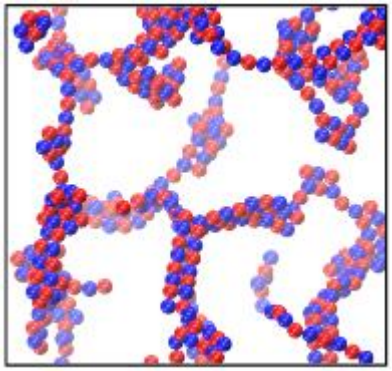

networks

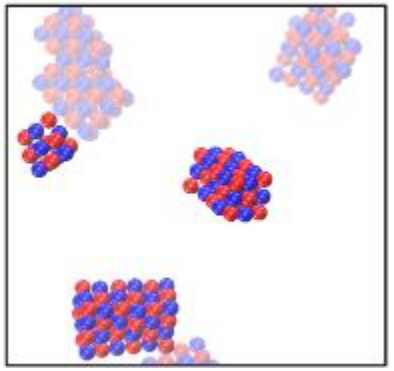

crystalline cluster

- Scale length depends on the numbers, the assembly pattern and the size of the fundamental unit, e.g. small molecule, large molecule, or nano-particle
- The assembly pattern can define the short range order and may be characterised by fractality, defects, **molecular dynamics & cooperativity**
- CQA : Product stability, e.g. protein aggregation impacts product efficacy and safety

TVIS

- A more recent addition to the suit of available PAT is the use of impedance measurements across a vial rather than within the vial (as in the CHRIST system)
- Hence the term Through Vial Impedance Spectroscopy

- Impedance is a frequency dependent parameter largely because both the impedance of a capacitance or an inductor are both dependent on the frequency of the applied field.
- By fitting the impedance spectrum one can extract the sample resistance and capacitance

TVIS could be deployed at the scale of a vial or a population of vials

The mesoscale is accessible by assessing the temperature dependence of the impedance

The challenge is to find ways in which these two attributes may be developed so that it becomes possible to bridge the scales (molecular to macroscopic signatures)

Through Vial Impedance Spectroscopy

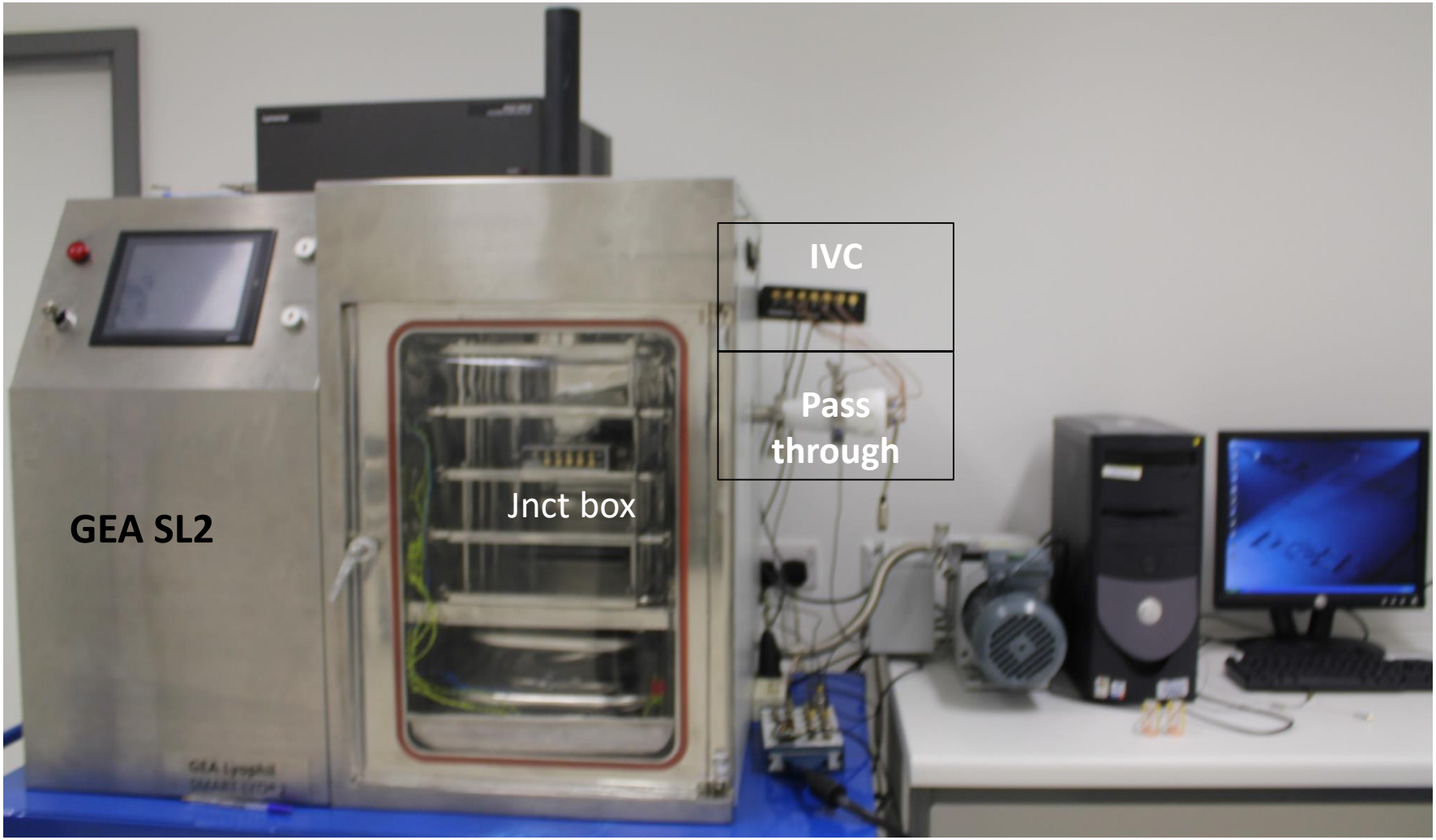

72
Insert text with

Vial designs

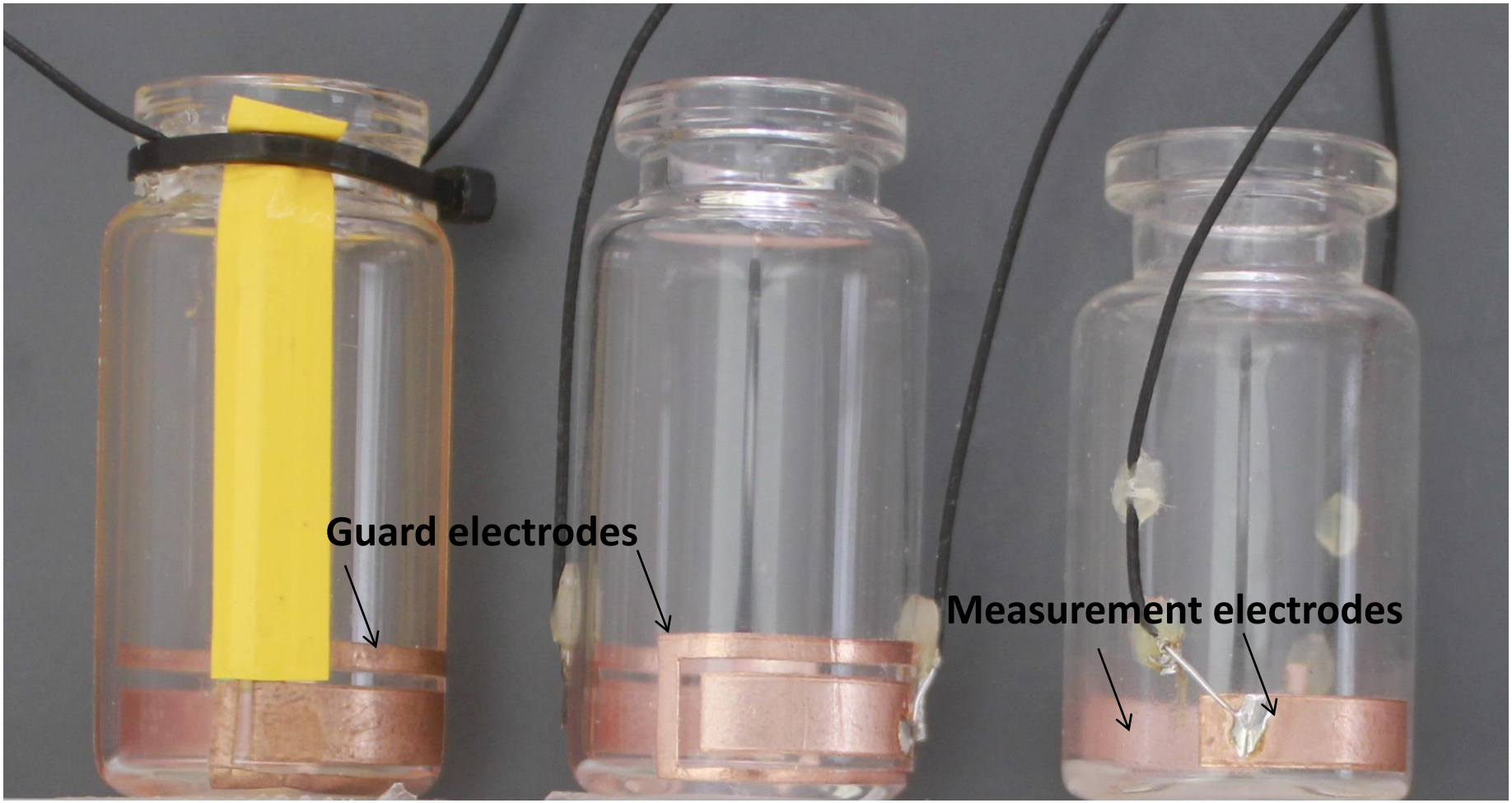

TVIS response surface

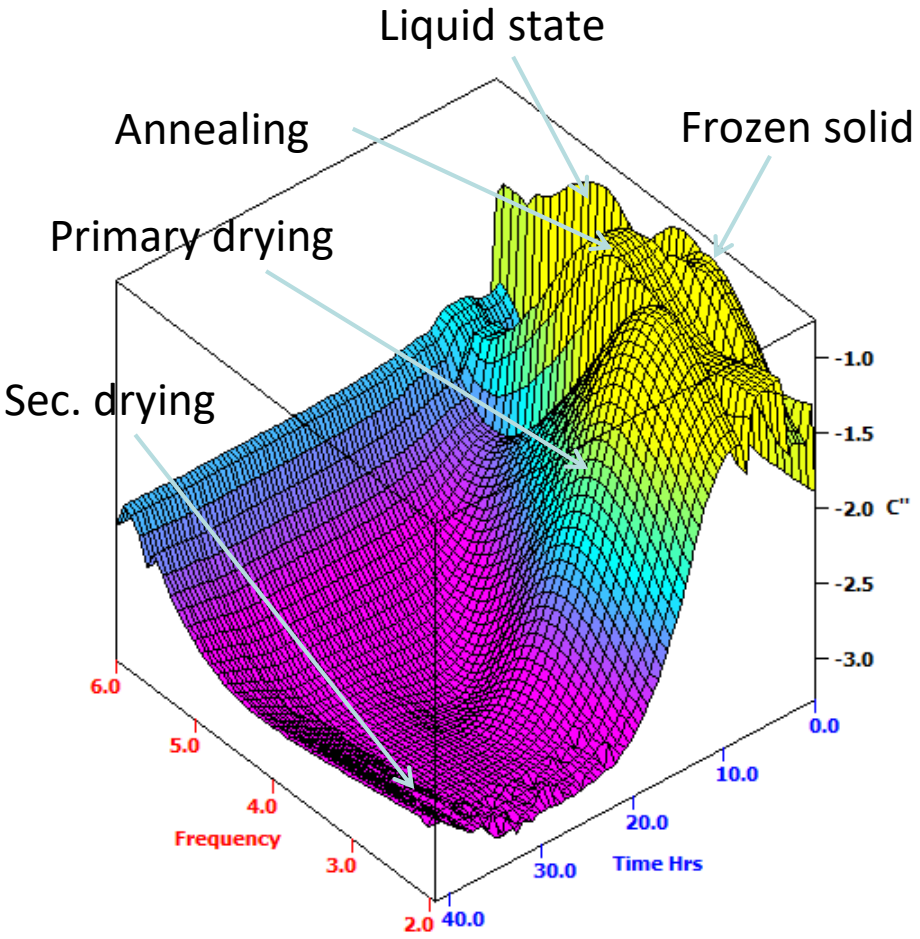

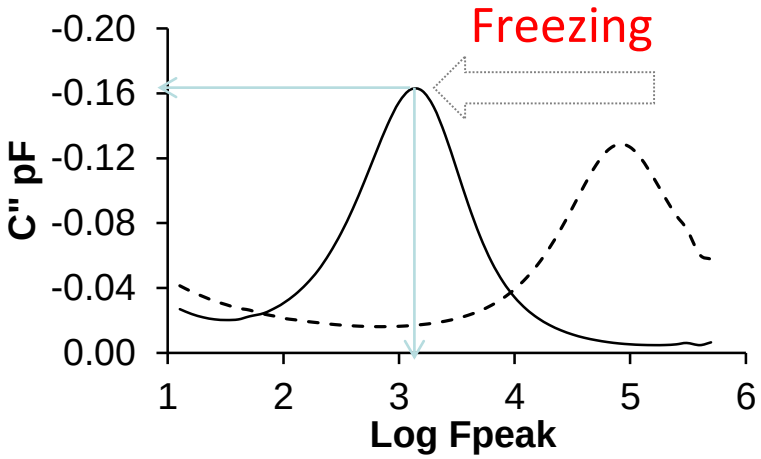

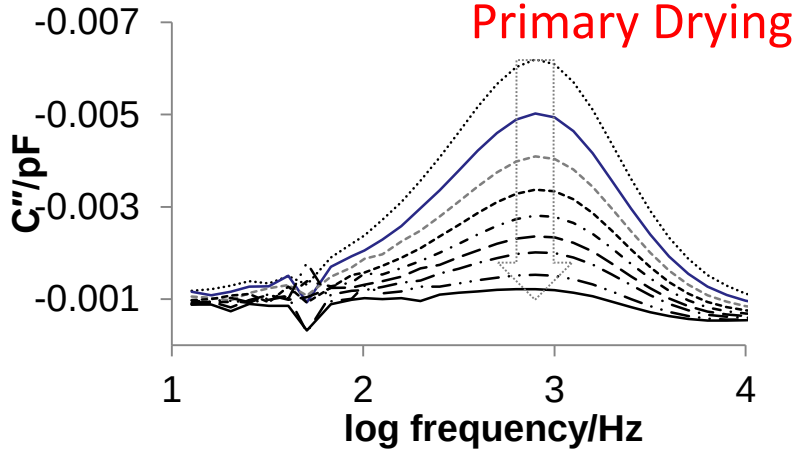

Through Vial Impedance Spectroscopy (TVIS)

- Electrodes attached to the external surface of a vial (either across the vial or on one side) or placed above the vial
- Composite impedance of the system depends on the size, position and orientation of the electrodes
- The sample has both resistive and capacitive properties whereas the container and any air space between the sample and the electrodes is predominantly capacitive in nature
- A typical circuit model would therefore be a capacitor modelling the glass wall (and any air space) and a parallel combination of a resistor and a capacitor modelling the electrical properties of the sample.

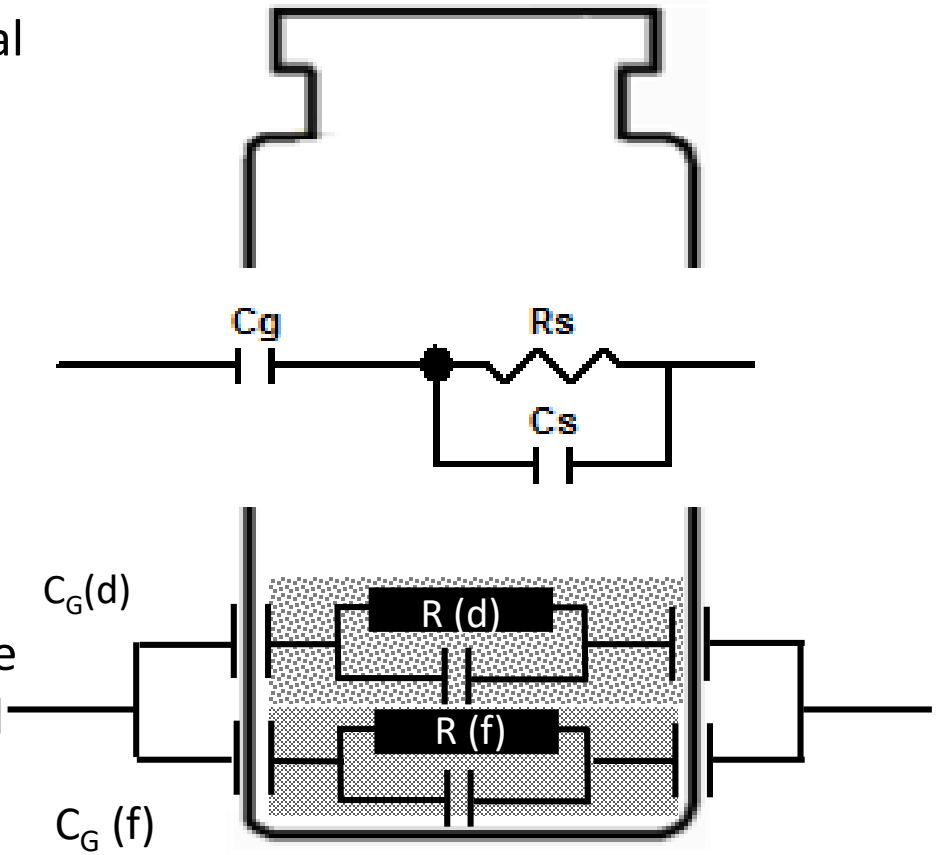

The impedance of the model can be calculated from the following equation

$$Z^* = \frac{1}{i\omega C*} = \frac{1}{i\omega C_G} + \frac{1}{\frac{1}{R_S} + i\omega C_S}$$

which re-arranges to

$$Z^* = \frac{1}{i\omega C_G} + \frac{R_S}{1 + i\omega R_S C_S} = \frac{1 + i\omega R_S(C_G + C_S)}{i\omega C_G - \omega^2 R C_G C_S}$$

Impedance can also be expressed in terms of a complex capacitance

$$C^* = C' + C'' = \frac{1}{i\omega Z^*} = \frac{C_G + i\omega R_S C_G C_S}{1 + i\omega R_S(C_G + C_S)}$$

From the complex capacitance formula, the expressions for real and imaginary capacitance can be calculated to explain the origin of interfacial polarization peak. This achieved by multiplying the nominator and denominator by the complex conjugate of the denominator and by grouping the real (C') and imaginary (C'') parts

$$C^* = \frac{1}{i\omega Z^*} = \frac{(C_G + i\omega R_S C_2 C_G)(1 - i\omega R_S(C_S + C_G))}{(1 + i\omega R(C_S + C_G))(1 - i\omega R_S(C_S + C_G))} = \frac{C_G + \omega^2 R_S^2 C_{2G} C_S(C_S + C_G) - i\omega R_S C_G^2}{1 + (\omega R_S((C_S + C_G))^2}$$

To obtain

$$C' = \frac{C_G + \omega^2 R_S^2 C_G C_S(C_S + C_G)}{1 + \left(\omega R_S\left((C_S + C_G)\right)\right)^2} \quad \text{and} \quad C'' = -\frac{\omega R_S C_G^2}{1 + (\omega R_S((C_S + C_G))^2}$$

Real Part Capacitance

- The value of real part of capacitance at ω→0 is

$$C' = C_{G(fl)} = f(v_{ice})$$

- and value at ω → ∞

$$C' = \frac{C_S C_G}{(C_S + C_G)}$$

- It follows that the step change in capacitance is

$$\Delta C' = C_G - \frac{C_S C_G}{(C_S + C_G)}$$

$$\Delta C' = \frac{C_G^2}{(C_S + C_G)}$$

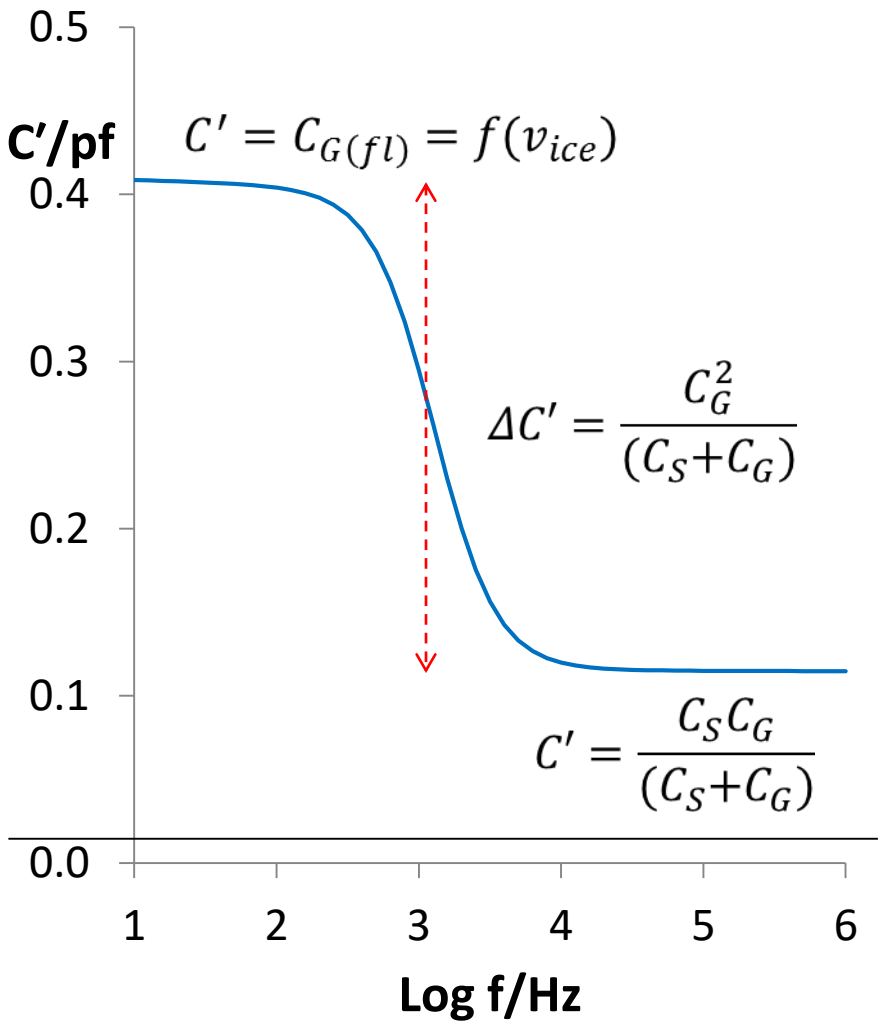

Imaginary Part Capacitance

At ω → 0, C″ = 0. As the frequency increases, C″ increases to a maximum (C''_{max}) then decreases to 0 as the frequency ω → ∞

$$C''_{max} = \frac{C_G^2}{2(C_S+C_G)}$$

at a frequency of

$$\omega_{max} = \frac{1}{R(C_S+C_G)} \text{ in radians}$$

Or

$$f_{max} = \frac{1}{2\pi R(C_S+C_G)} \text{ in cycles per second}$$

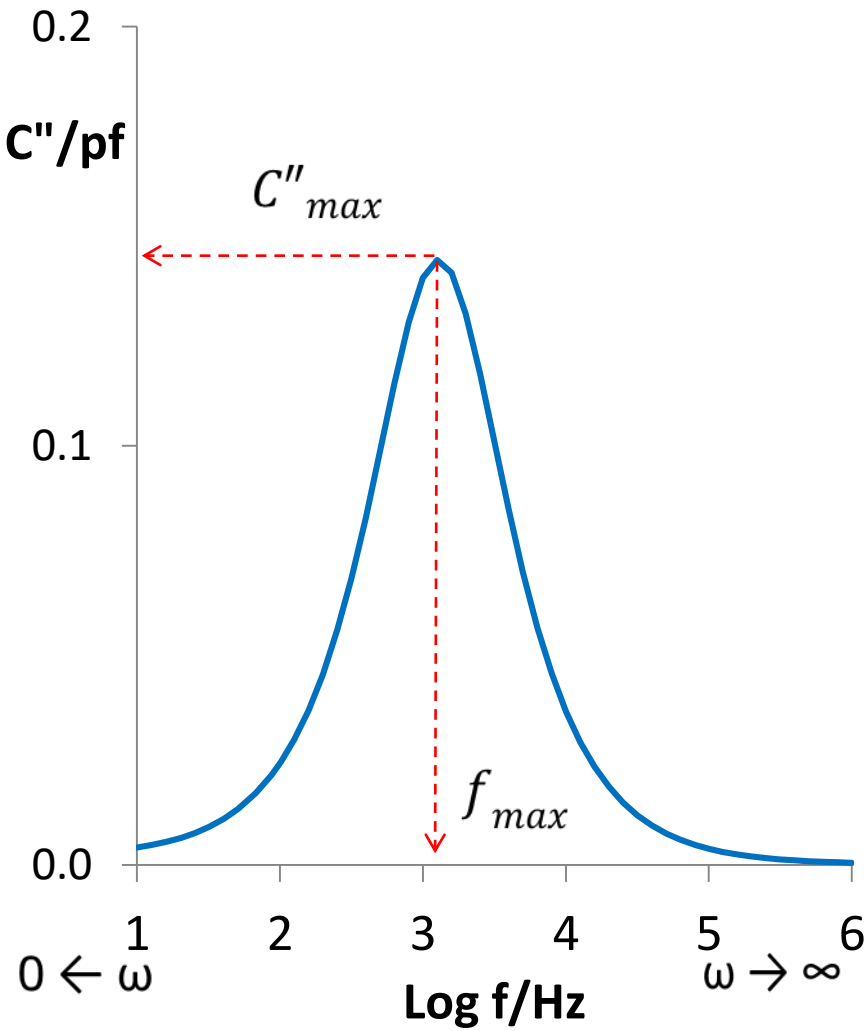

Removal of the guard electrode

- Right shows example spectra of frozen distilled water using two different TVIS vials, one with guard electrodes and the other without
- Removal of guard electrodes has increased the amplitude of pseudo-relaxation peak almost three times with respect to corresponding peak with guard electrodes.

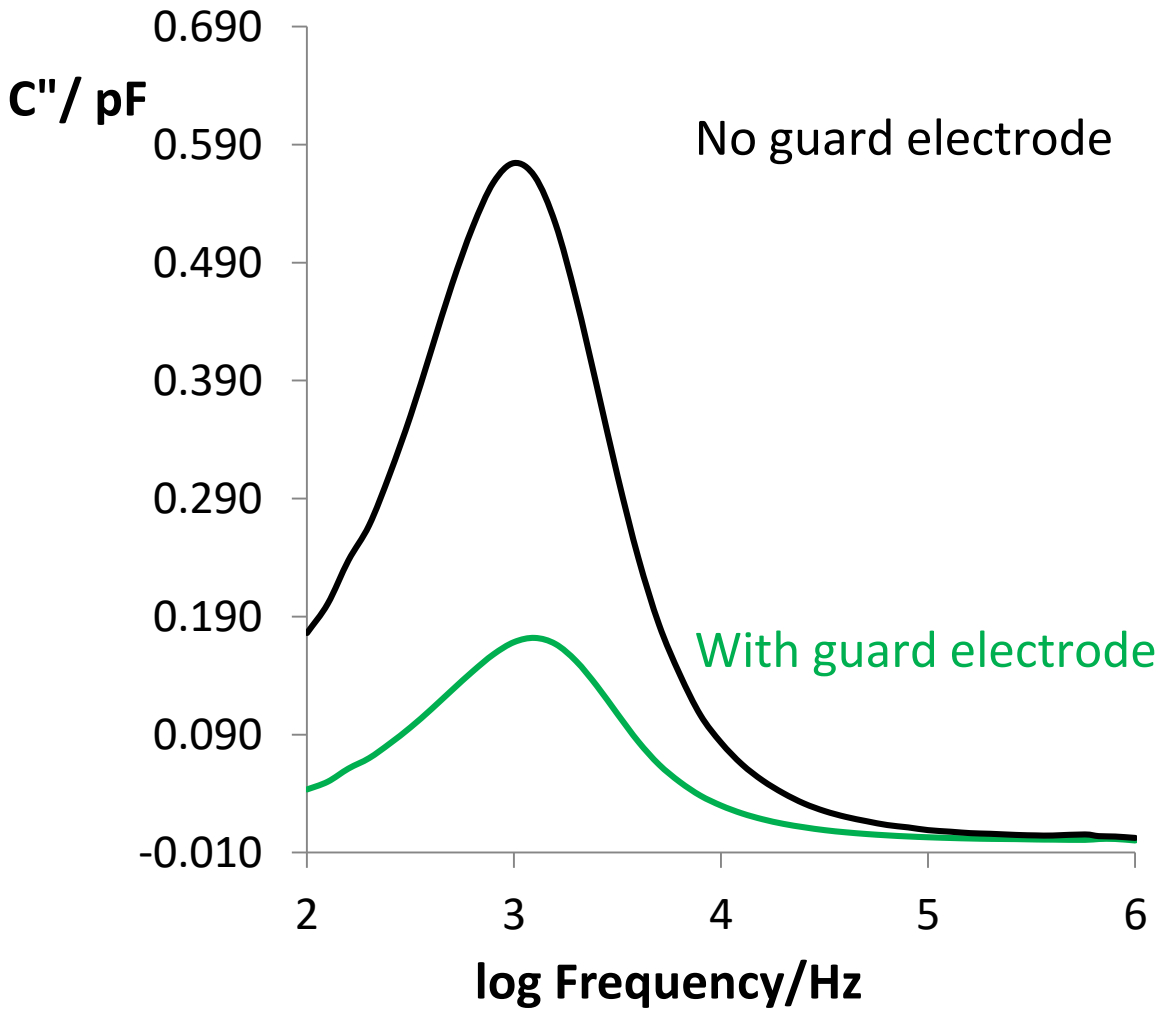

Product Characterization – Ice formation

Fpeak profile records freezing step (B-E) which progress through 2 discrete stages; solidification(B-D) and equilibration(D-E). Time duration for the former increase with the fill height while the latter remain broadly unchanged as it is related to thermal coefficient of the vial base.

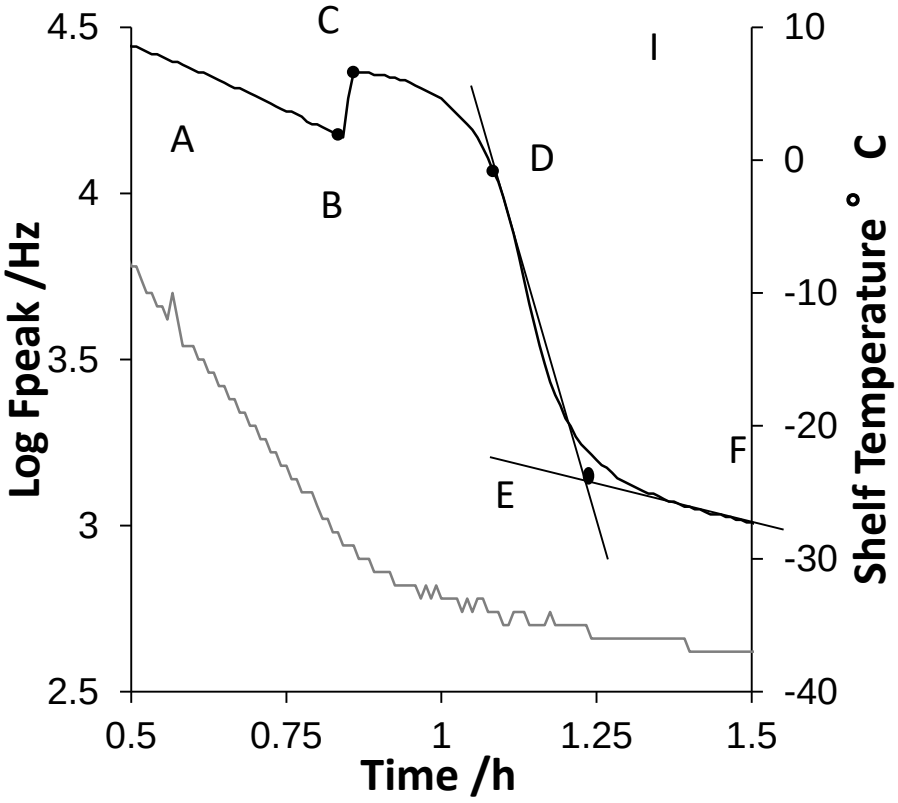

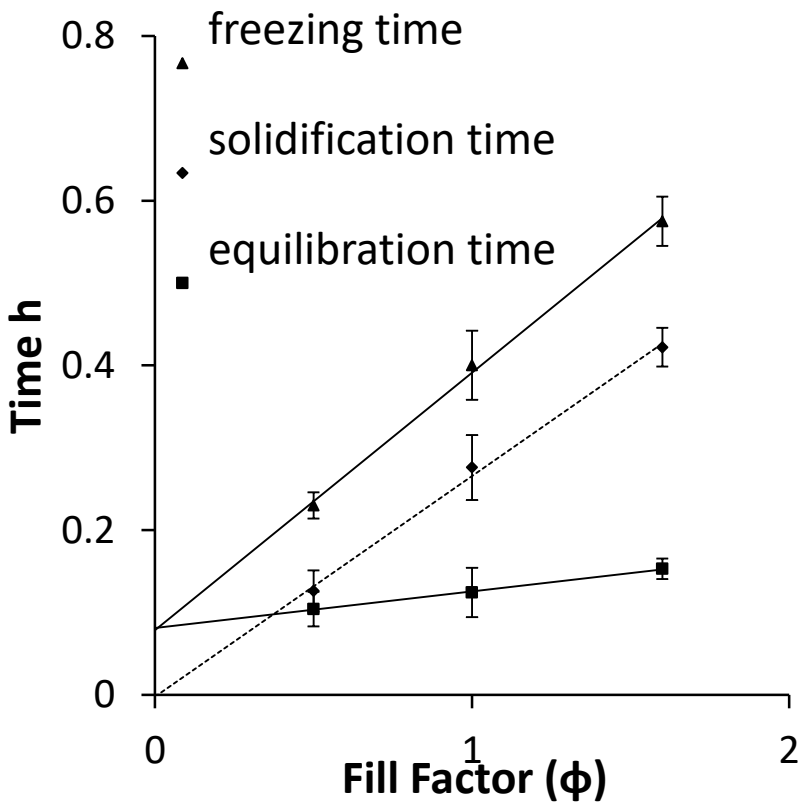

Product Characterization : Glass transition, Eutectic Crystallization, Collapse

Smith G et al (2013) Eur J Pharm Biopharm 85 (3)1130-40

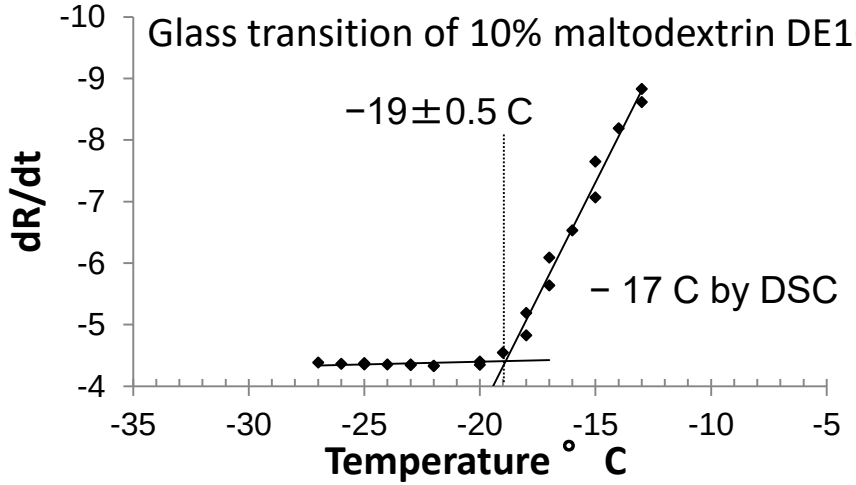

Arshad MS et al (2014) Eur J Pharm Biopharm 87(3):598-605

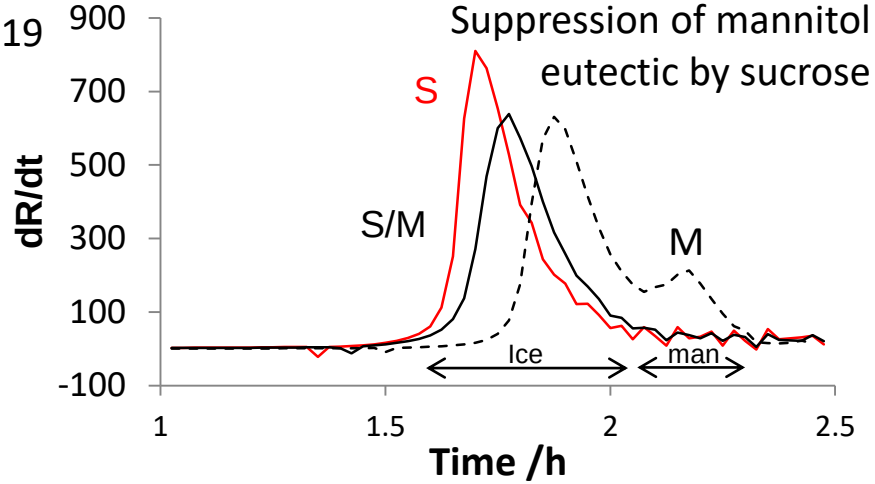

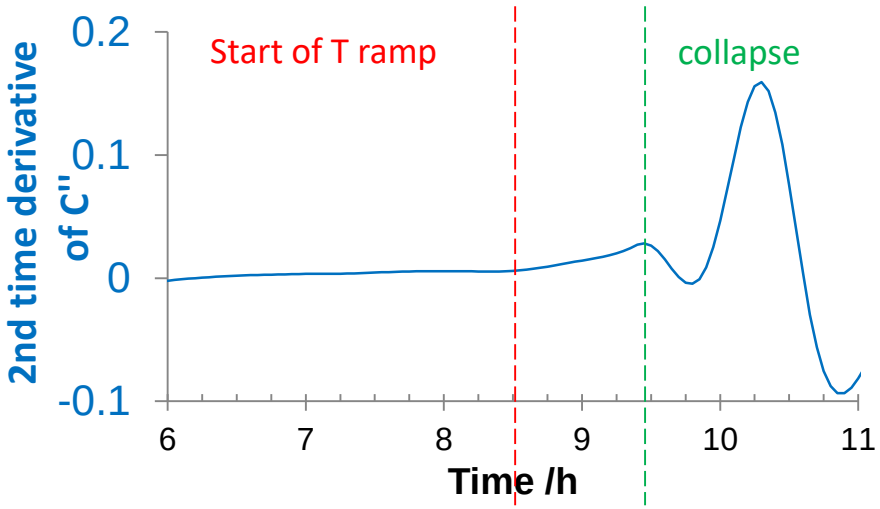

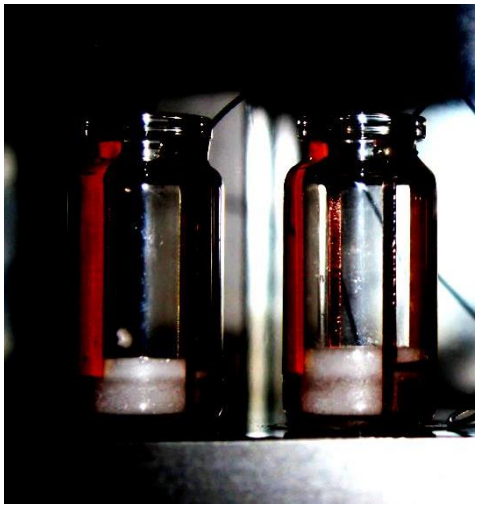

Smith G et al (2014) Pharmaceutical Technology 38(4)

Phase separation

- The discontinuities in the gradients of C were recorded at -15 ° C and -22 ° C (estimated from the inflection point) while the changes in R were less clear as the gradient changed over a longer period of time.
- The lower glass transition temperature (T'_G) from the impedance profiles (relative to the DSC data) is a likely consequence of the slower cooling rate in the vial which might favour increased ice formation and a more concentrated unfrozen fraction.

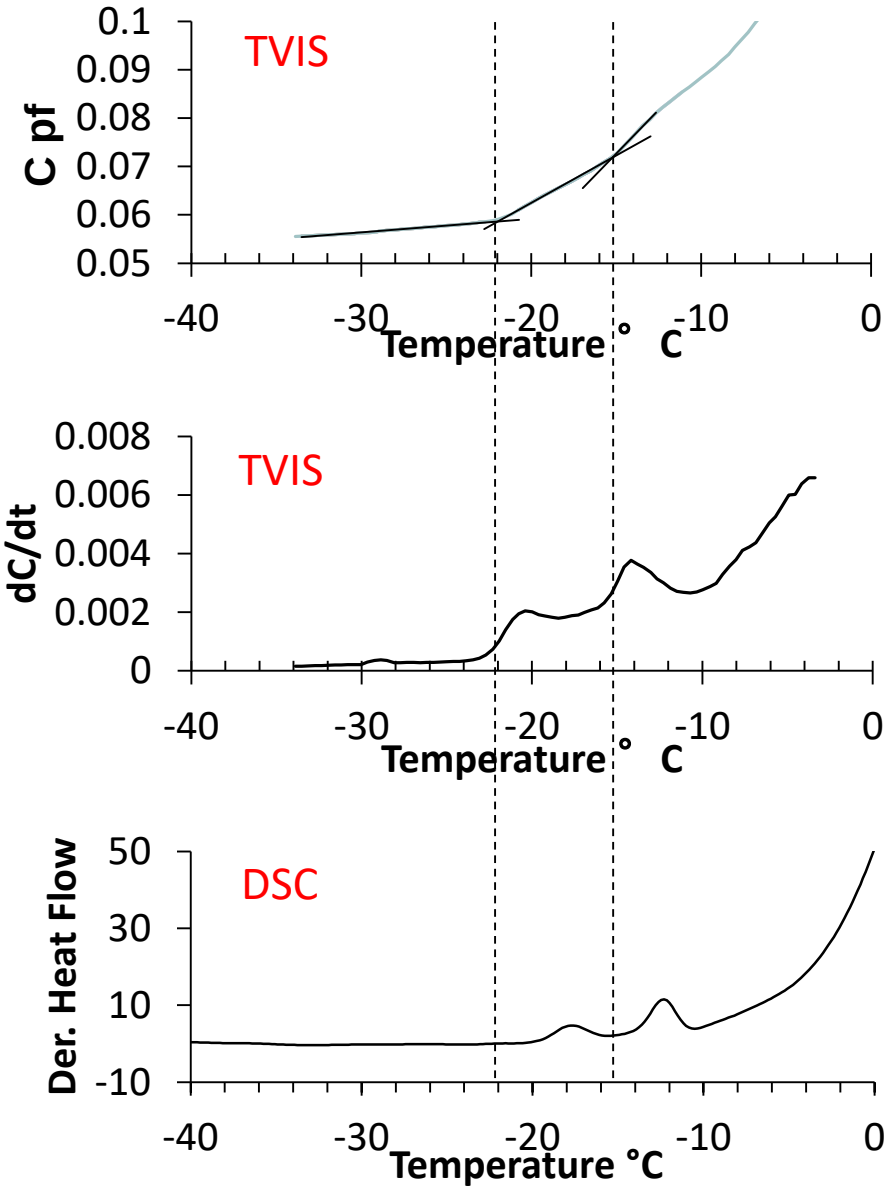

Product Characterization : Temperature

- The f_{peak} showed a good correlation with the product temperature during product cooling (A), freezing (B) and annealing (C)
- Provided there is no change in phase, then a linear correlation exists between Log F and temperature (A, C-D)
- Temperature coefficient for log F_{peak} in the frozen state (C-D) is ~0.04 which is approx. x3 of the temperature coefficient in the solution state

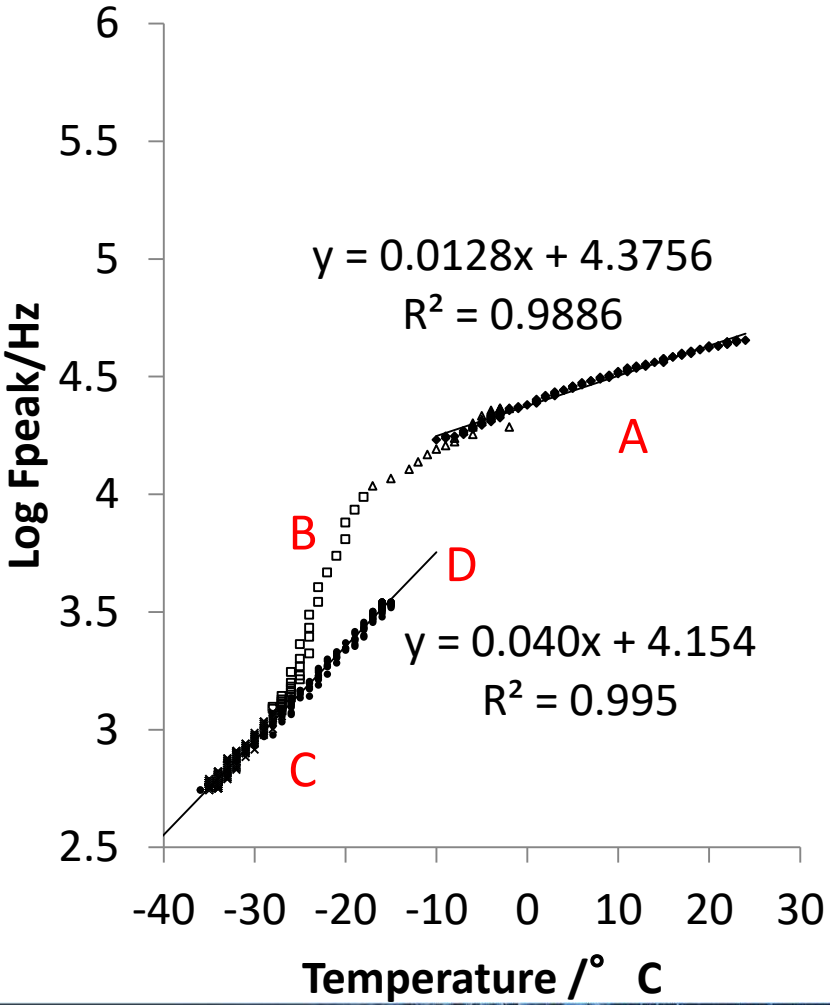

Model of temperature profile within vial

- Divide mass of frozen solid into segments (0 to 2, or 0 to 9). Each segment is modelled by the following circuit

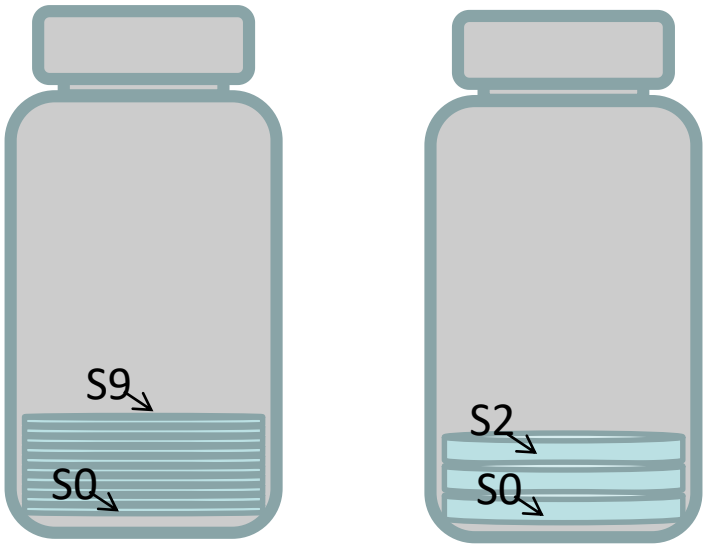

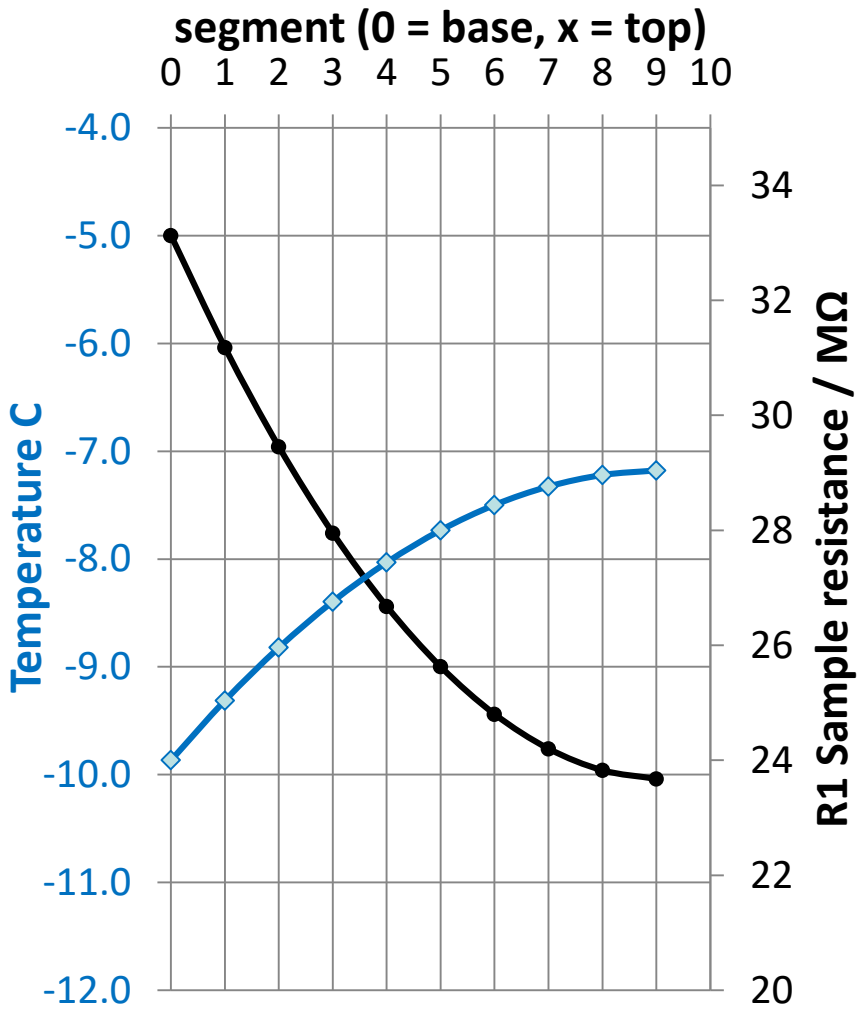

Contact electrode : Parallel elements

- Positioning the contact electrode on the walls surrounding the sample means that the sample segments (n = S1-3) are presented in parallel with one another, but in series with the wall impedance

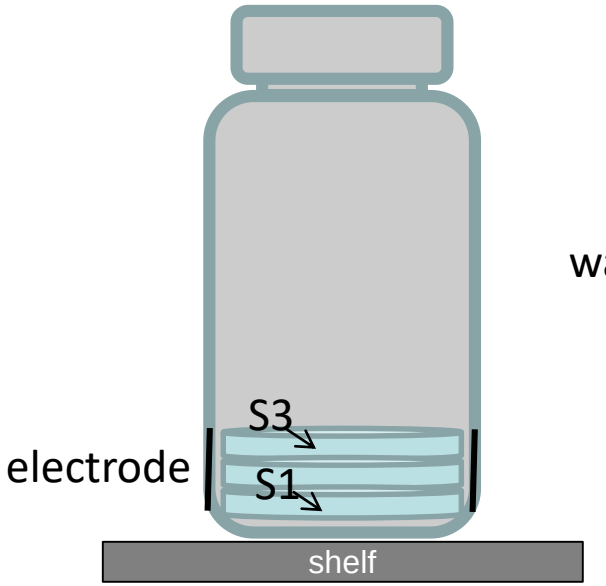

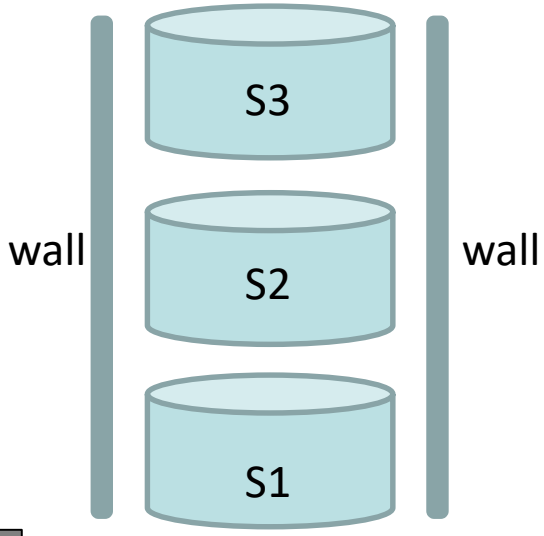

$$C_n^{*}\ (i\omega) = \frac{1}{R_n} + i\omega C_n\ (n = 1 \text{ to } 3)$$

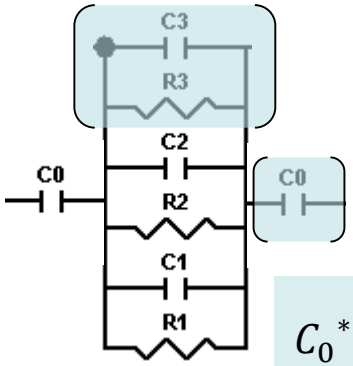

$$C_0^{*}\ (i\omega) = \frac{1}{i\omega C_0}$$

$$C_s^{*}\ (i\omega) = C_1^{*}\ (i\omega) + C_2^{*}\ (i\omega) + C_3^{*}\ (i\omega)$$

Side electrodes

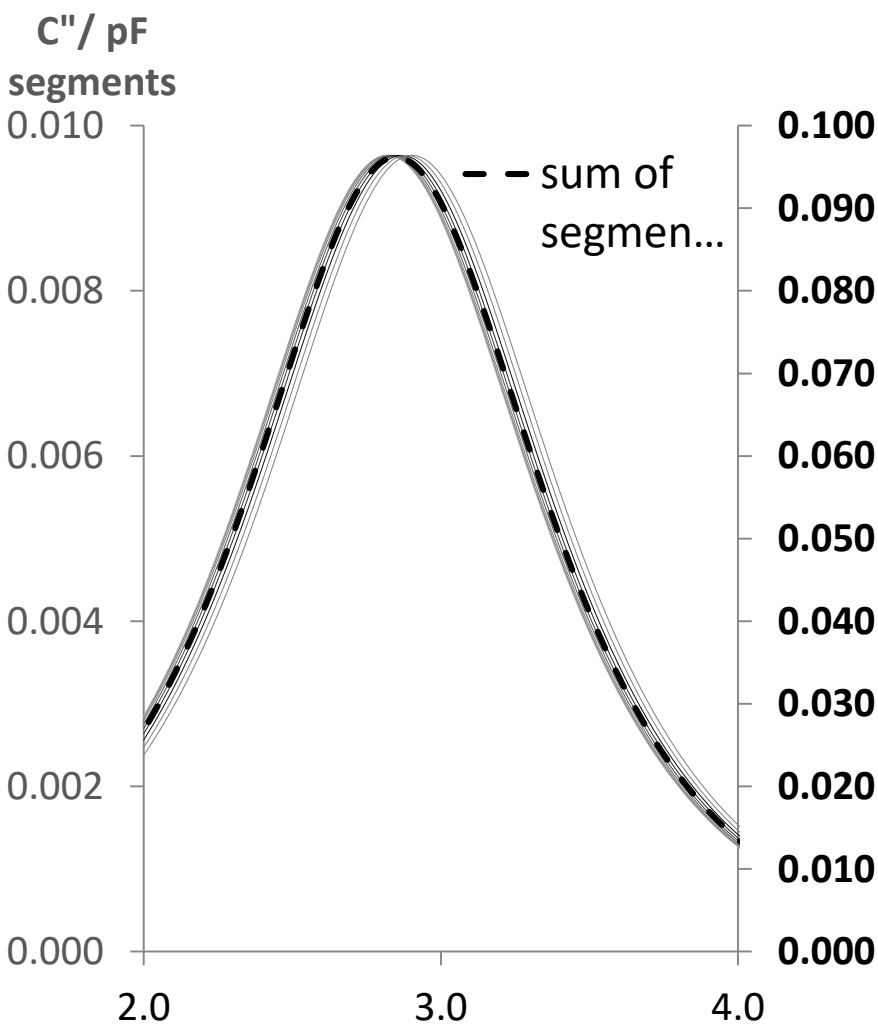

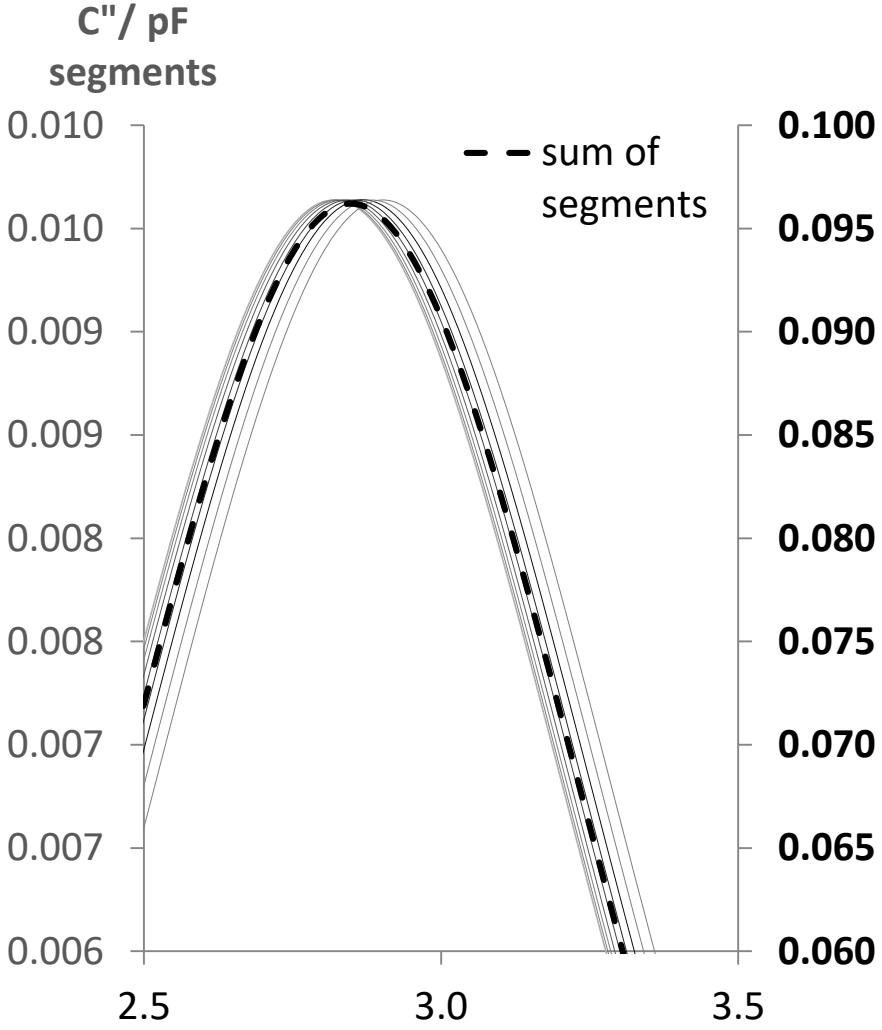

$$f_{max} = \frac{1}{2\pi R(C_S + C_G)}$$

Macroscale: single vial

ELSEVIER
Available online at www.sciencedirect.com
SCIENCE DIRECT®
Journal of Food Engineering 67 (2005) 467–475
JOURNAL OF FOOD ENGINEERING
www.elsevier.com/locate/jfoodeng

Temperature distribution in a vial during freeze-drying of skimmed milk
Sung Song, C. et al

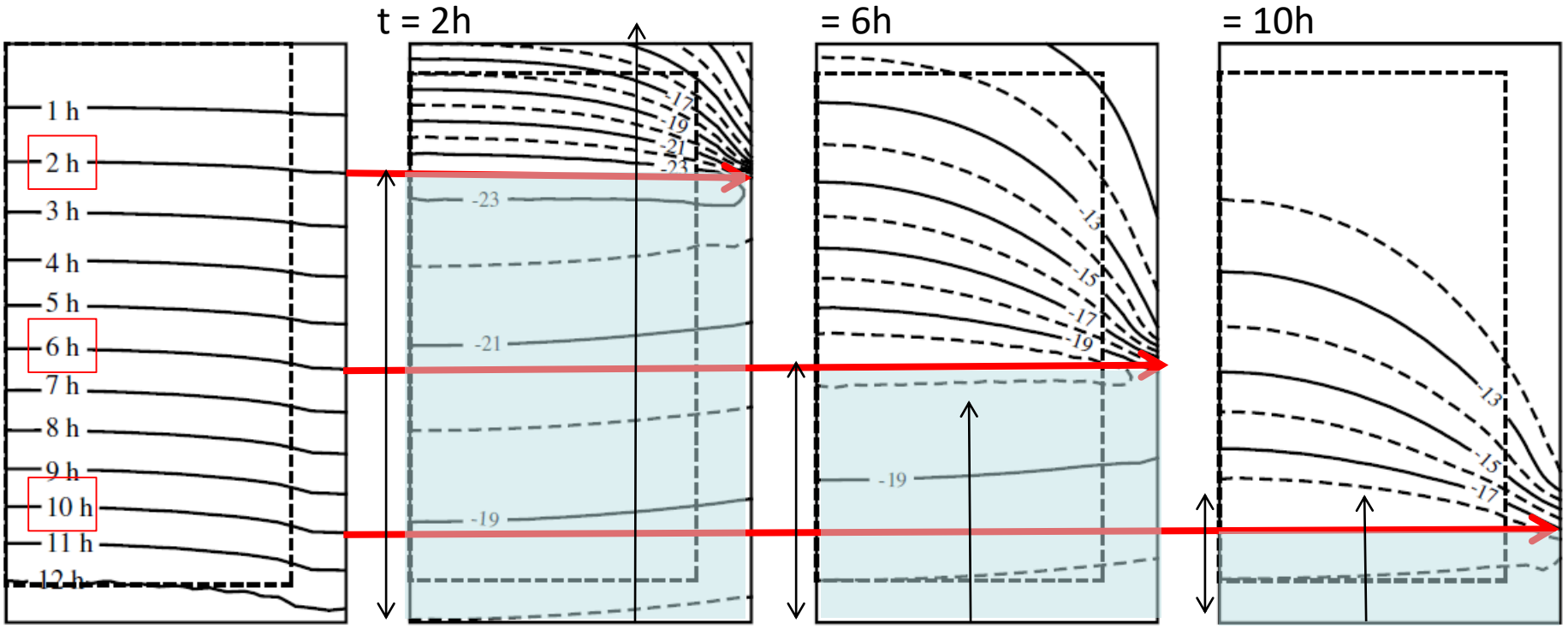

Δ T = 6 to 7 K = ~2 K = ~1 K

Calculated temperature profile at time 2 h, 6 h and 10 h
Temperature gradient in frozen layer is one dimensional – but in the dry layer its curved owing to the impact of wall heating

Calculated position of sublimation interface

Temperature variation in primary drying

- Temperature calibration in the frozen state
- Derivative of peak height is an indicator of drying rate
- When the drying rate peaks the temperature increases

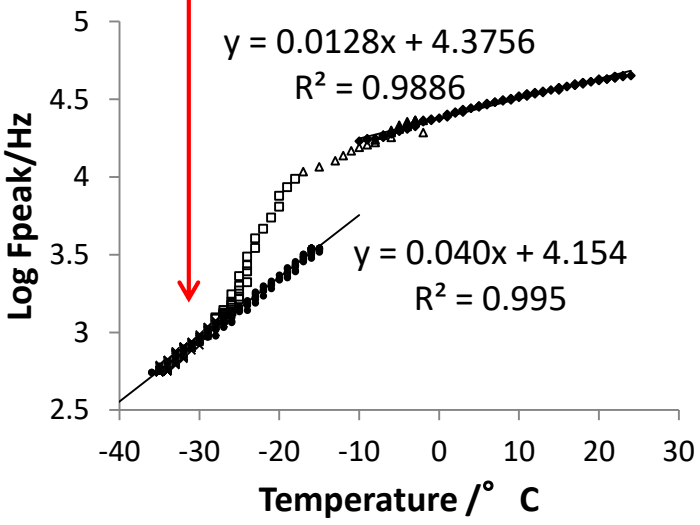

3% sucrose

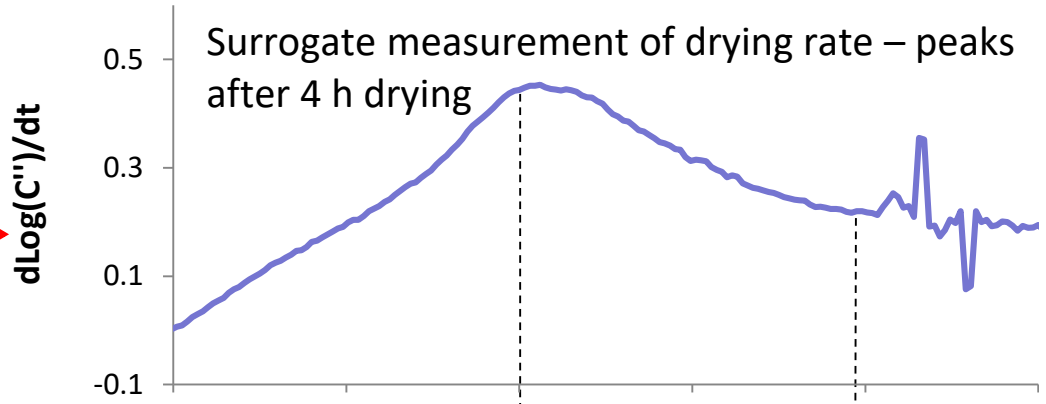

$$f_{max} = \frac{1}{2\pi R(C_S + C_G)}$$

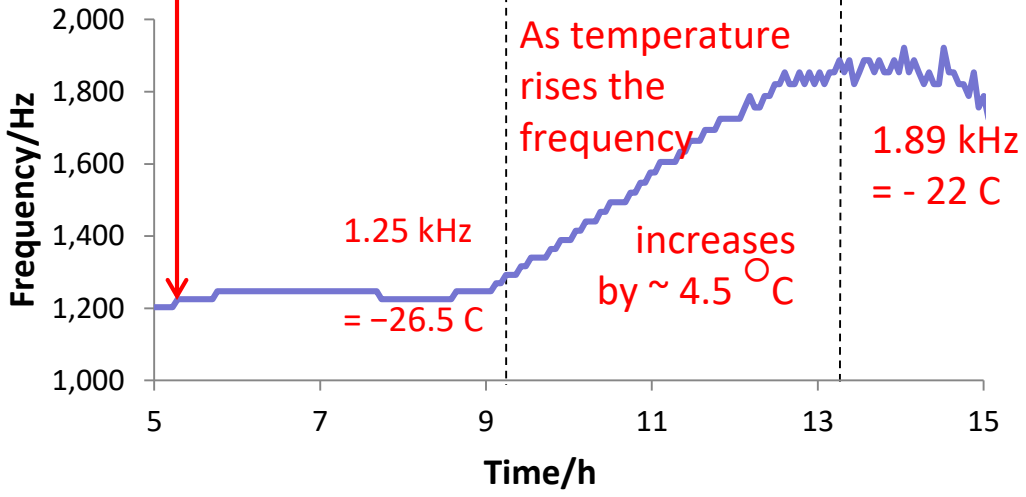

ISL-FD conference and seminar, Barcelona, Spain, 06-10 July 2015

Effect of the Vacuum Induced Nucleation on process and on final product homogeneity

Irene Oddone
Department of Applied Science and Technology
Institute of Chemical Engineering
Politecnico di Torino

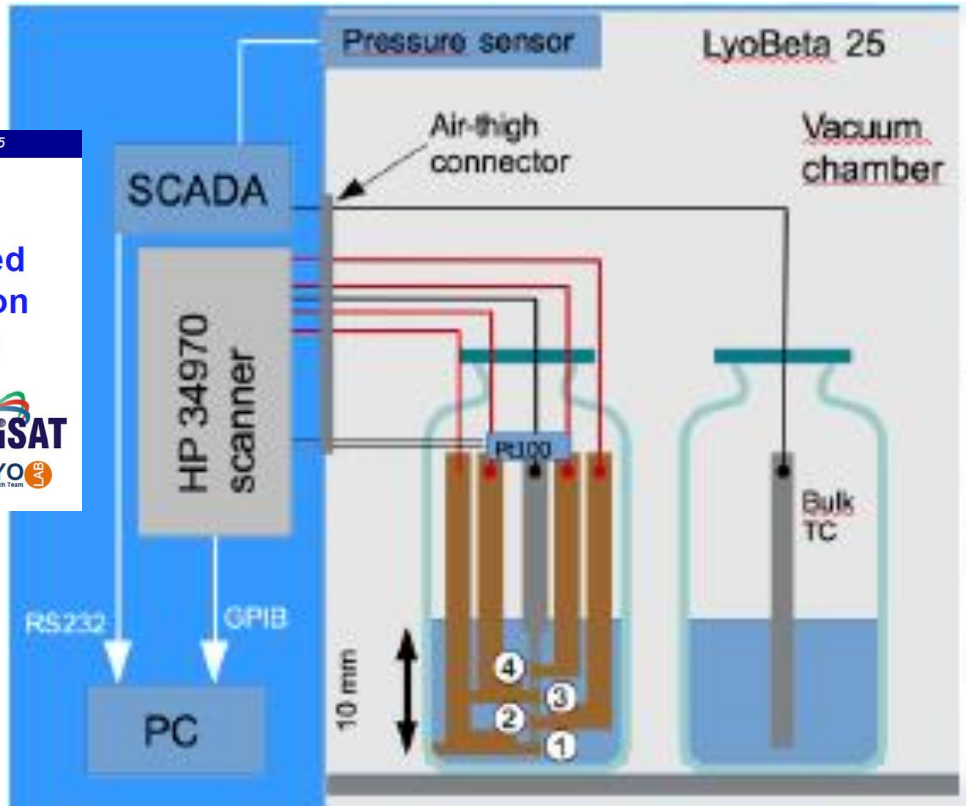

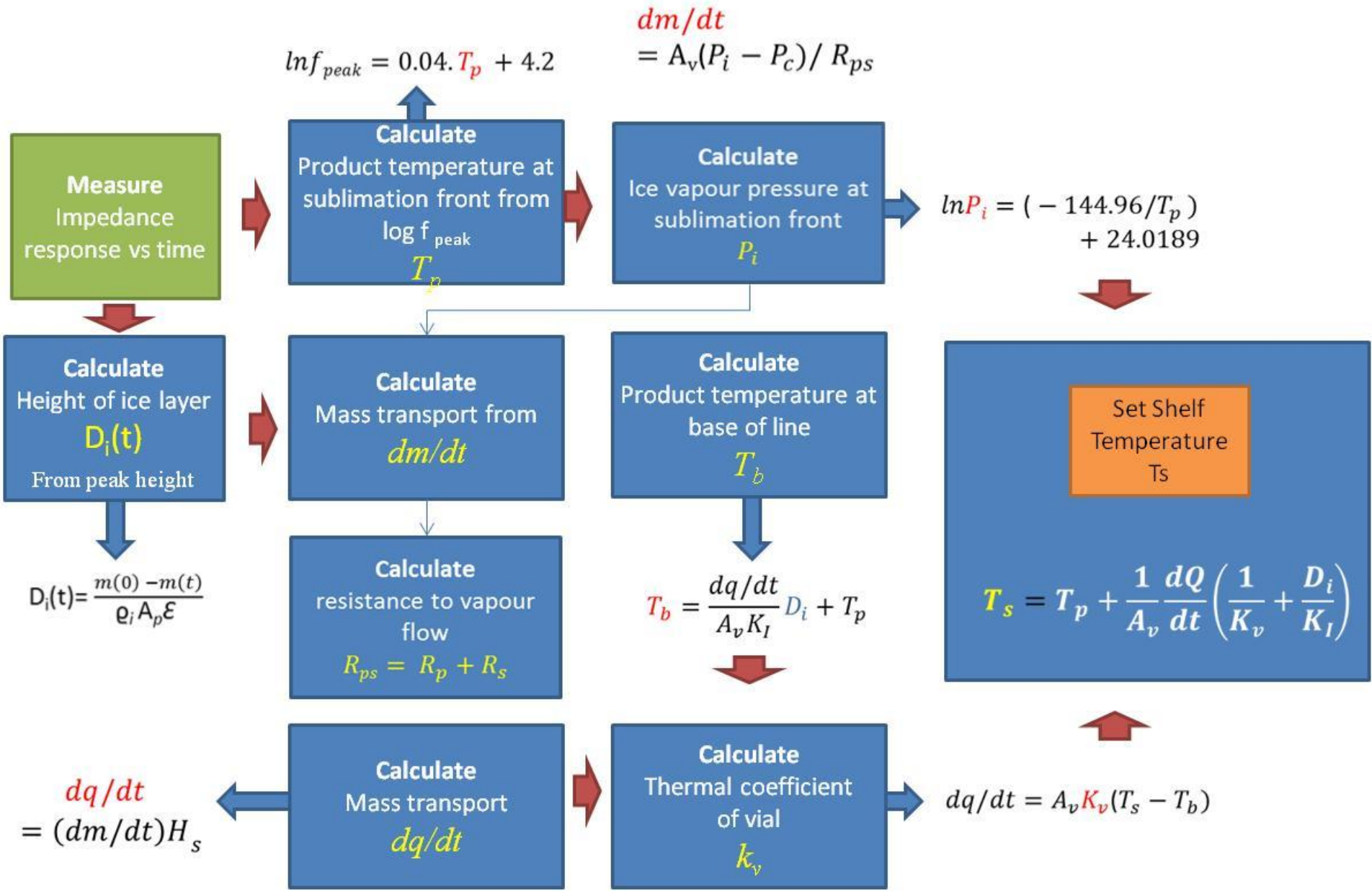
$lnf_{peak} = 0.04.T_p + 4.2$
$dm/dt = A_v(P_i - P_c)/R_{ps}$
Measure Impedance response vs time
Calculate Product temperature at sublimation front from log f peak T_p
Calculate Ice vapour pressure at sublimation front P_i
$lnP_i = (-144.96/T_p) + 24.0189$
Calculate Height of ice layer $D_i(t)$ From peak height
Calculate Mass transport from dm/dt
Calculate Product temperature at base of line T_b
Set Shelf Temperature Ts
$D_i(t) = \frac{m(0) - m(t)}{\varrho_i A_p \varepsilon}$
Calculate resistance to vapour flow $R_{ps} = R_p + R_s$
$T_b = \frac{dq/dt}{A_v K_I} D_i + T_p$
$T_s = T_p + \frac{1}{A_v}\frac{dQ}{dt}\left(\frac{1}{K_v} + \frac{D_i}{K_I}\right)$
$dq/dt = (dm/dt)H_s$
Calculate Mass transport dq/dt
Calculate Thermal coefficient of vial k_v
$dq/dt = A_v K_v (T_s - T_b)$

Maltodextrin DE19 10% w/v Annealing

- Capacitance decrease only 3%

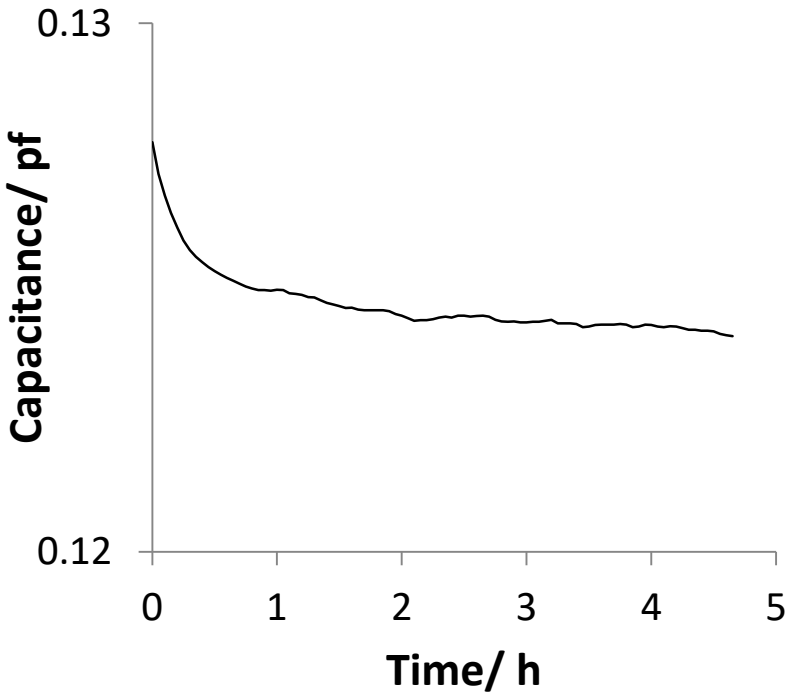

- Resistance decreases by approx. 30% during annealing hold stage

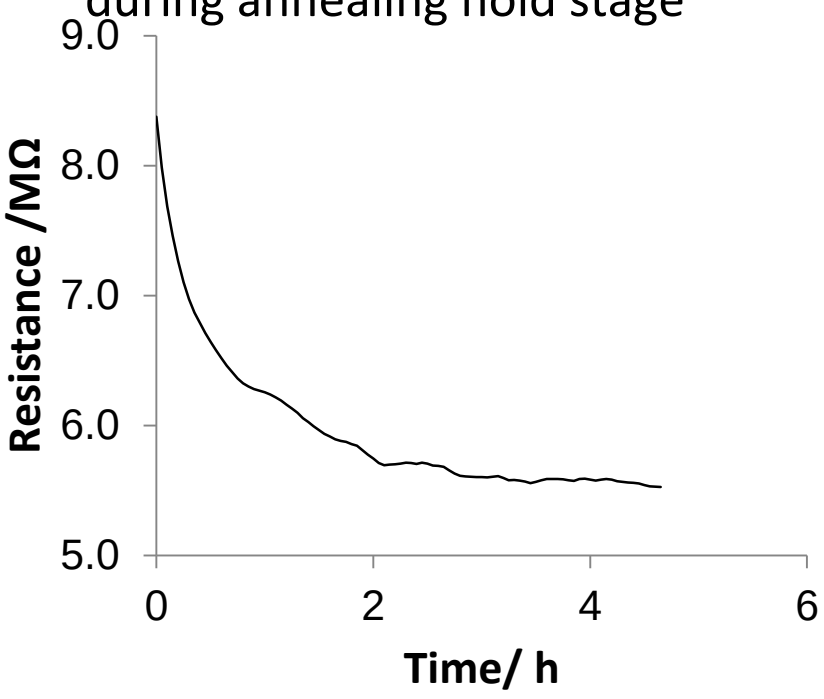

Simplification of the unfrozen mass by recrystallization effectively lowers the electrical resistance

Smith, G. et al (2014) J Pharm Sci 103 (6) 1799–1810

Completion of Annealing (Maltodextrin 10% w/v)

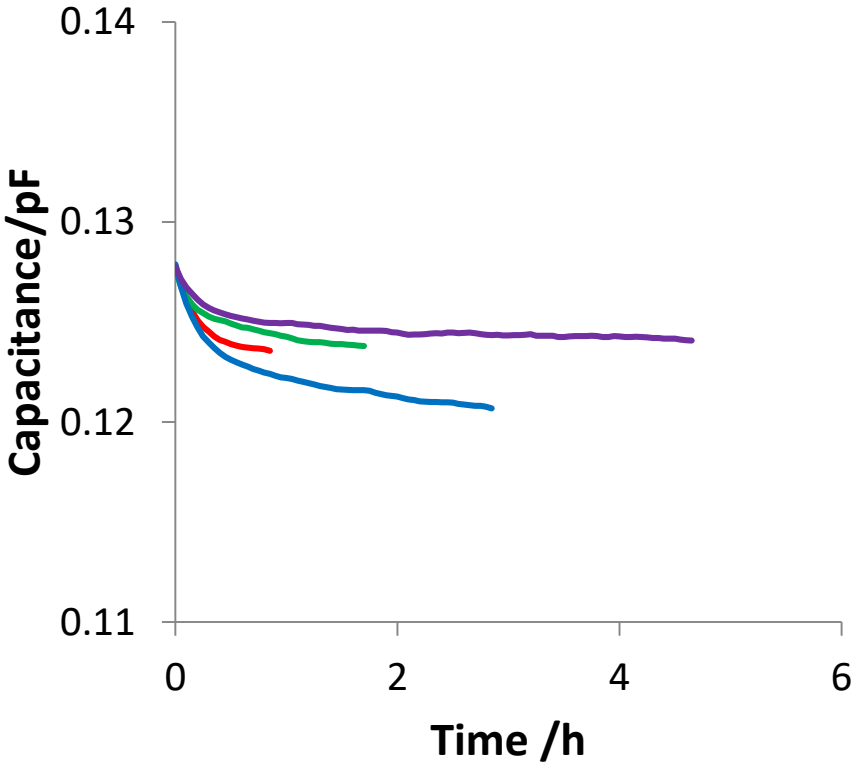

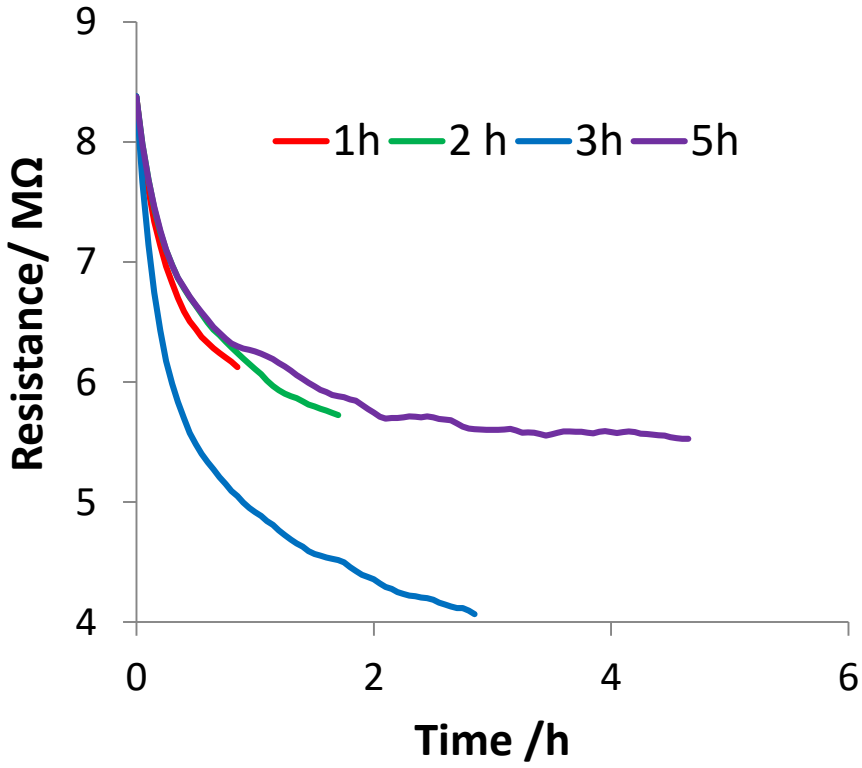

The capacitance of the formulation changes minimally while the resistance changes significantly and plateaus at 3-4 h

Simplification of the unfrozen mass by recrystallization effectively lowers the electrical resistance (i.e. recrystallization)

Glass transition on annealing

- There are no appreciable differences in T_G on both ramp up and ramp down suggesting that the concentration of the unfrozen fraction does not change with annealing

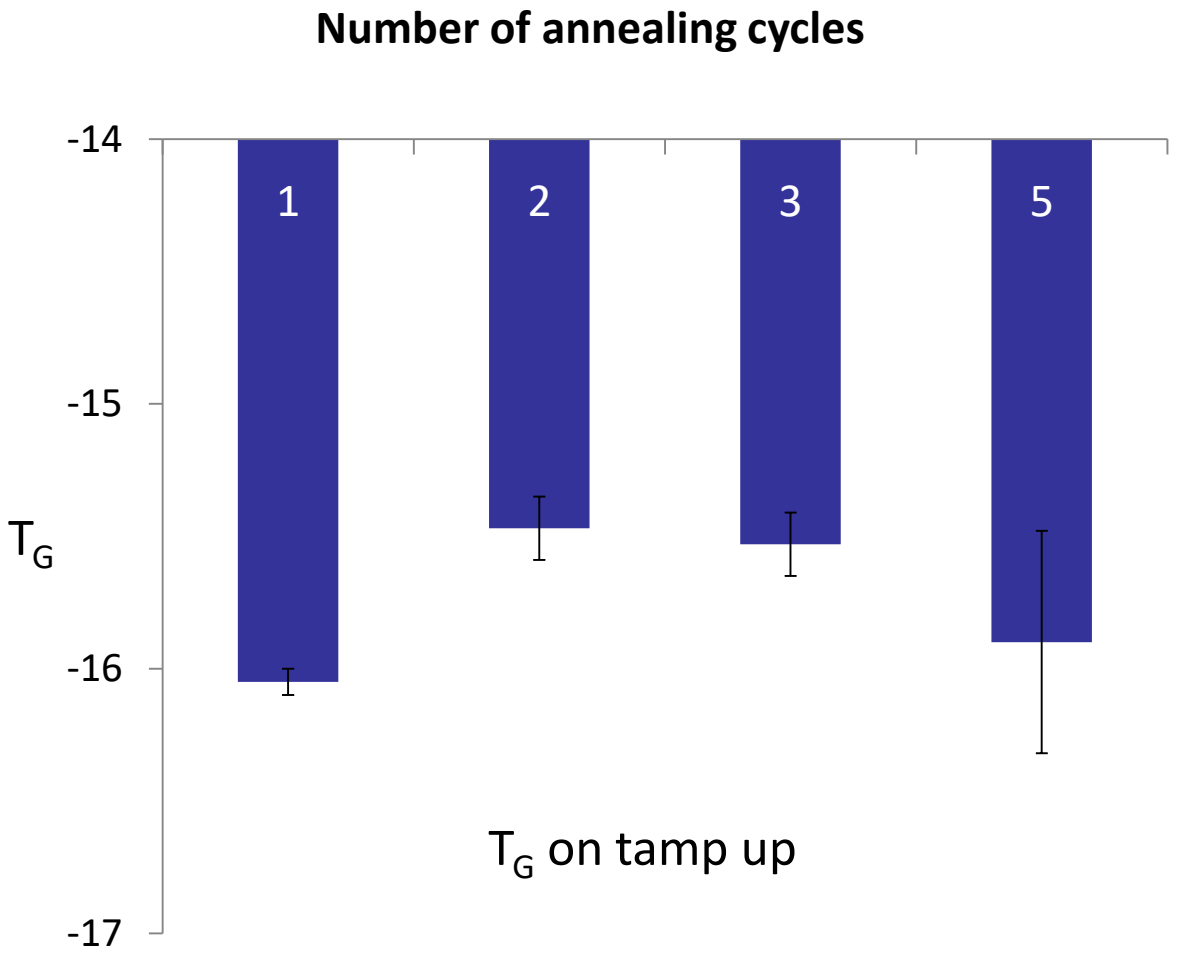

Arrhenius Fit to describe the below Tg' resistance

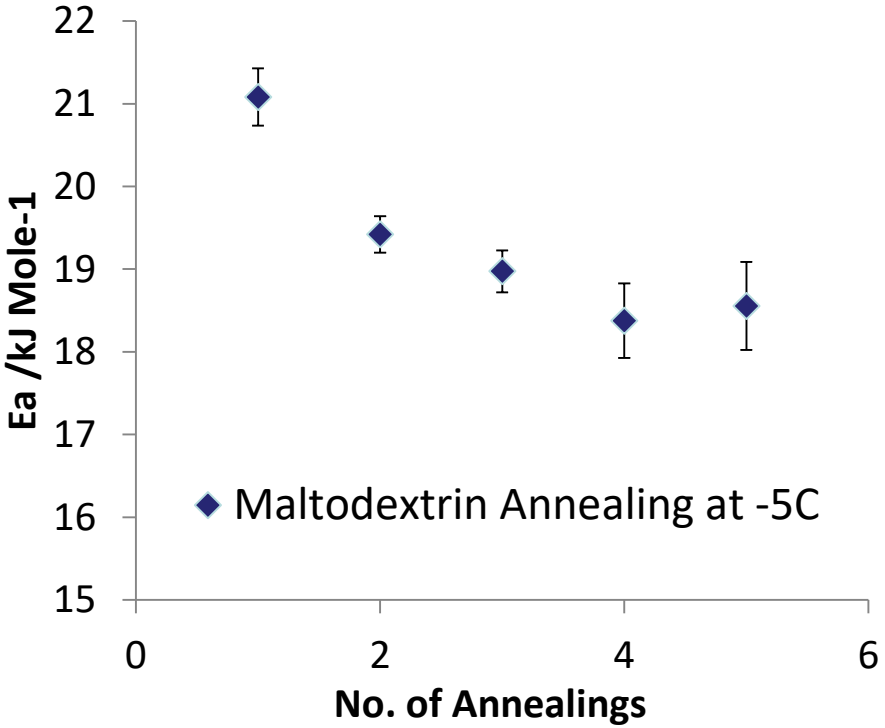

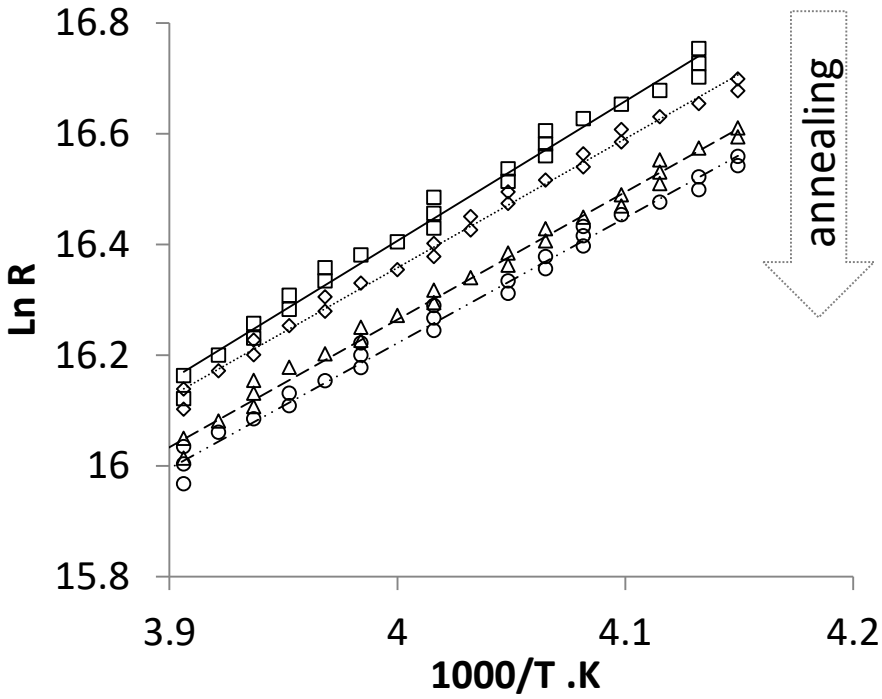

The product resistance and the activation energy for charge transport (E_a) in the sub-Tg' temperature region decreases following annealing. The explanation is that the unfrozen fraction has a super high viscosity and that the ice structure now dominates the resistance. Reduction in E_a is again consistent with a simplification in ice structure

Impact of annealing temperature

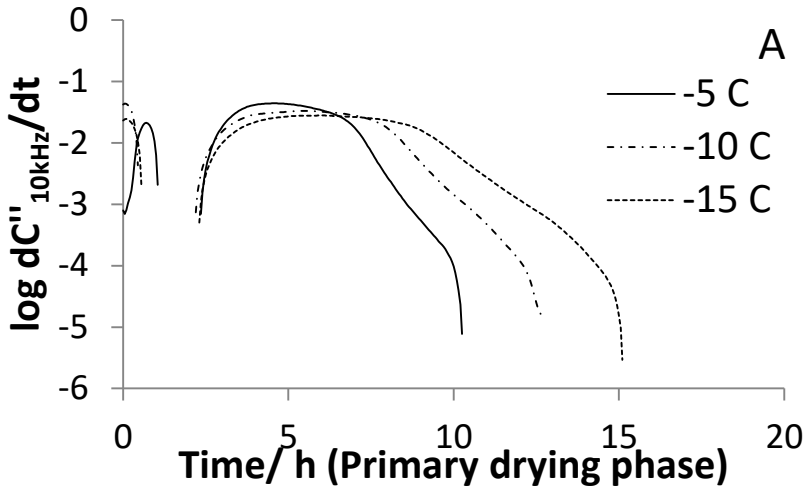

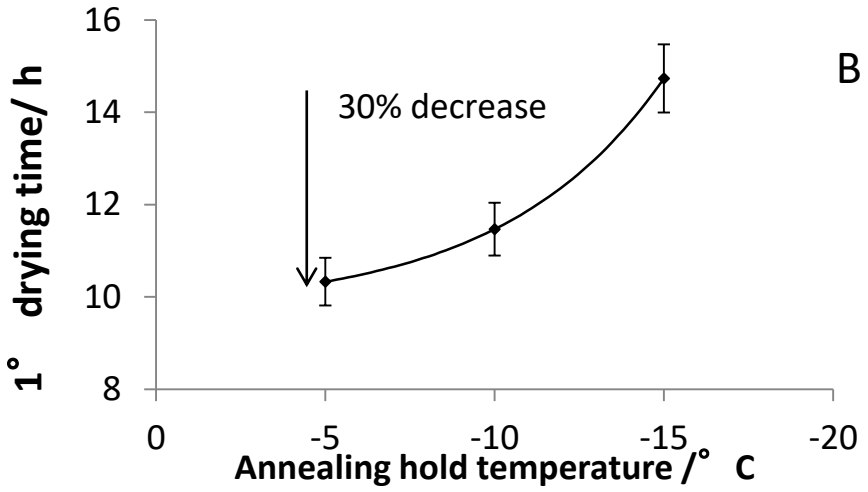

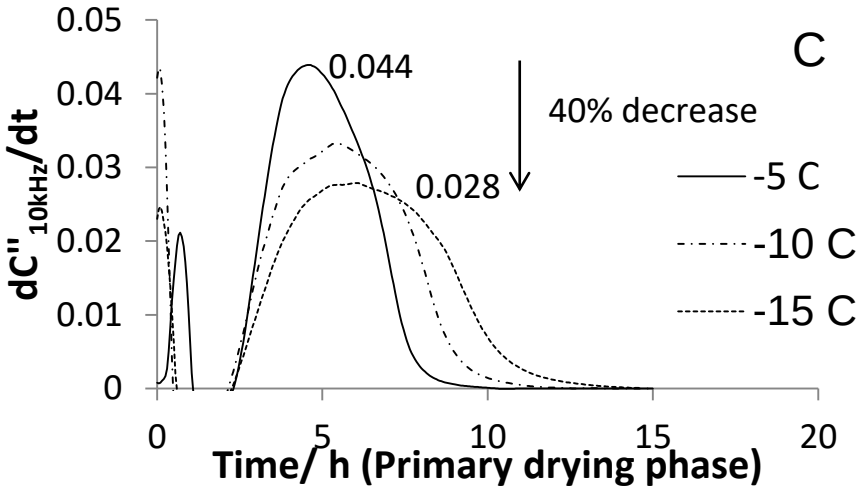

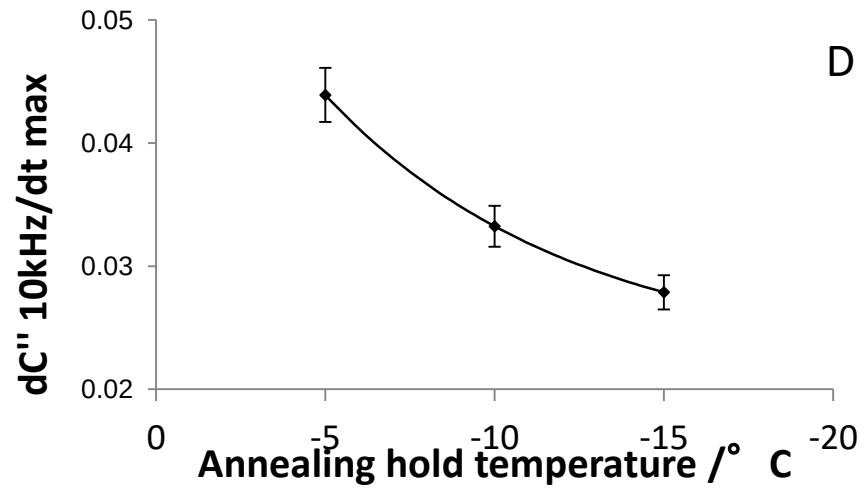

Christ MICROBALANCE

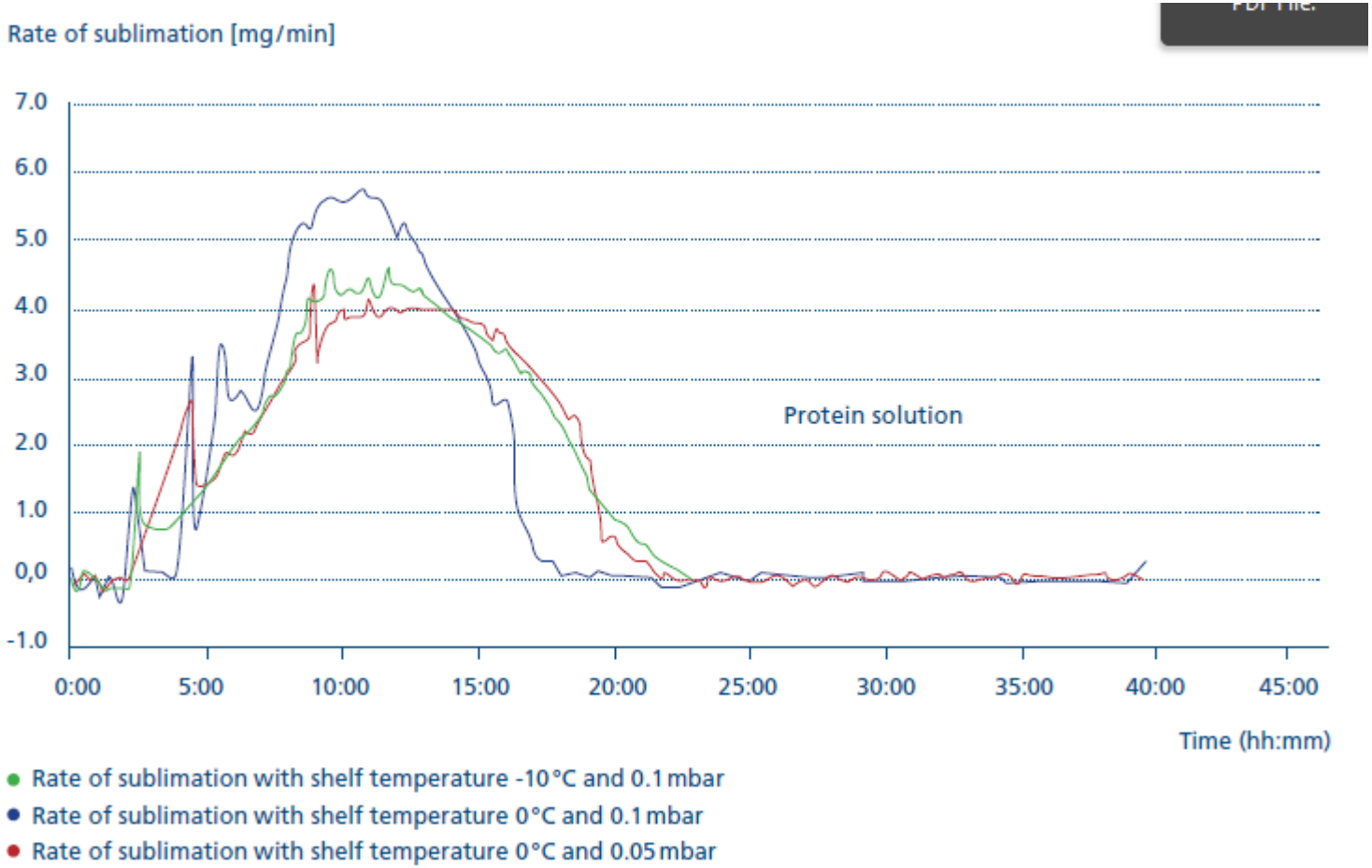

Meso-scale in liquids and glasses

- Liquids and glasses are known as structurally disordered materials which are often described in terms of molecular dynamics and co-operativity.

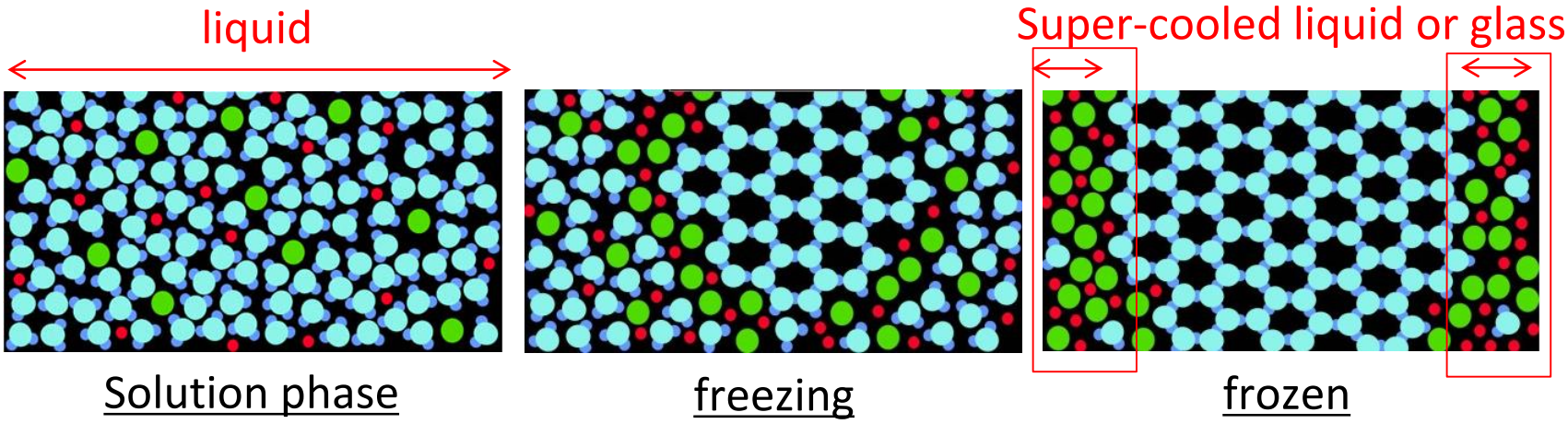

- The solid state (glass) is achieved when the temperature is reduced sufficiently to increase the viscosity to 10^{13} poise
- Scale length and shape of the cooperative unit (CRR) depends on temperature. CRR can be ~ nm close to T_g and the shape compact; whereas >T_g the CRR becomes longer and more string like (Nature Physics 2, 268 - 274 (2006))
- The unfrozen fraction will inevitably contain some residual water (which in turn impacts the glass transition temperature)

Cooperativity (N_B) and fragility (m)

- N_B is the number of molecules involved in viscous flow (i.e. the structural relaxation) at the glass transition, T_g
- The fragility index is determined from the temperature dependence of the viscosity (deviation from Arrhenius)
- As the fragility index increases so does the scale length of the cooperative unit
- The model predicts that the scale length (ξ) for the cooperative unit in a typical fragile system is in the region of 1-3 nm.

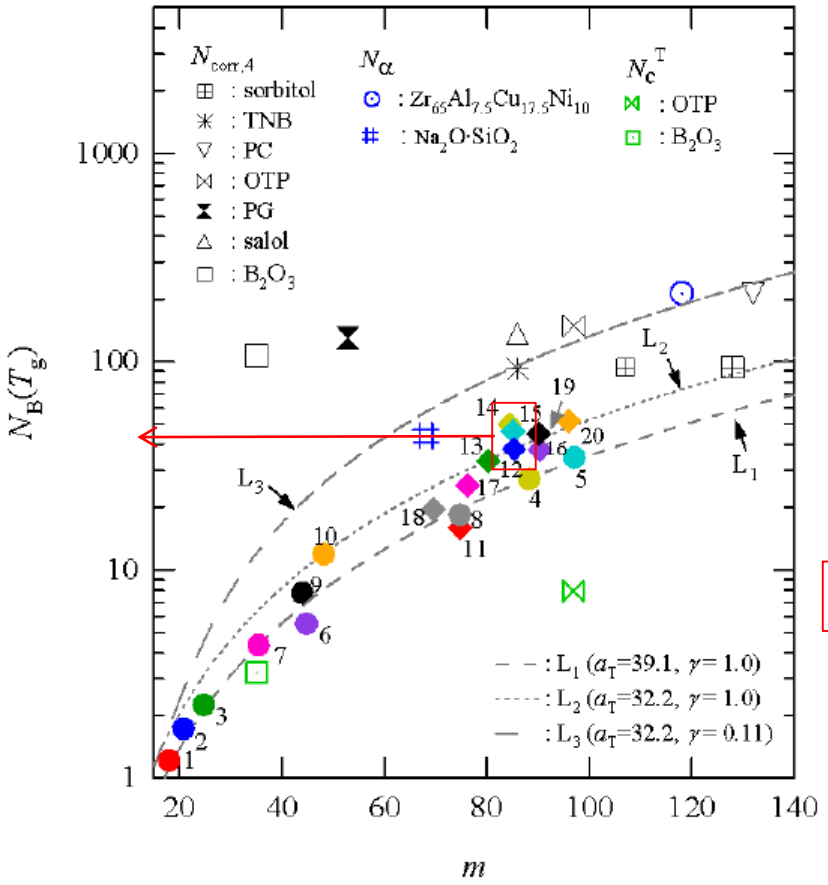

No.	Glass-forming material
1.	SiO_2
2.	GeO_2
3.	$K_2O{\cdot}3SiO_2$
4.	$Li_2O{\cdot}2B_2O_3$
5.	$SrO{\cdot}2B_2O_3$
6.	As_2Se_3
7.	GeS_2
8.	Se
9.	$Zr_{46.75}Ti_{8.25}Cu_{7.5}Ni_{10}Be_{27.5}$
10.	$Pd_{48}Ni_{32}P_{20}$
11.	$Pd_{77}Cu_{6.5}Si_{16.5}$
12.	$Au_{76.9}Ge_{13.65}Si_{9.45}$
13.	$50ZrF_4$-$40BaF_2$-$2NaF$-$8AlF_3$
14.	$[Ca(NO_3)_2]_{0.4}[RbNO_3]_{0.6}$ (CRN)
15.	Sorbitol
16.	Xylitol
17.	Tripropylene glycol (TPG)
18.	Dipropylene glycol (DPG)
19.	Propylene Glycol (PPO-4000)
20.	1:8 $NaCF_3SO_3$-PPO(4000)

Physics Procedia 48 (2013) 113-119

VTF Fit to describe the above Tg' resistance

- Above T_g the temperature dependence of the product resistance follows the Vogel-Tammann-Fulcher function.

- The curvature of the resistance plot decreases following annealing which relates to the increased strength of the glassy material.

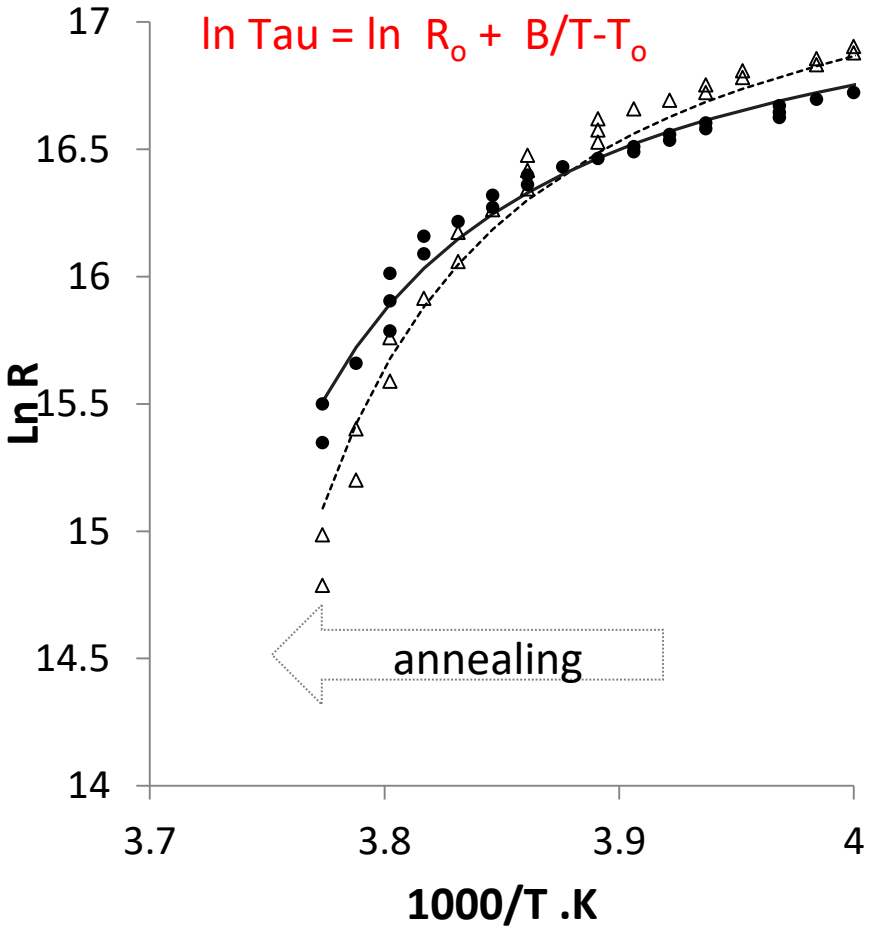

Annealing impact on glassy matrix

- The fragility is a dimensionless parameter employed to explain the strength of a glassy material, it is calculate from

$$F_{1/2}=1 - (T/T_g)$$

- Fragility index range from 0-1 in the increasing order of strength.
- The fragility (or the steepness index) of the glassy material increase from 0.38 to 0.44 after annealing.
- Link b/w fragility and (i) moisture content of the unfrozen phase ?, (ii) ease of moisture desorption during 2 drying ??

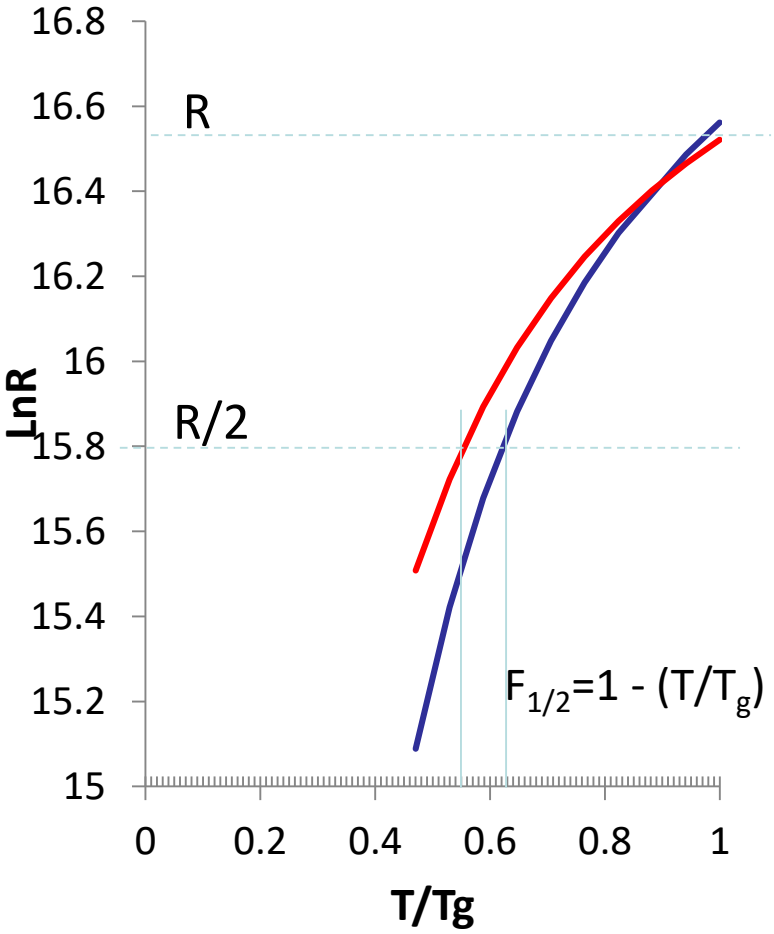

Macroscale 2 Clusters of vials

- Steady state sublimation rate can vary by up to 50% across the shelf

Mini-piloting

- Mini-pilot studies should aim to capture the impact of the radiant heating.
- Aim: determine the minimum cluster size across which both core and edge processing effects can be determined
- Screen formulations for low impact from to edge effects (radiant heating)

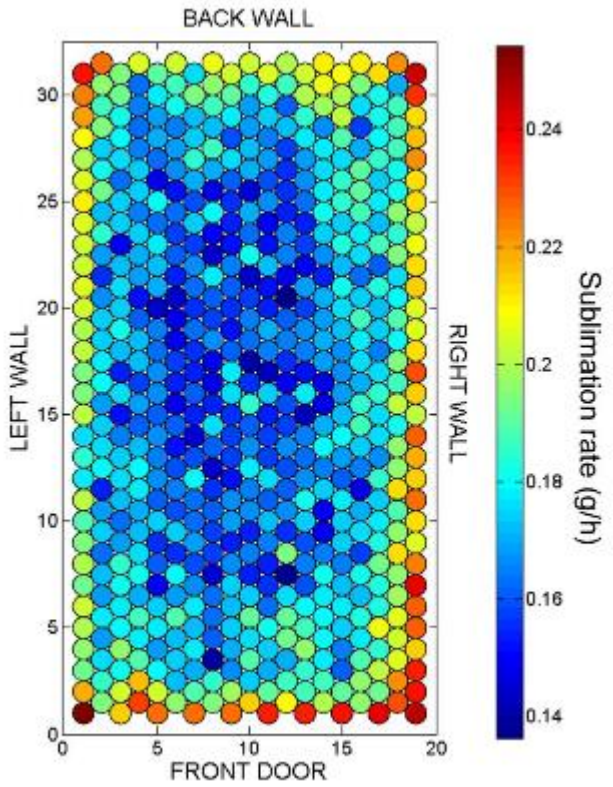

Kauppinen, A. (2015) 26thAnn. Symp. Finnish Soc. Phys. Pharm., Kuopio, Finland

Spatial mapping: Primary drying times

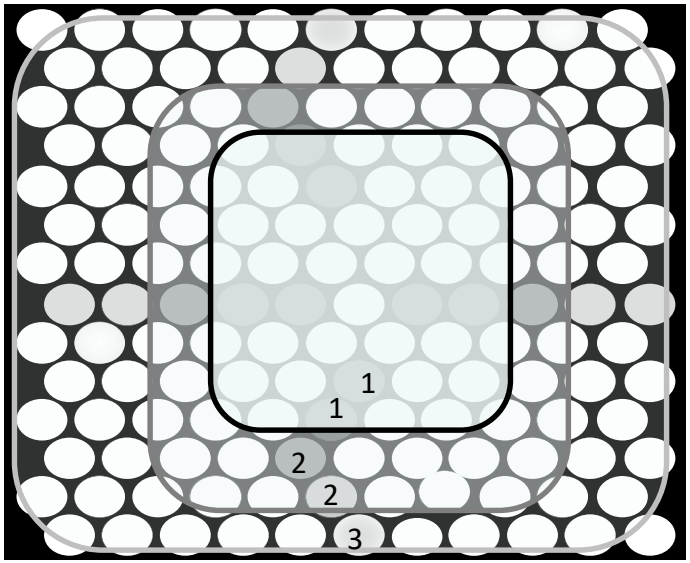

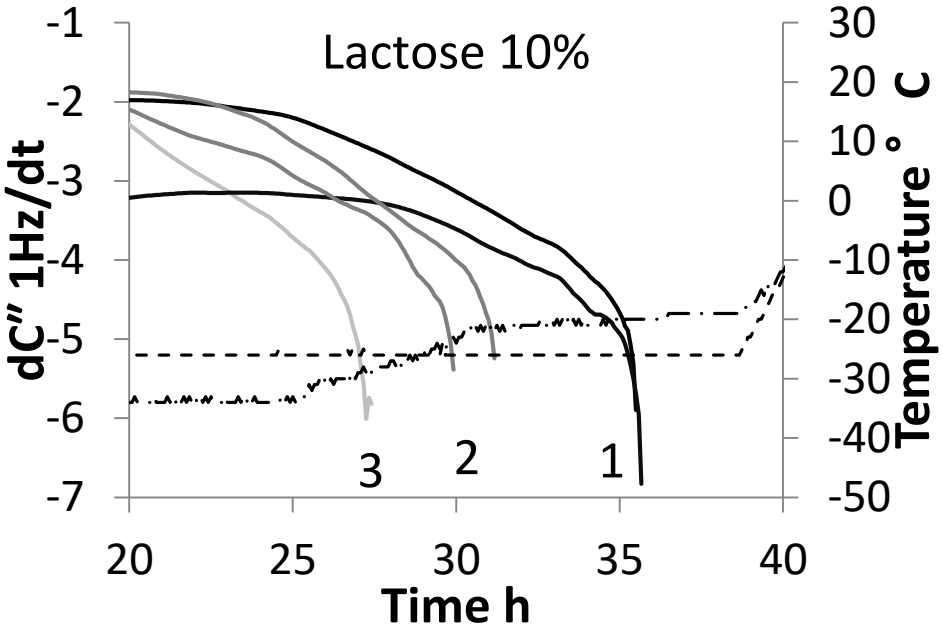

1. Primary drying time distribution across the shelf identifies three distinct spatial regions characteristic of thermal variations in the shelf.
2. Edge effects – may extend across three vials around the periphery of the shelf

Drying times & surrogate drying rates

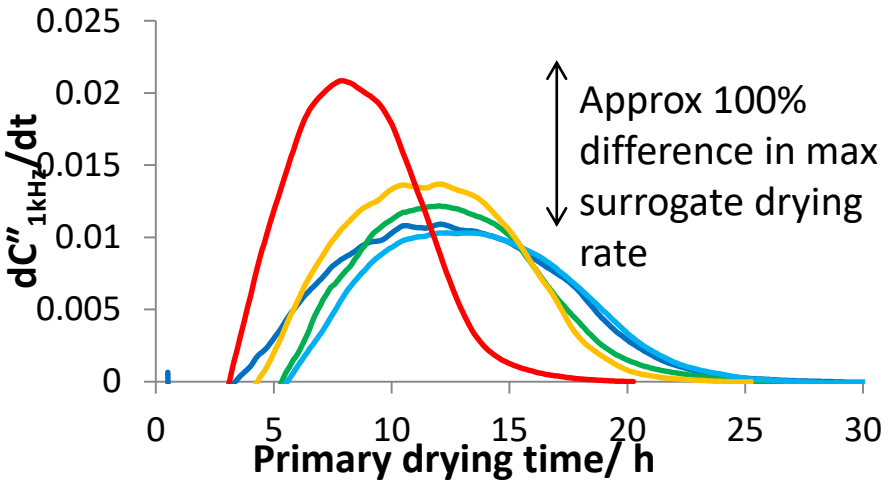

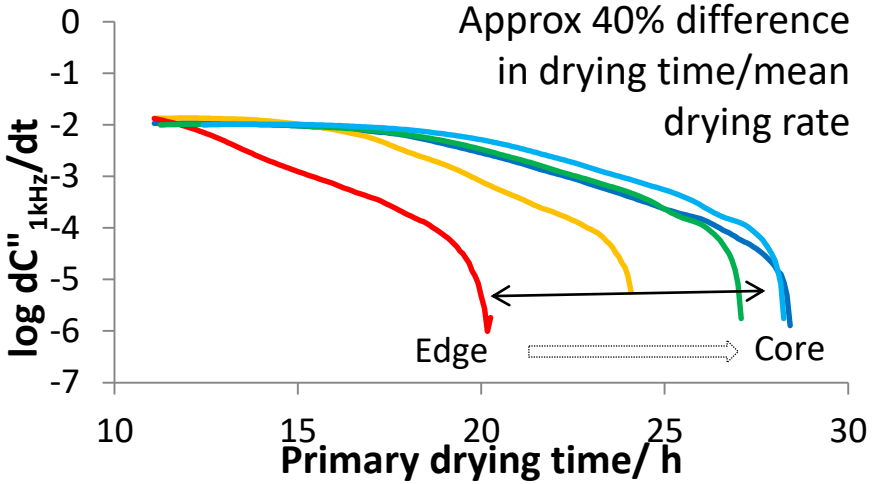

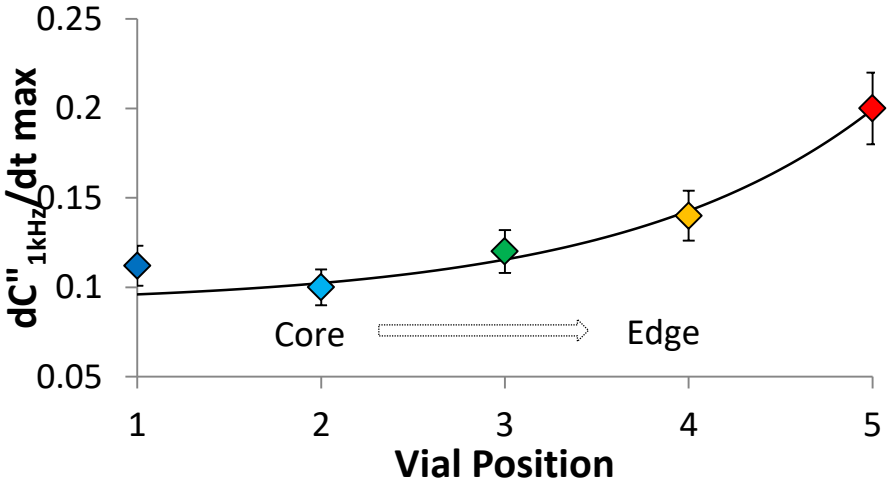

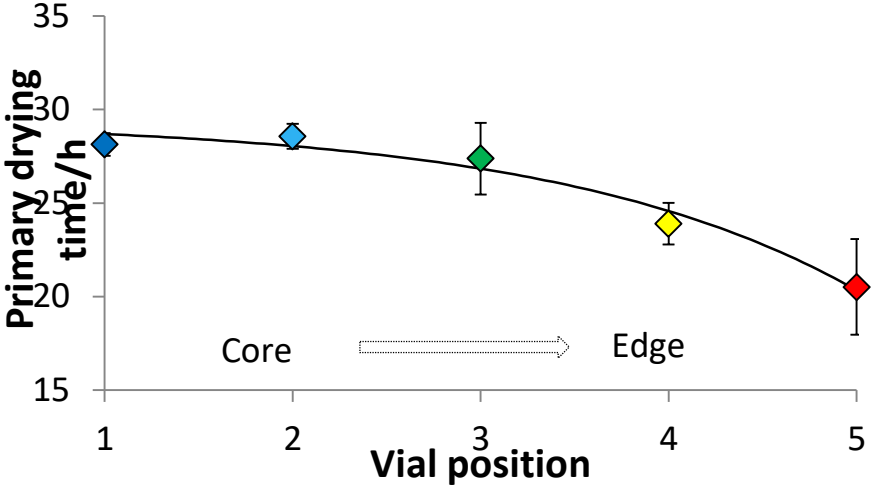

Normalised Drying Curves – surrogate rates

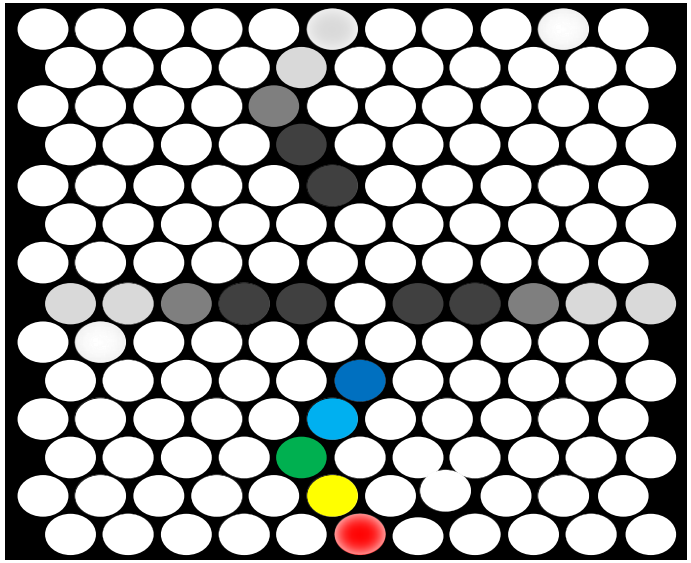

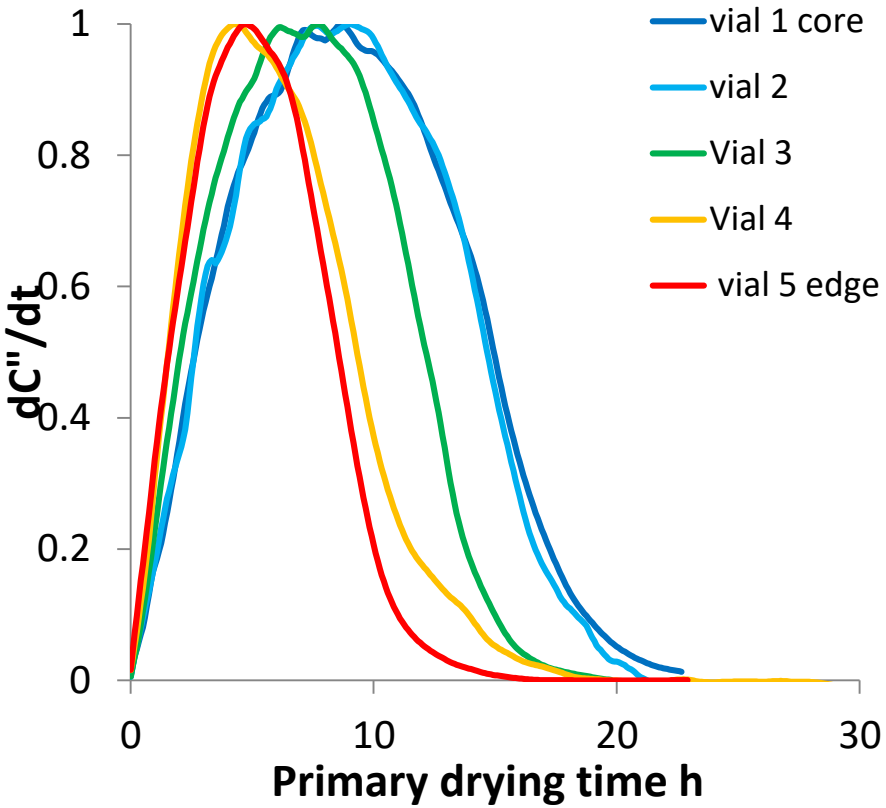

Normalised Drying Curves – drying times

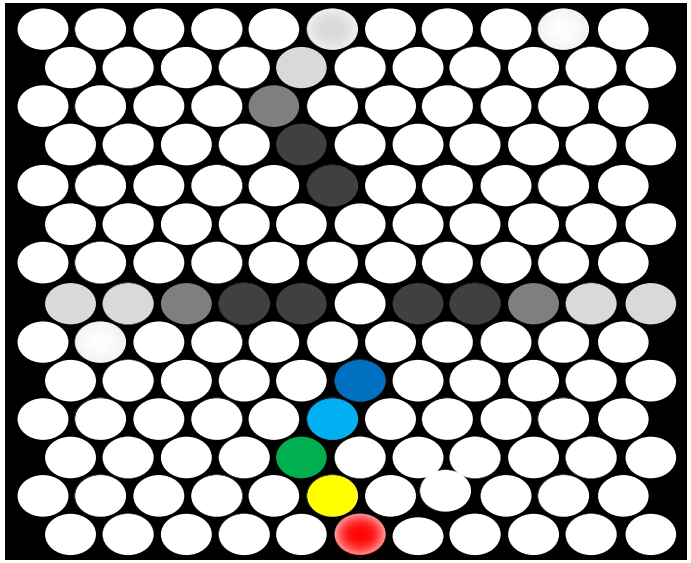

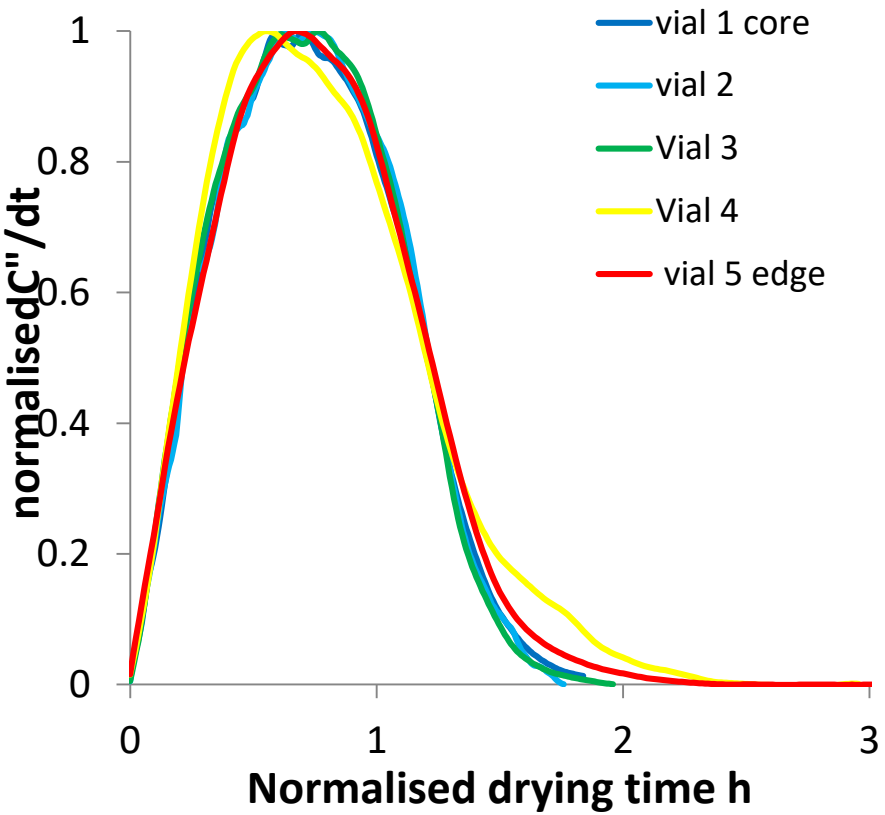

Shape of the drying front ?

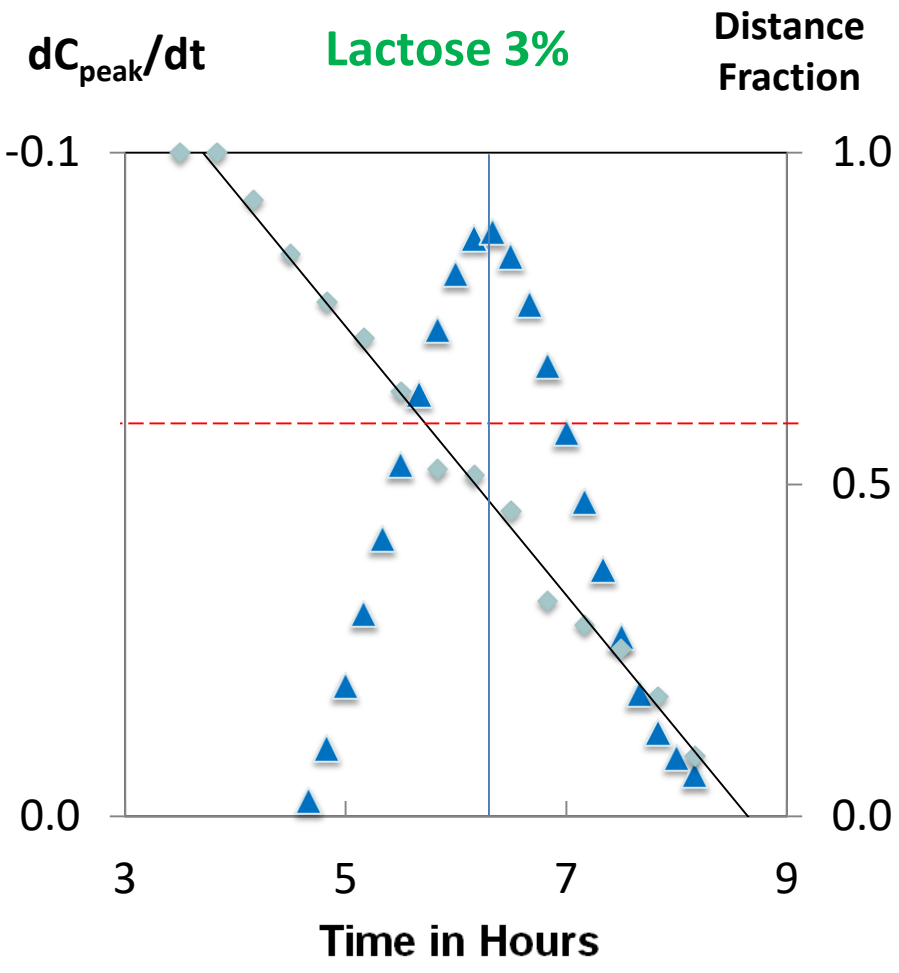

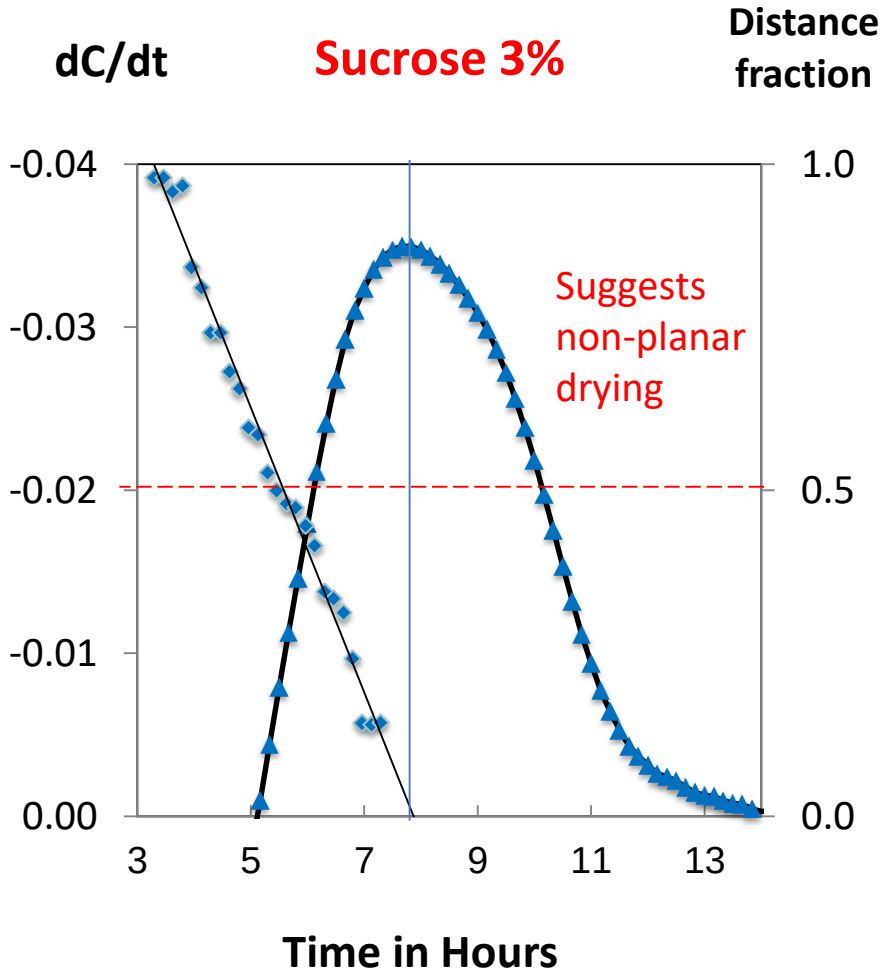

TVIS the Future : Scale Down to Scale Up

Collaborative R&D project

- GEA Pharma Systems, BlueFrog,
- National Institute for Biological Standards and Control,
- Genzyme Ireland,
- De Montfort University

3 year project to implement TVIS across different scales:

- microtitre plates up to pilot scale

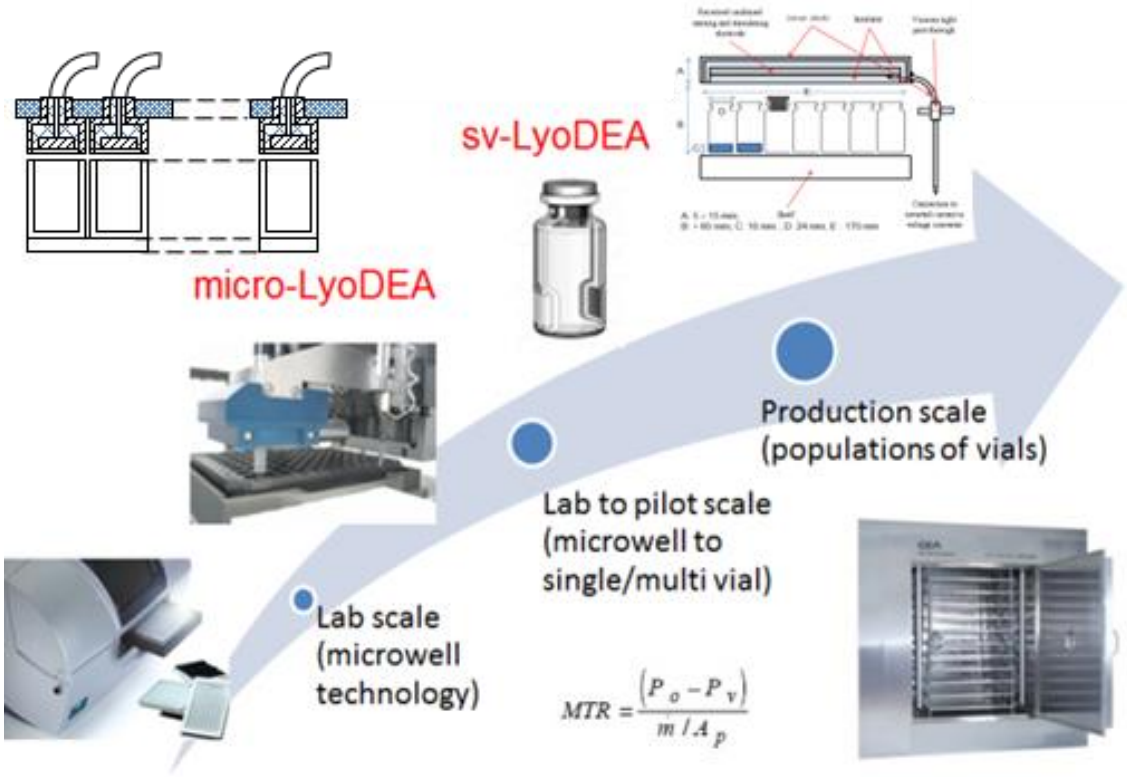

BIOSTART

Supported by UK government Innovate UK

Oportunities and Challenges

- TVIS registers thermal events through changes in the sample resistance associated with the exo thermic processes of ice formation and eutectic formation
- TVIS registers the glass transition through a discontinuity in either the capacitance or resistance as a function of temperature/time
- Primary drying (loss of ice) is monitored through changes in the strength of the dielectric loss peak (or step in the real part capacitance) – requires calibration (e.g. microbalance)
- Temperature control might be possible through monitoring of log f_{peak} – requires calibration with external TCs
- Mechanisms of annealing where elucidated from changes in resistance with time (during the heating-hold phase) and from the absence of any changes in T_G
- Drying rate profiles may provide information on the shape of the drying front and the influence of formulation on the susceptibility to radiant heating.
- Meso-structural information was extracted through the (non-Arrhenius) temperature dependence of the resistance
- Opportunities to track the physical characteristics of collections of vials is proposed.

Acknowledgements

- **Evgeny Polygalov**. Senior Research Fellow. Leicester School of Pharmacy. De Montfort University
- Dr **Sohail Arshad**. Assistant Professor Pharmaceutics, Faculty of Pharmacy, Bahauddin Zakariya University, Multan, Pakistan
- Dr **Irina Ermolina**. Senior Lecturer. Leicester School of Pharmacy. De Montfort University
- **Julian Taylor** and **Trevor Page**. GEA Pharma Systems, Eastleigh, United Kingdom
- **Tim McCoy** Genzyme
- **Paul Matejtschuk** NIBSC
- Technology Strategy Board and Innovate UK

Collapse in situ imaging of collapse

- **Optical coherence tomography-based freeze-drying microscopy provides in situ assessment of the collapse temperature**
- T_C can be a few degrees different to T_C measured by conventional FDM
- Possible consequence of the differences in T_G prime that results from the freezing process impacting the amount of ice that forms.

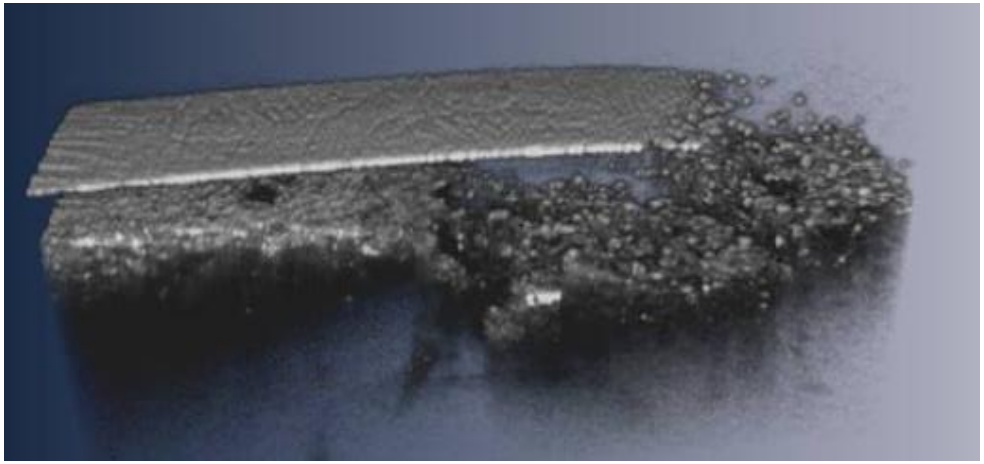

Mujat et al. (2012) Biomedical Optics Express **3** 55-63